Biotechnologically modified calcium phosphate cement for the stabilization of osteoporotic vertebral compression fractures

Dissertation

in partial fulfilment of the requirements for the degree of
doctor rerum naturalium (Dr. rer. nat.)

submitted to the Faculty Council of the School of Medicine
at Friedrich-Schiller-University of Jena

Francesca Gunnella

born on 03.04.1988 in Rieti, Italy

August 2018

Reviewers:

1. .....
2. .....
3. .....

Date of public disputation:

TABLE OF CONTENT

ABBREVIATIONS

CPC	calcium phosphate cement
PLGA	poly (l-lactide-co-glycolide acid)
BMPs	bone morphogenetic proteins
GDF5	growth differentiation factor 5
BMP-2	bone morphogenetic protein-2
ELISA	enzyme-linked immunosorbent assay
PMMA	polymethylmethacrylate
BMD	bone mineral density
BMPR-I	bone morphogenetic protein receptor-I
BMPR-II	bone morphogenetic protein receptor-II
β-TCP	beta-tricalcium phosphate
μCT	microcomputed tomography

ABSTRACT

Osteoporosis is characterized by reduced bone mass and disruption of bone architecture, resulting in an increased risk of fragility fractures, most of which are located in the lumbar spine. Bioresorbable calcium phosphate cement (CPC), mechanically stabilized by the addition of poly(l-lactide-co-glycolide) acid (PLGA) fibers, may be suitable for the vertebroplasty/kyphoplasty of osteoporotic vertebral fractures. However, additional targeted delivery of osteoinductive bone morphogenetic proteins (BMPs) in the CPC may be required to counteract the augmented local bone catabolism and support complete bone regeneration.

The present work thus aimed at: **1)** analyzing the release kinetics of three BMPs (**GDF5**, **BB-1** and **BMP-2**) from an injectable brushite-forming PLGA fiber-reinforced CPC and their bioactivity *in vitro*; **2)** generating and characterizating a minimally invasive large animal sheep model for lumbar ventrolateral vertebroplasty; and **3)** testing the PLGA-fiber reinforced CPC loaded with low-dose BMP-2 in the newly established model.

The quantification of the release by ELISA within 30/31 days showed a maximum of 34% and 17% of the applied dosages (2, 10, 200, and 1000 µg/ml) respectively, for GDF5 and BB-1 (BMP-2: 25.7% release of 400 µg/ml within 14 days).The addition of 5% and 10% PLGA fibers augmented the BMP release within 14 days. Notably, in several cell lines the BMPs released within 3 days demonstrated bioactivity, in selected cases augmented by the addition of 10% fibers. In order to develop a large animal model suitable for preclinical studies, lumbar defects were created by a ventrolateral percutaneous approach in aged, osteopenic, female sheep (L1: untouched; L2: empty defect; and L3: CPC). The minimally invasive model resulted in short operation time and postoperative recovery, very limited local trauma, and high experimental reproducibility.

The model was then used for the vertebral injection of CPC containing different dosages of BMP-2 (1, 5, 100, and 500 µg). Three and 9 months after operation, BMP-2 improved all parameters of bone formation, bone resorption, and bone structure, as well as the compressive strength. The BMP-2 effects on bone formation were dose-dependent, with 5 to 100 µg as the optimal dosage.

Overall the results confirmed the suitability of the drug-loaded CPC as a carrier for a one-time delivery of osteogenic proteins such as BMP-2 in minimally invasive surgery. Thus, the new CPC may represent an alternative to the bioinert, supraphysiologically stiff polymethylmethacrylate cement currently used to treat osteoporotic vertebral fractures by vertebroplasty/kyphoplasty.

ZUSAMMENFASSUNG

Osteoporose ist durch eine verminderte Knochenmasse und gestörte Knochenarchitektur charakterisiert. Dies führt zu einem erhöhten Risiko für Knochenbrüche, die am häufigsten in der Lendenwirbelsäule auftreten. Ein durch Poly(lactid-co-glycolid) (PLGA) Fasern mechanisch stabilisierter, bioresorbierbarer Calcium-Phosphat Zement (CPC) könnte für die Behandlung von osteoporotischen Wirbelkörperfrakturen mittels Vertebroplastie/Kyphoplastie geeignet sein. Trotzdem ist möglicherweise eine zusätzliche, gezielte Bereitstellung von osteoinduktiven Wachstumsfaktoren (bone morphogenetic proteins; BMPs) in dem CPC notwendig, um dem erhöhten lokalen Knochenabbau entgegenzuwirken und die komplette Knochenregeneration zu unterstützen. Die Ziele der vorliegenden Arbeit waren daher: **1)** die Analyse der Freisetzungskinetik von drei BMPs (**GDF5**, **BB-1** und **BMP-2**) aus einem injizierbaren, Brushit-bildenden, PLGA-Faser verstärkten CPC und deren Bioaktivität in vitro; **2)** die Etablierung und Charakterisierung eines minimal-invasiven Großtiermodells im Schaf für die lumbale ventrolaterale Vertebroplastie; und **3)** die Testung eines PLGA-Faser verstärkten, mit niedrig dosiertem BMP-2 beladenen CPC in dem neu etablierten Modell.

Die Quantifizierung der Freisetzung mittels ELISA zeigte, dass innerhalb von 30/31 Tagen max. 34% der eingesetzten Konzentrationen (2, 10, 200 und 1000 µg/ml) von GDF5 bzw. 17% von BB-1 freigesetzt wurden (BMP-2: 25.7% Freisetzung von 400 µg/ml innerhalb von 14 Tagen). Der Zusatz von 5 und 10% PLGA Fasern verstärkte die BMP Freisetzung innerhalb von 14 Tagen. Bemerkenswerterweise zeigten die innerhalb von 3 Tagen freigesetzten BMPs in verschiedenen Zell-Linien Bioaktivität, die in ausgewählten Fällen durch den Zusatz von 10% Fasern verstärkt wurde.

Zur Entwicklung eines für präklinische Studien geeigneten Großtiermodells wurden über einen ventrolateralen perkutanen Zugang lumbale Defekte in alten osteopenischen weiblichen Schafen erzeugt (L1: unbehandelt; L2: Leerdefekt; und L3: CPC). Dieses minimal-invasive Modell resultierte in einer kurzen Operationszeit und postoperativen Erholungsphase, sehr begrenztem lokalen Trauma und hoher experimenteller Reproduzierbarkeit.

Das Modell wurde dann für die vertebrale Injektion von CPC mit verschiedenen Dosierungen von BMP-2 benutzt (1, 5, 100, und 500 µg). Drei und 9 Monate nach der Operation verbesserte BMP-2 alle Parameter der Knochenbildung, Knochenresorption und Knochenstruktur sowie die Druckfestigkeit. Die BMP-2 Effekte auf die Knochenbildung waren dosisabhängig, mit 5 bis 100 µg als der optimalen Dosierung.

Zusammenfassend bestätigten die Resultate die Eignung des Wirkstoff-beladenen CPC als Träger für die einmalige Bereitstellung von osteogenen Proteinen wie z.B. BMP-2 in minimal-invasiver Chirurgie. Daher könnte der neue CPC eine Alternative für den bioinerten, supraphysiologisch steifen Polymethylmethacrylat-Zement darstellen, der derzeit für die Behandlung von osteoporotischen Wirbelkörperfrakturen mittels Vertebroplastie/Kyphoplastie eingesetzt wird.

1. INTRODUCTION

1.1 Osteoporosis

Osteoporosis, literally "porous bone", is a systemic skeletal disease regarded as a major socioeconomic health problem worldwide, characterized by the loss of bone mass leading to high individual disease load and severely impaired quality of life (Reginster and Burlet 2006, Hernlund, Svedbom et al. 2013). The considerably reduced bone mass and disturbed microarchitecture results in a loss of mechanical strength and increased fracture risk (Hernlund, Svedbom et al. 2013). There are different ways in which osteoporosis can develop and lead to a more fragile skeleton (Unnanuntana, Rebolledo et al. 2011). Studies of bone turnover have shown that the major cause of decreased bone mass in human osteoporosis is not the decrease in bone formation, but rather an increase in bone resorption (Hernlund, Svedbom et al. 2013). During childhood and adolescence, bone deposition exceeds bone resorption, so that the skeleton grows in size and bone mineral density (BMD). Up to 90 percent of the peak bone mass is acquired by age 18 in girls and by age 20 in boys, which makes youth the best time to "invest" in the individual's bone health. The amount of bone tissue in the skeleton, known as bone mass, keeps increasing until around age 30 (Sykaras and Opperman 2003). At that point, bones have reached their maximum strength and density, known as peak bone mass. Factors such as hormones (Riggs, Jowsey et al. 1969), nutrition (Cashman 2007), and physical exercise (Englund, Littbrand et al. 2009) can dramatically affect the peak bone mass. Women tend to experience only minimal loss of total bone mass between age 30 and menopause. But in the first few years after menopause, most women go through rapid bone loss, which then slows, but continues throughout the postmenopausal years. This loss of bone mass leads to a condition called osteopenia, which becomes osteoporosis when mechanical demands exceed the stability of the skeletal structure (Urist 1965).

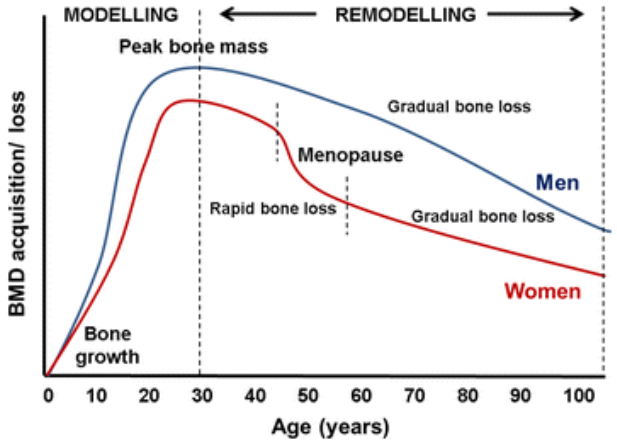

Figure 1.1: Peak bone mass and bone loss according to age for men and women. [*Kruger MJ, Nell TA. Bone mineral density in people living with HIV: a narrative review of the literature. AIDS Res Ther 2017:14(1)35*]

Osteoporosis has been operationally defined on the basis of BMD assessment. According to the World Health Organization (WHO) criteria, it is defined as a BMD that lies 2.5 standard deviations or more (T-score of < -2.5 SD) below the average peak bone mass for the young healthy population [age of approximately 30; (Namkung-Matthai, Appleyard et al. 2001)]. This criterion has been widely accepted, and provides both a diagnostic and an intervention threshold. Based on BMD values, ranging from grade 0 (normal bone density) to grade 3 (severe osteoporosis), the WHO introduced a classification of osteoporosis, in which different forms can be recognized (Table 1.1).

Due to its prevalence worldwide, osteoporosis is considered a serious public health concern. Currently it is estimated that over 200 million people worldwide suffer from this disease (Hernlund, Svedbom et al. 2013). The prevalence of osteoporosis among women in the largest countries in the European Union (Germany, France, Italy, Spain, and UK; EU5) using the WHO criteria is shown in Table 1.2.

The treatment of osteoporosis consists of a combination of antiresorptive and anabolic agents (estrogen receptor modulators and bisphosphonates); however, it is important to recognize that non-pharmacologic approaches are also needed to limit the fracture risk (Rizzoli, Branco et al. 2014). They include: maintaining adequate intake of calcium, vitamin D, and protein; using proper techniques when lifting; performing adequate weight-bearing physical activity and exercise to maintain or improve balance and posture; making appropriate lifestyle changes, such as smoking cessation and moderating alcohol intake.

DEFINITION	BMD MEASUREMENT	T-SCORE
NORMAL	Within 1SD of mean BMD for young adult women	T-score >-1
OSTEOPAENIA	BMD 1-2.5 SD below the mean for young adult women	T-Score btn -1 and -2.5
OSTEOPOROSIS	BMD >2.5 SD **below** mean for young adult women	T-Score <-2.5
SEVERE OSTEOPOROSIS	BMD >2.5 SD below mean for young adult women in a patient who has already experienced >1 fractures	T-Score <-2.5 with fragility fractures

Table 1.1: World Health Organization (WHO) criteria for diagnosing osteoporosis using bone density measurements. [*Kanis JA, et al. The diagnosis of osteoporosis. J Bone Miner Res 1994; 9:1137–1141*]

Age group (years)	France	UK	Germany	Italy	Spain	EU5
50-54	135	127	192	128	95	695
55-59	200	175	265	180	126	974
60-64	286	276	328	276	175	1,385
65-69	271	308	489	335	215	1,672
70-74	364	65	718	464	270	2,236
75-79	484	411	672	546	368	2,543
80-84	526	417	686	558	357	2,612
50-84	**2,266**	**2,079**	**3,350**	**2,487**	**1,606**	**12,117**

Table 1.2: Number (in thousands) of women with osteoporosis according to age in the European Union Five (EU5) countries using female-derived reference ranges at the femoral neck. [*Ström O, et al. Osteoporosis: burden, health care provision and opportunities in the EU: a report prepared in collaboration with the International Osteoporosis Foundation (IOF) and the European Federation of Pharmaceutical Industry Associations (EFPIA), 2011*]

1.2 Osteoporotic vertebral compression fractures

Osteoporosis increases the number of atraumatic fractures and contributes to the severity of traumatic fractures. The clinical fracture threshold is reached at a loss of cancellous bone mass of $\geq$ 40%, leading to fractures mostly localized in the lumbar spine (Bush 1991). The incidence of clinically diagnosed vertebral fractures rises steeply with age and the female to male incidence ratio after age adjustment is around 2:1 (Cooper and Melton 1992). A 50-year-old white woman has a 32% risk of suffering from a vertebral fracture during her remaining lifetime (Cummings, Black et al. 1989). Untreated vertebral compression fractures can cause debilitating back pain, spinal deformity, disability, reduction of respiratory function, and increased risk of death (Leidig, Minne et al. 1990). Although the impact of the vertebral compression fractures on health remains to be accurately quantified, a considerable number of patients suffer from long-term pain and disability. Moreover, osteoporosis can impair social relations, which in turns contributes to the development of severe depression (Gold 1996). The adverse effects of osteoporotic fractures are likely to increase in the future with the growing number of elderly people (Melton 1997).

1.2.1 Fracture healing

Bone heals by a regenerative process to restore the metabolic and mechanical functions of the injured tissue (Fig. 1.2). Immediately following a trauma, localized tissue hypoxia occurs (Einhorn and Gerstenfeld 2015), and a hematoma is generated which consists of cells from both peripheral and intramedullary blood, as well as bone marrow cells. The injury initiates an

inflammatory response, which is necessary for the healing to progress (Fig. 1.2A). The response causes the hematoma to coagulate in between and around the fracture ends, as well as within the medulla, forming a template for callus formation (Gerstenfeld, Cullinane et al. 2003).

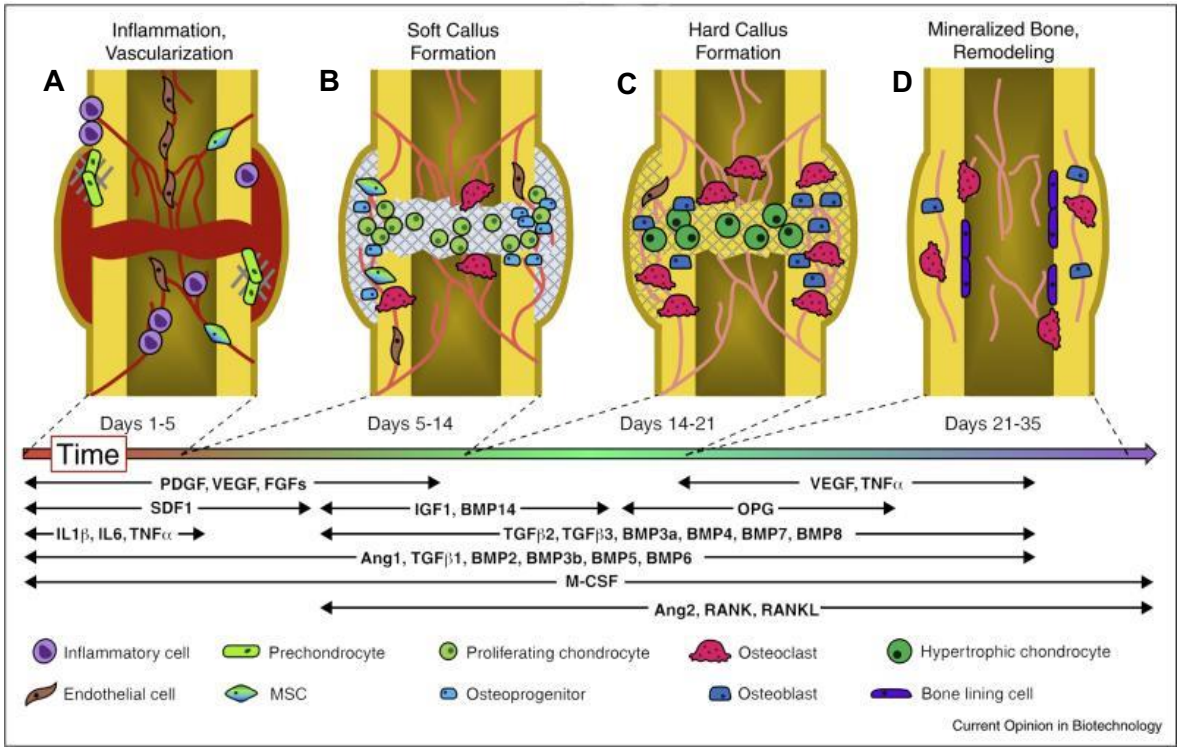

Figure 1.2: A spatiotemporal cascade of multiple endogenous factors controls normal bone regeneration during fracture repair in four stages. PDGF = platelet derived growth factor; VEGF = vascular endothelial growth factor; FGF = fibroblast growth factor; TNF = tumor necrosis factor; SDF = stromal cell-derived factor; IGF = insulin-like growth factor; BMP = bone morphogenetic protein; OPG = osteoprotegerin; IL = interleukin; TGF = transforming growth factor; Ang = angiopoietin; M-CSF = macrophage colony stimulating factor; RANK = receptor activator of nuclear factor kB; RANKL = RANK-ligand. [*Newman MR et al. Curr Opin Biotechnol 2016; 40:125-132*]

Although prolonged or chronic expression of inflammatory cytokines has negative effects on bone, joints, and implanted material, a brief and highly regulated secretion of proinflammatory molecules following acute injury is critical for tissue regeneration (Gerstenfeld, Cullinane et al. 2003). The acute inflammatory response peaks within the first 24 hours and is largely completed after 7 days, although proinflammatory molecules also play an important role in later phases of the regeneration process (Cho, Kim et al. 2007). The initial proinflammatory response involves secretion of tumor necrosis factor-α (TNF-α), interleukin-1 (IL-1), IL-6, IL-11, and IL-18 (Gerstenfeld, Alkhiary et al. 2006), which recruit inflammatory cells and promote angiogenesis (Fig. 1.2A-B). Following the formation of the primary hematoma, a fibrin-rich granulation tissue is formed. Within this tissue, endochondral formation of cartilage occurs in between the fracture ends and outside of the fracture below the periosteum. The granulation tissue is also mechanically less stable, whereas the cartilaginous tissue forms a soft callus which already gives the fracture a stable structure

[(Dimitriou, Tsiridis et al. 2005); Fig 1.2B]. At the same time, an intramembranous, subperiostal ossification response occurs directly adjacent to the distal and proximal ends of the fracture, generating a hard callus (Fig. 1.2C). It is the final bridging of the hard callus that ultimately provides the fracture with a semi-rigid structure, which allows weight bearing [(Gerstenfeld, Alkhiary et al. 2006); Fig. 1.2D]. The generation of the callus tissue is dependent on the local recruitment of mesenchymal marrow stem cells (mMSCs) from surrounding soft tissues, cortex, periosteum, and bone marrow, as well as the systemic supply of stem cells from the circulation following their mobilization into the peripheral blood from remote hematopoetic sites. Fracture callus mMSCs adjacent to the newly formed bone and the periosteum differentiate into chondrocytes, shaping an early fracture callus with new bone at its periphery, fibroblast-like cells in its center, and chondrocytes sandwiched in between these two layers. As healing progresses, differentiation of the fracture callus cells into chondrocytes proceeds from the periphery of the callus and the original periosteum towards the center and the circumferential edges of the callus. Chondrocytes closest to the periosteum and new bone are the first to become hypertrophic and form calcified cartilage. Osteoblasts derived from the pre-existing bone beneath the calcified cartilage, form bone on the calcified cartilage stratum until the fracture gap is bridged with new bone. Subsequent bone remodeling enhances the mechanical properties of the newly formed bone and returns it to its former shape. During this process, transforming growth factor-beta (TGF-β) superfamily members are pivotal. TGF-β2, -β3, and GDF5 are involved in chondrogenesis and endochondral ossification, whereas BMP-5 and BMP-6 have been suggested to induce osteoblast proliferation and intramembranous ossification at periosteal sites (Cho, Gerstenfeld et al. 2002, Marsell and Einhorn 2009).

Although bone is one of the few organs in the body that can spontaneously heal and restore function without scarring, bone healing is unsuccessful when the bone loss produces a critical-size defect (i.e., a defect exceeding the healing capacity of a few millimeters in human; or even in cases of non critical-size defects in elderly people and people affected by diabetes, nicotin abuse, compromised vascularity or osteoporosis).

1.2.2 Cellular and molecular basis of osteoporosis

A limited fracture healing capacity in osteoporosis is known from animal studies (Walsh, Sherman et al. 1997, Namkung-Matthai, Appleyard et al. 2001), and is associated with a dramatically increased failure rate of implant fixation (Barrios, Brostrom et al. 1993). The age-related bone loss resulting in osteoporotic vertebral compression fractures is based on a dysbalance between the underproduction of osteoblasts and the subsequently diminished bone formation on one hand, and the overproduction and overactivation of osteoclasts with augmented bone resorption on the other hand (Egermann, Schneider et al. 2005). In this context, estrogen deficiency seems to play an important role in the pathogenesis of osteoporosis and osteoporotic fractures (Augat, Simon et al.

2005). Osteoblasts and mMSC osteoblast precursors (Komm, Terpening et al. 1988), osteocytes (LeGeros 1982), and osteoclasts (del Real, Wolke et al. 2002) all express functional estrogen receptors (ERs). This may be the basis for the finding that mMSCs from post-menopausal women have a lower growth rate and a deficient ability to differentiate along the osteogenic lineage in comparison to mMSCs from pre-menopausal women (Rodriguez, Garat et al. 1999). In addition, aging decreases the expression of osteoblast- specific transcription factors such as Runx2 and Dlx5 in mMSCs, but increases the expression of the adipocyte-specific transcription factor PPARγ2. Both changes decrease the number of mMSC-derived osteoblasts, but increase the number of mMSC-derived adipocytes (Moerman, Teng et al. 2004) and thus decrease the ratio between these two cell populations. This creates unfavorable conditions for bone stem cell participation in fracture repair and commonly leads to a failure of osteoporotic fractures to heal (Egermann, Schneider et al. 2005). It is now clear that ligand binding to ERs induces a conformational change that promotes receptor dimerization and binding to specific DNA promoter sequences called estrogen response elements [EREs; (Smith and O'Malley 2004)]. The ligand-bound receptor then forms a complex with coactivator proteins, which activates the general transcriptional machinery and increases the expression of target genes through chromatin remodeling. ERs can also recruit corepressors, which negatively regulate ER-dependent gene expression. In addition to this classical modality of gene activation, alternative mechanisms account for estrogen's ability to both stimulate and repress the expression of genes encoding critical osteoclastogenic factors such as IL-6, TNF-α, and M-CSF (Stein and Yang 1995). Although many estrogenic effects are mediated by nuclear ERs, some responses originate in the plasma membrane. In fact, estrogen induces rapid non-genomic effects (within seconds or minutes) in various cell types, including bone cells, which are mediated by signaling through a membrane receptor. Estrogen's ability to inhibit osteoblast apoptosis, but to induce osteoclast apoptosis, is linked to its ability to increase ERK1 and ERK2 phosphorylation and repress JNK activity (Kousteni, Bellido et al. 2001, Kousteni, Han et al. 2003).

The result of estrogen deficiency is thus a dramatic elevation in the number of basic multicellular units (BMUs), defined anatomical spaces in which bone remodelling occurs, through increased activation frequency of osteoclasts [number of new remodeling units activated in each unit of time; (Weitzmann 2006)]. The enhanced activation frequency of osteoclasts expands the remodeling space, increases cortical porosity, and enlarges the resorption area on trabecular surfaces. This phenomenon is primarily caused by increased osteoclast formation, but also by increased osteoclast recruitment to bone surfaces (Weitzmann 2006). Estrogen deficiency also augments the erosion depth by prolonging the resorption phase of the remodeling cycle through increased osteoclast lifespan due to reduced apoptosis (Hughes, Dai et al. 1996).

Although estrogen has direct effects on bone cells, animal studies have identified additional unexpected regulatory effects of estrogen centered at the level of the adaptive immune response

(Cenci, Toraldo et al. 2003), with the potential of indirectly influencing bone formation and resorption.

However, subtle differences in the genetic code and environmental factors may explain why one person's osteoblasts or osteoclasts are more active or responsive to their environment and thus, why estrogen deficiency in postmenopausal women does not necessarily lead to osteoporosis.

In addition, in older people angiogenesis is impaired, due to age-related changes in the hemostatic cascade, growth factor expression, and endothelial cell formation (Reed and Edelberg 2004). These changes result in delayed and impaired neovascularization and are therefore also likely to have an impact on wound and fracture healing in older people.

However, estrogen deficiency after menopause is not the only reason for osteoporosis since osteoporosis also affects men. By age 65 or 70, men and women are losing bone mass at the same rate as the absorption of calcium decreases (Nordin 1997). Such a decrease with age could be due to: 1) a decline in serum calcitriol, possibily due to a declining renal function; 2) a reduced gastrointestinal response to calcitriol; 3) a decline in serum 25-Hydroxyvitamin D3 ($25OHD_3$) due to low exposure to sunlight and/or a lower capacity of the skin to synthetize vitamin D; and 4) in the case of men, a decrease in testosteron levels.

The receptor activator nuclear factor-κB ligand (RANKL) as a regulator of osteoclast activity, is also involved in the pathogenesis of osteoporosis and thus represents a new therapeutic target (McClung 2007). By binding to its receptor RANK on osteoclastic precursors, RANKL controls the differentiation, proliferation, and survival of osteoclasts. Mice that are deficient in osteoprotegerin (OPG), a natural inhibitor of RANKL, exhibit osteoporosis, whereas over-expression of OPG in mice results in reduced numbers of osteoclasts and high bone mass (Simonet, Lacey et al. 1997, Bucay, Sarosi et al. 1998). Perturbations in the ratio of OPG to RANKL have been demonstrated to occur with estrogen deficiency, hyperparathyroidism, and other disorders that stimulate bone resorption (Hofbauer, Gori et al. 1999, Hofbauer, Khosla et al. 1999). RANKL is also expressed by lymphocytes and synovial fibroblasts and may mediate bone loss associated with inflammatory conditions (Kong, Feige et al. 1999, Takayanagi, Iizuka et al. 2000).

1.2.3 Treatment of osteoporotic vertebral fractures: vertebroplasty/kyphoplasty

Therapeutic options for acute vertebral body fractures include established surgical procedures such as spondylodesis. However, innovative, minimally invasive methods such as vertebroplasty and balloon-kyphoplasty are increasingly used (Phillips, Pfeifer et al. 2003). The latter are advantageous because they allow: 1) reduction of the hospitalization time compared to the traditional "open surgery" in which the vertebrae are exposed by an incision through the skin and muscles; 2) clear improvement of lumbar biomechanics in the large majority (90%) of the patients;

and 3) rapid and substantial reduction of pain (Lavelle, Khaleel et al. 2008). Significant pain relief usually occurs within 24 h after treatment (Cotten, Boutry et al. 1998).

The standard treatment for vertebral compression fractures consists of conservative management, including bed rest, bracing, and analgesics to relieve pain and regain functions of daily living (Boonen, Wahl et al. 2011). However, these practices are often insufficient in improving pain and mobility (Lyritis, Mayasis et al. 1989, Hallberg, Rosenqvist et al. 2004). In addition, long-term use of narcotic analgesics and anti-inflammatory drugs is poorly tolerated by elderly patients. Narcotics may result in sedation and impaired balance increasing the risk of falling and additional fractures. Prolonged bed rest may cause bone loss that exacerbates the underlying disease state (Krolner and Toft 1983), and can lead to rapid deconditioning, pulmonary compromise and increased mortality (Lau, Ong et al. 2008). Operative interventions such as open surgical fusions and the use of metal implants to treat unstable vertebral compression fractures have thus gained popularity (Deyo 2010); however, such interventions frequently cause failures and non-unions due to the low bone quality in osteoporotic patients, muscle injuries, and prolonged back pain. Pain relief is the principal objective when treating vertebral compression fractures in the elderly population (Boonen, Wahl et al. 2011), and the pain intensity potentially influences a patient's acceptance of surgical complication risks and thus the decision to consent to lumbar fusion (Bono, Harris et al. 2013). For such reasons, minimally-invasive vertebroplasty and kyphoplasty can recognizably increase the quality of life in patients with an osteoporotic vertebral fracture by improving lumbar biomechanics and stability and thus relieving pain. The technique of vertebroplasty, originally developed and published in 1987 by the French radiologist Galibert and the French neurologist Deramond (Galibert P 1987), consists of the direct percutaneous injection of a biomaterial, usually a methyl methacrylate cement, under pressure into a lesioned vertebral body. Percutaneous balloon kyphoplasty, approved by the US food and drug administration (FDA) since 1998 (Belkoff, Mathis et al. 2001), is a modification of this technique. The principle of kyphoplasty is to restore vertebral body anatomy by inflating balloons and then reinforce the anterior column of the vertebra with cement. The principal indications for these two procedures were initially osteolytic metastasis and myeloma, painful or aggressive hemangioma, and osteoporotic vertebral collapse (Cotten, Boutry et al. 1998). Nowadays, the main target population are patients with painful, therapy-resistant osteoporotic vertebral fractures not responding to analgesics, rest, bracing, or other conservative therapies for a period of 6 months (Voormolen, Mali et al. 2007). However, vertebroplasty is contraindicated in coagulation disorders due to the large diameter of the injection needle. Extensive vertebral destruction and significant vertebral collapse (i.e., vertebra reduced to less than one-third of its original height) may result in a technically challenging surgical procedure. The complication rate associated with both procedures is relatively low [7%; (Yaltirik, Ashour et al. 2016)], but serious complications can occur. These risks include spinal cord compression, nerve root compression, venous embolism, and pulmonary embolism including cardiovascular collapse (Burton and Mendel 2003). Hulme *et al*. reviewed 69 clinical studies and reported hardly any

difference between vertebroplasty and kyphoplasty concerning vertebral height restoration and pain relief (Hulme, Krebs et al. 2006).

Kyphoplasty may be superior to vertebroplasty in patients with large kyphotic angles, vertebral fissures, fractures in the posterior edge of the vertebral body or significant height loss in the fractured vertebrae (Yaltirik, Ashour et al. 2016). Radiography and computed tomography (CT) must be performed in the days preceding vertebroplasty to assess: 1) the extent of the vertebral collapse; 2) the location and extent of the lytic process; 3) the visibility and degree of involvement of the pedicles; 4) the presence of cortical destruction or fracture, especially of the posterior wall; and 5) the presence of epidural or foraminal stenosis. The decision to perform such procedures should be made by a multidisciplinary team, because the choice among open spine surgery, vertebroplasty, radiation therapy, medical treatment, or a combination thereof depends on a number of factors.

1.3 Calcium phosphate cements (CPCs) as a biomaterial

Bone cements, applied as filler materials in vertebral augmentation procedures such as vertebroplasty and kyphoplasty, are basically self-curing systems, generally supplied as separately packaged powder and liquid phases and mixed prior to use during surgery. These materials undergo subsequent *in situ* polymerization following injection into the vertebral body and harden to provide adequate mechanical support to the vertebral column (Deb 1999). At present, polymethylmethacrylate (PMMA) cement is the most widely used material for vertebroplasty and kyphoplasty, with extensive records of in vitro and in vivo analyses (Yimin, Zhiwei et al. 2013). Although the use of high-viscosity PMMA cement is thought to significantly reduce the rate of cement leakage, it may lead to limited penetration into trabecular bone and thus compromise the mechanical strength of the augmented vertebral body (Baroud, Crookshank et al. 2006, Hulme, Krebs et al. 2006). At the same time, PMMA cement shows some disadvantages such as monomer toxicity, thermal necrosis caused by high polymerization temperatures (Belkoff, Mathis et al. 2001), lack of bioactivity and biodegradability, and risk of leakage or fractures in adjacent vertebral bodies (Hulme, Krebs et al. 2006, Nouda, Tomita et al. 2009). Moreover, PMMA cement-based therapies for vertebral compression fractures may permanently exclude and eliminate mMSCs from the vertebral bone marrow space due to cellular toxicity, thus hampering endogenous bone healing. Due to such safety concerns on PMMA cements, calcium phosphate cement (CPC) has been used as an alternative to PMMA or acrylic bone cements and other injectable, drug-releasing biomaterials. In early 1980s, researchers discovered self-setting calcium orthophosphate cements (Table 1.3), which contain a powder with one or more solid compounds of calcium phosphate salts and an aqueous liquid (LeGeros 1982). Mixed in an appropriate ratio, a paste is formed which sets at body temperature by entanglement of the crystals precipitating within the paste. Therefore, calcium phosphate cements can be shaped according to the defect dimensions and set in situ. After setting, the

calcium phosphate crystals typically form a microporous structure with pores smaller than 1 µm (Chow 2001, del Real, Wolke et al. 2002). CPCs show several advantages: 1) excellent osteoconductivity for bone ingrowth and remodeling; 2) bioactivity, which means the ability to bind directly to the surrounding bone without the formation of fibrous tissue (Cao and Hench 1996); 3) a setting reaction at body temperature (Bohner 2001, Blattert, Jestaedt et al. 2009); and 4) biocompatibility and resorbability (depending on the calcium phosphate). Once implanted, CPCs can be resorbed by two different mechanisms, i.e., active resorption, which is regulated by living cells such as osteoclasts, and/or passive resorption via chemical dissolution or hydrolysis in the body fluids. However, CPCs exhibit poor tensile, shear, and mechanical strength, which limits their applicability to non- or moderate-load-bearing situations (Canal and Ginebra 2011). Because of their intrinsic porosity, the strength of CPCs is lower than that of calcium phosphate ceramics. All these factors may contribute to a residual instability of the vertebral body following cement augmentation (He, Zhai et al. 2015). In addition, for minimally invasive in vivo application in an osteoporotic vertebra, the CPC paste must have two features i.e., injectability and cohesion. Injectability means that the cement paste can be extruded through a long, small needle (e.g., 2 mm diameter and 10 cm length) without demixing. Demixing occurs when the mixing fluid is too liquid compared with the size of the cement powder particles, resulting in filter pressing: the liquid is extruded without the CaP particles. A cement paste with an appropriate cohesion sets in a fluid without disintegrating. This can be achieved by decreasing the powder-to-liquid ratio in the preparation process. The resulting CPC paste is less viscous and can be more easily injected (Khairoun, Boltong et al. 1998). Thus, for an injectable CPC a low powder-to-liquid ratio (< 2.4) has to be maintained, which on the other hand limits the mechanical strength of the resulting CPC (Maenz, Kunisch et al. 2014). Depending upon the pH value of the self-setting paste, calcium orthophosphates (Fig. 1.3) can only form two major end-products after hardening: 1) at pH > 4.2, a precipitated poorly crystalline hydroxyapatite (HA) or calcium-deficient hydroxyapatite (CDHA); and 2) at pH < 4.2, dicalcium phosphate dihydrate (DCPD), also called brushite (Xia, Grover et al. 2006). Thus, the existing self-setting calcium orthophosphate formulations are divided into the two major groups of apatite-forming and brushite-forming CPCs, on the basis of which bone substitution materials have been developed for orthopaedic surgery (e.g., for vertebroplasty and lumbar fusion). Brushite cement is injectable since it hardens under physiological conditions, shows a high biocompatibility after implantation, and is more rapidly bio-resorbable than apatite cement (Elliott 1997). In contrast, the crystals in the apatite cements can be easily detached from the bulk of the hardened cement, especially after partial dissolution, since the force linking the newly formed crystals is weak. These crystals can then be ingested by osteoclasts and other cells (Yuan, Li et al. 2000).

Ca/P-molar Ratio	Compounds and their abbreviations	Chemical formula	Solubility at 25° C, $-\log(K_S)$	pH stability range in acqueous solutions at 25° C
0.5	Calciumdihydrogenphosphate Monohydrat (MCPM)	$Ca(H_2PO_4)_2 \cdot H_2O$	1.14	0.0-2.0
0.5	Calciumdihydrogenphosphate	$Ca(H_2PO_4)_2$	1.14	a
1.0	Calciumhydrogenphosphate-Dihydrate, **brushite**	$CaHPO_4 \cdot 2H_2O$	6.59	2.0-6.0
1.0	Calciumhydrogenphosphate, monetite	$CaHPO_4$	60.90	a
1.33	Octacalciumphosphate	$Ca_8(HPO_4)_2(PO_4)_4 1. 5H_2O$	96.6	5.5-7.0
1.5	α-Tricalciumphosphate (α-TCP)	$\alpha\text{-}Ca_3(PO_4)_2$	25.5	b
1.5	β-Tricalciumphosphate (β-TCP)	$\beta\text{-}Ca_3(PO_4)_2$	28.9	b
1.2-2.2	Amorphous calcium phosphates	$Ca_xH_y(PO_4)_z \cdot nH_2O$, n=3-4,5	23-32	5.0-12.0 (c)
1.5–1.67	Calcium-deficient hydroxyapatite (**CDHA**)	$Ca_{10-x}(HPO_4)_x(PO_4)_{6-x}(OH)_{2-x}$, $0 < x < 1$	85.1	6.5-12.0
1.67	Hydroxyapatite (**HA**)	$Ca_{10}(PO_4)_6(OH)_2$	116.8	9.5-12.0
2.0	Tetracalcium phosphate	$Ca_4(PO_4)_2O$	38-44	b

a – Stable at temperatures above 100°C
b – These compounds cannot be precipitated from aqueous solutions
c – Always metastable

Table 1.3: Existing calcium orthophosphates and their main properties. [*Dorozhkin SV. Calcium Orthophosphates: Applications in Nature, Biology and Medicine. Pan Stanford: Singapore, Singapore 2012*]

Figure 1.3: Two commercial calcium orthophosphates. [*Dorothzkin S, Self-Setting Calcium Orthophosphate Formulations, J Funct Biomater 2009; 4:209-311*]

1.3.1 Calcium phosphate cements for bone drug delivery

A biomaterial with an intended use as a drug carrier must have the ability to incorporate a drug, to retain it at a specific target site, and to deliver it progressively to the surrounding tissues. For this purpose, injectable and biodegradable biomaterials with an intrinsic porosity are advantageous. Since the hardening of the CPC takes place at room or body temperature, drugs, biologically active molecules or even cells can be incorporated without thermal denaturalization or loss of activity during preparation or implantation (Ginebra, Canal et al. 2012). These features make CPCs attractive candidates for a local and controlled supply of drugs in the treatment of different skeletal diseases, such as bone tumors, osteoporosis or osteomyelitis.

One possibility is to homogeneously incorporate drugs into CPCs by adding them to either the powder or the liquid phase of the cement (Ginebra, Traykova et al. 2006). This can be achieved by blending drug powder with the solid phase or by dissolving it within the liquid phase, in the latter case usually resulting in a more homogenous distribution. When the drug is instead incorporated into the powder phase of the CPC, only partial dissolution of the drug particles will take place depending on the solubility of the drug in the reactant liquid phase of the CPC. Different approaches are to either incorporate the drug by impregnation of pre-set CPC solid blocks or granules with a drug solution or to incorporate the drug in polymeric microspheres before blending them with the CPC.

CPCs can be used as carriers for different types of drugs or active principles which are classified in three groups: 1) low molecular weight drugs; 2) ions; and 3) high molecular weight biomolecules. The first group is represented by antibiotics [gentamicin (Bohner, Lemaitre et al. 2000), vancomycin (Hofmann, Mohammed et al. 2009), ciprofloxacin (Hofmann, Mohammed et al. 2009), doxycycline (Alkhraisat, Rueda et al. 2010)], non-steroidal anti-inflammatory drugs [NSAIDs, e.g., ibuprofen (Girod Fullana, Ternet et al. 2010), acetylsalycylic acid (Ginebra, Rilliard et al. 2001)], and anti-cancer drugs [cisplatin (Tahara and Ishii 2001), paclitaxel (Lopez-Heredia, Kamphuis et al. 2011)]. The second group is represented by ions targeting bone remodeling processes (calcium, phosphate, strontium, silicate, zinc, and magnesium) and ions with antimicrobial activity (e.g., silver) to treat and prevent infections. The third group is represented by growth factors and other proteins. In the last years, recombination techniques have promoted the industrial production of human growth factors in large quantities and high purity. However, drug carriers have to be tailored for the controlled administration of these factors at adequate therapeutic levels, and thus their vectoring toward local tissue targets and cells. In fact, a one-time application of a supra-physiological concentration of a therapeutic protein alone does not induce tissue formation and regeneration, since it diffuses very rapidly from the implantation site and has a short half-life (Tayalia and Mooney 2009). Resorbable CPCs with a homogeneous distribution of a growth factor not only on their surface, but in the whole bulk of the cement, allow for a more prolonged release of the growth factor during degradation of the cement (Ginebra, Traykova et al. 2006) and are thus defined as “depot systems” (Verron, Khairoun et al. 2010). Using primary rat bone cells, Blom et

al. recently studied the effect of the incorporation of human recombinant TGF-β1 (rhTGF-β1) into a CPC composed of α-TCP, TTCP, and DCPD on the first stages of bone formation in vitro, and demonstrated that the addition of rhTGF-β1 stimulated the differentiation of pre-osteoblastic cells (Blom, Klein-Nulend et al. 2002). The stimulating effect of TGF on bone growth was later confirmed in preclinical animal studies (Blom, Klein-Nulend et al. 2001). Other proteins with a relevant function in bone tissue, such as collagen I and osteocalcin, have already been incorporated in CPCs with the aim of improving their biological and mechanical properties (Knepper-Nicolai, Reinstorf et al. 2002). Of great interest are also osteoinductive bone morphogenetic proteins (BMPs) from the transforming growth factor beta (TGF-beta) superfamily of genes, which can be delivered from the CPC to further enhance new bone formation (Verron, Khairoun et al. 2010).

1.4 Bone morphogenetic proteins (BMPs)

Bone morphogenetic proteins (BMPs), a unique group of glycoproteins, were first identified in the 1960s as mediators of the osteoinductive activity of demineralized bone for ectopic bone formation in adult animals (Urist 1965, Reddi and Huggins 1972). This is based on their capacity to induce the differentiation of multipotent mesenchymal stem cells into osteoblasts, thus leading to bone formation even outside bone tissue.

Currently, about 20 different BMPs have been identified and grouped into subfamilies according to their amino acid homology (Table 1.4). BMPs are synthesized as large inactive precursors containing an N-terminal signal peptide, followed by a prodomain controlling appropriate folding, and a C-terminal mature polypeptide (Xiao, Xiang et al. 2007). Once secreted, BMPs mainly act as homodimers (Bragdon, Moseychuk et al. 2011), and bind to two types of serine/threonine kinase receptors, namely typeI (BMPR-I) and type II receptors [BMPR-II; (Rosenzweig, Imamura et al. 1995)]. Once bound to a BMPR-I, the ligand/receptor complex recruits BMPR-II, which in turn phosphorylates the BMPR-I on its cytoplasmic domain containing a glycine/serine-rich domain [GS domain; (Miyazono, Kamiya et al. 2010)]. The BMP signal is then transduced to target genes through Smad-dependent (canonical) or Smad-independent pathways (Fig. 1.4A). BMPs are potent growth factors and have pivotal roles in osteogenic cell differentiation and the regulation of bone formation, maintenance, and repair (Scarfi 2016). The osteoinductive capacity of BMPs has been confirmed by both in vitro studies and clinical trials (Sierra-Garcia, Castro-Rios et al. 2016). Genetic engineering allows the production of large amounts of BMPs for clinical use, and clinical trials have shown the benefits of FDA-approved recombinant human BMP-2 and BMP-7 for the treatment of bone defects. Several synthetic and natural biomaterials have been tested as BMP carriers, ranging from hydroxyapatite and organic polymers to collagen (Carreira, Zambuzzi et al. 2015), metals, glass, and ceramics. Implantation of these protein-loaded carrier leads to cell adhesion and subsequent carrier degradation, which eventually releases the drug/protein at the specific site. However, several problems such as insufficient protein delivery or inactivation of the protein have been frequently reported (Agrawal and Sinha 2017). Depending on their inorganic,

organic, or synthetic composite nature, different carriers have different physiochemical and biological properties and thus show different efficacy in delivering bone morphogenetic proteins, with a profound influence on the clinical outcome.

Name/type of BMP	Characteristics of BMP
BMP-1	Not part of TGF-ß family; induction of cartilage formation
BMP-2	Osteoinductive, osteoblast differentiation and apoptosis
BMP-3 (osteogenin)	Most abundant BMP in bone, inhibits osteogenesis
BMP-4	Osteoinductive, lung and eye development
BMP-5	Chondrogenesis
BMP-6	Osteoblast differentiation, chondrogenesis
BMP-7 (osteogenic protein-1)	Osteoinductive, kidney and eye development
BMP-8 (osteogenic protein-2)	Osteoninductive
BMP-9 (growth differentiation factor-2)	Nervous system development, autocrine-paracrine role in the hepatic reticulo-endothelial system
BMP-10	Cardiac development
BMP-11 (growth differentiation factor-8)	Neuronal tissue formation
BMP-12 (growth differentiation factor-7)	Tendon-iliac tissue formation
BMP-13 (growth differentiation factor-6)	Tendon and ligament-like tissue formation
BMP-14 (growth differentiation factor-5)	Enhanced bone formation and tendon healing
BMP-15	Follicle-stimulating hormone activity
BMP-16	Skeletal repair and regeneration
BMP-17	Data not found
BMP-18	Data not found

Table 1.4: Characteristics of various BMPs. [modified from *Jain AP et al. Bone morphogenetic proteins: The anomalous molecules. J Indian Soc Periodontol 2013; 17:583-6*]

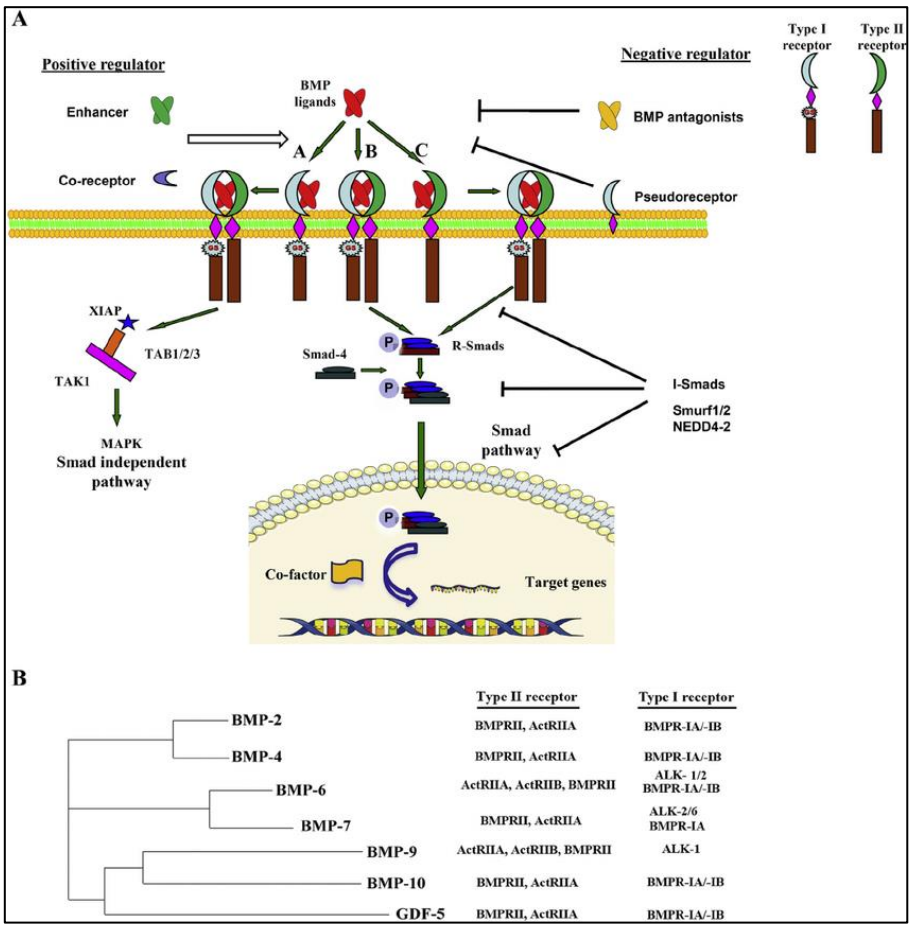

Figure 1.4: BMP signal transduction. (A) BMP signaling pathways. A) If BMP ligands first bind to the type I receptor and then recruit the type II receptor, which activates TAB1/2/3 through XIAP, the Smad-independent MAPK pathway is activated. B) Simultaneous binding of BMP ligands to type I and type II receptors leads to activation of the Smad-dependent pathway. The pathway-restricted Smads (R-Smads, Smads1, 2, 3, 5 or 8) are recruited and translocated into nuclei with the assistance of Smad-4 and regulate the transcription of target genes. C) If BMP ligands first bind to the type II receptor and then recruit the type I receptor, the Smad-dependent pathway is activated. Regulation of BMP signaling can occur extracellularly during the process of ligand binding to the receptors or intracellularly during the signal transduction by inhibitory Smads called I-Smads. (B) BMPs and their specific receptors. Key downstream signaling molecules of BMP/GDF are indicated through the use of a dendrogram tree. [*Lin Y, Jiang W. Bone morphogenetic proteins in tumour associated angiogenesis and implication in cancer therapies Cancer Lett 2016; 380(2):586-97*]

1.5 Animal models of osteoporosis

Various animal models of osteoporosis have been utilized for the preclinical testing of pharmaceutical agents and the evaluation of treatment options. The ideal animal model should mimic the anatomy, biomechanics, cell biology, and pathological changes seen in the human skeleton and at the same time should be reproducible, meet appropriate ethical standards, and be economical and efficient. Most basic investigations of osteoporosis have been conducted in rats (Li, Shen et al. 1997), but this model is of limited utility because it lacks true lamellar bone and does not show trabecular remodelling in the same way as human bone, especially in younger animals (Erben 1996). In addition, long-term bone loss following ovariectomy alone in the rat is not as dramatic as the bone loss in postmenopausal women (Thompson, Simmons et al. 1995) and cortical bone studies are limited due to the absence of Haversian systems. Most importantly, the rat is too small to permit major orthopaedic surgery.

Consequently, there is a need for large animal models in osteoporosis-related research to facilitate preclinical evaluation of pharmaceutical, surgical, and mechanical treatments. To meet this demand, several large animals species have been used, including dogs, cats, mini-pigs, sheep, and non-human primates (Newman, Turner et al. 1995). In particular the sheep may be a useful model for bone-related studies because: 1) the size and mechanical characteristics of the sheep skeleton are comparable to humans, which makes their large vertebral bodies well suitable for conventional surgical procedures (Wilke, Kettler et al. 1997, Turner 2002); 2) older sheep display Haversian bone remodelling (Turner 2002); 3) sheep display similar remodeling processes and biomechanical behaviour (Potes 2008); 4) sheep are genetically closer to humans than rodents and mice; 5) ewes ovulate spontaneously and have sex hormone profiles similar to women (O´Connell 1999); 6) sheep are relatively inexpensive to maintain, docile and easy to handle; 7) their use generally raises fewer ethical concerns than the use of domestic pets or non-human primates. The main challenge associated with the use of sheep for osteoporosis studies, however, is that they do not naturally attain the same degree of bone loss during their adult life (3 –10 years) as humans (Aerssens, Boonen et al. 1998), which have an almost 10-fold longer life span. In addition, ewes do not undergo menopause; therefore, ovariectomy combined with immobilization, low calcium diet, and weekly steroid injections (e.g., glucocorticoids) are successfully used to induce osteopenia and/or osteoporosis in these animals (Schorlemmer, Gohl et al. 2003). However, compared to existing sheep osteoporosis models with numerous design, logistic or ethical disadvantages, physiologically aged sheep (age 8 – 10 years) may be a suitable model of non-menopausal, senile osteopenia with moderately thinned bone structure, considerably diminished bone formation, and substantially augmented bone erosion (own unpublished work).

In the past years, sheep have been used as a model for “open surgery” techniques, but reproducible and safe models of minimally invasive, percutanoeus vertebroplasty in sheep have only been recently developed (Bungartz, Maenz et al. 2016, Oliveira, Potes et al. 2016). However, several

anatomic differences from human vertebrae have to be taken into consideration. Because of the orientation angle of the lumbar facet joints and pedicles, as well as the relatively short and sagittally oriented pedicles, a conventional transpedicular approach is associated with the risk of pedicle fracture and vertebral foramina disruption. In addition, the access angle is limited, resulting in smaller and isolated defects (Oliveira, Potes et al. 2016), and a higher risk of cement leakage into the vertebral foramen (Benneker and Hoppe 2013). To overcome these limitations, a parapedicular approach (Fig. 1.5) and proper sizing of the instruments are recommended (Carreira, Zambuzzi et al. 2015).

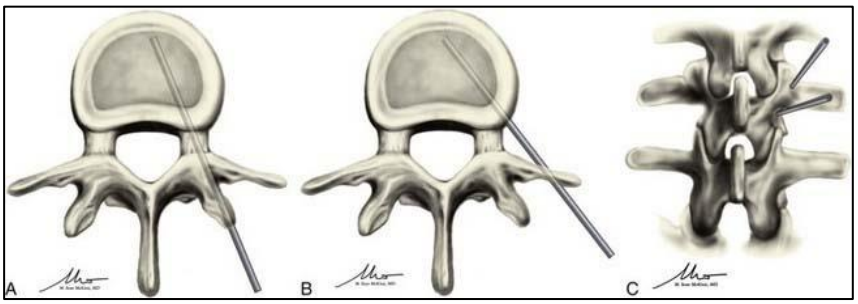

Figure 1.5: Surgical approaches to the vertebral body. A) Axial view of the needle trajectory for the transpedicular approach. B) Axial view of the ideal needle trajectory for the parapedicular approach. C) Posterior view of the spine showing both the transpedicular (superior) and parapedicular (inferior) points of entry. [*https://clinicalgate.com/osteoporotic-fractures*]

2. AIM OF THE WORK

Calcium phosphate cements (CPCs), first described in the 1980s, have been successfully used in the clinical field as bone filling material and represent a promising alternative to PMMA for the surgical treatment of osteoporotic vertebral compression fractures since they are biodegradable, have a Young modulus comparable with that of cancellous bone, and are regarded as osteoconductive by providing a scaffold for the formation of new bone. Own studies have recently demonstrated that the incorporation of PLGA fibers in a brushite-forming CPC on one hand results in an increase of diametral tensile strength, biaxial flexural strength, flexural strength, and work of fracture (Fig. A.2), and on the other hand enhances bone formation upon in vivo application. To further stimulate bone formation, the CPC can be used as a carrier system for osteoinductive growth factors such as bone morphogenetic proteins (BMPs). The main aim of the present work is the development of a BMP-containing CPC which shows high biocompatibility and osteoinductivity and is suitable for the stabilization of osteoporotic compression fractures.

The thesis is structured in three parts based on published or submitted papers:

1. **Gunnella F**, Kunisch E, Maenz S, Bossert J, Jandt KD, Plöger F, Kinne RW. In vitro release of bioactive bone morphogenetic proteins (GDF5, BB-1, and BMP-2) from a PLGA fiber-reinforced, brushite-forming calcium phosphate cement (submitted to *The Spine Journal* 03-2018; under peer-review process).
2. Bungartz M, Kunisch E, Horbert V, Xin L, **Gunnella F**, Mika J, Borowski J, Bischoff S, Schubert H, Sachse A, Illerhaus B, Günster J, Jandt KD, Kinne RW, Brinkmann O. First-time systematic postoperative clinical assessment of a minimally invasive approach for lumbar ventrolateral vertebroplasty in the large animal model sheep. *The Spine Journal* 2016;16(10):1263-1275.
3. **Gunnella F**, Kunisch E, Bungartz M, Maenz S, Horbert V, Xin L, Mika J, Borowski J, Bischoff S, Schubert H, Hortschansky P, Sachse A, Illerhaus B, Günster J, Bossert J, Jandt KD, Plöger F, Kinne RW, Brinkmann O. Low-dose BMP-2 is sufficient to enhance the bone formation induced by an injectable, PLGA fiber-reinforced, brushite-forming cement in a sheep defect model of lumbar osteopenia. *The Spine Journal* 2017;17(11):1699-1711.

3. In vitro release of bioactive bone morphogenetic proteins (GDF5, BB-1, and BMP-2) from a PLGA fiber-reinforced, brushite-forming calcium phopshate cement

Gunnella F, Kunisch E, Maenz S, Bossert J, Jandt KD, Plöger F, Kinne RW

Submitted to *The Spine Journal*
Ref.: Ms. No. SPINEE-D-18-00238

Preface

Particular properties of the CPC, such as biodegradability, fast setting ability and osteointegrative capacity, make them very attractive candidates as carriers for specific drug purposes. In the case of bone pathologies, proteins called BMPs, which are the most vital growth factors in bone formation and healing, can be incorporated in the CPC to further increase its osteoinductive capacity. This promising strategy leads to a sustained release and thus prolongs the half-life of growth factors. Several BMPs have been tested for their therapeutic efficacy in animal models of osteopenia. This has led to the approval of several clinical products containing rhBMP-2 or rhBMP-7 for either fracture treatment or spinal fusion in the 2000s, however with growing safety concerns. Recently, GDF-5 (also known as BMP-14) has shown positive effects in a sheep model of lumbar osteopenia by enhancing middle to long-term bone formation via changes in bone structure, formation, resorption, and compressive strength (Bungartz, Kunisch et al. 2017). A mutant GDF5 protein called BB-1, which carries two point mutations (methionine to valine at positions 453 and 456) in the BMPR-I binding site of GDF-5 and thus shows increased affinity to the BMPR-I (Kasten, Beyen et al. 2010), also significantly enhanced the bone formation induced by a PLGA-fiber reinforced CPC in sheep lumbar osteopenia for at least 3 months after a single therapeutic application (Gunnella, Kunisch et al. 2018). On the basis of the encouraging in vivo effects of GDF5, BB-1 and BMP-2, the present study aimed at analyzing the quantity and bioactivity of these BMPs released from a biodegradable, brushite-forming CPC in vitro.

Elsevier Editorial System(tm) for The Spine Journal

Manuscript Draft

Manuscript Number:

Title: In vitro release of bioactive bone morphogenetic proteins (GDF5, BB-1, and BMP-2) from a PLGA fiber-reinforced, brushite-forming calcium phosphate cement

Article Type: Basic Science

Section/Category: Basic Science/Physiology

Keywords: Brushite-forming calcium phosphate cement; fiber reinforcement; growth factor release; ALP activity; bone regeneration

Corresponding Author: Professor Raimund Wolfgang Kinne, MD

Corresponding Author's Institution: Experimental Rheumatology Unit, Department of Orthopedics, Jena University Hospital, Waldkrankenhaus "Rudolf Elle"

First Author: Francesca Gunnella, MSc

Order of Authors: Francesca Gunnella, MSc; Elke Kunisch, PhD; Stefan Maenz, PhD; Jörg Bossert; Klaus D Jandt, PhD; Frank Plöger, PhD; Raimund Wolfgang Kinne, MD

Abstract: Background context: Biodegradable calcium phosphate cement (CPC), mechanically stabilized by the addition of poly (l-lactide-co-glycolide) acid (PLGA) fibers, represents a promising option for the surgical treatment of osteoporotic vertebral fractures. The targeted delivery of bone morphogenetic proteins (BMPs) with the CPC further promotes bone regeneration in large animal models of lumbar osteopenia. However, little is currently known on the quantity and bioactivity of BMPs released from the CPC.
Purpose: The present study thus aimed at analyzing the quantity and bioactivity of BMPs released from a biodegradable, brushite-forming CPC.
Study Design/Setting: This is an in vitro release and bioactivity study of BMPs.
Methods: CPC discs or cuboids with/without PLGA fibers (5 and 10%) and containing different dosages of GDF5, BB-1, and BMP-2 (2, 10, 200, 400, and 1000 µg/ml of BMP) were ground and either extracted in phosphate-buffered saline (PBS) or in pure sheep serum/cell culture medium containing 10% fetal calf serum (FCS) for up to 31 days. The concentration of the released BMP was quantified by ELISA and the bioactivity of the extracts of BMP-free (control) or BMP-loaded CPC was determined by assessing the alkaline phosphatase (ALP) activity in several osteogenic cell lines after 3 days of exposure [C2C12, C2C12BR1b (with overexpressed BMP-receptor-1b), MCHT-1/26, and ATDC-5].
Results: Whereas there was practically no release of the BMPs in PBS, the cumulative release in medium+FCS or sheep serum within 30/31 days was 34, 24, 10, and 13%, respectively, of the applied dosages 2, 10, 200, and 1000 µg/ml for GDF5 and 6, 17, 7, and 8.5%, respectively, for BB-1 (BMP-2: 25.7% release of 400 µg/ml within 14 days). The addition of 5% and, in particular, 10% PLGA fibers augmented the BMP release within 14 days

(dosage 400 µg/ml; $p \leq 0.05$ for 10% versus 0% PLGA in the case of GDF5; $p \leq 0.05$ for 10% versus 0 and 5% PLGA in the case of BMP-2; maximal GDF5 and BMP-2 release of 22.6% and 43.7% respectively). Notably, the BMPs released from the CPC were bioactive, as demonstrated by an increased ALP activity in comparison to negative controls in one or several cell lines. In selected cases, this ALP activity was further augmented by the addition of 10% PLGA fibers.
Conclusions: Depending on the applied dosage and sample geometry, between 10 and 34% of GDF5 and between 6 and 17% of BB-1 were released in a bioactive form from the CPC within 30/31 days (BMP-2: 25.7% within 14 days), and this release was augmented by the presence of PLGA fibers. These data show that bioactive BMPs are released from CPC ± PLGA fibers and suggest their active contribution to the healing of bone defects after therapy with BMP-loaded CPC in large animal models.

In vitro release of bioactive bone morphogenetic proteins (GDF5, BB-1, and BMP-2) from a PLGA fiber-reinforced, brushite-forming calcium phosphate cement

Francesca Gunnella[a], Elke Kunisch[a], Stefan Maenz[b,c], Jörg Bossert[b], Klaus D. Jandt[b,c,d], Frank Plöger[e], Raimund W. Kinne[a*]

[a] Experimental Rheumatology Unit, Department of Orthopedics, Jena University Hospital, Waldkrankenhaus "Rudolf Elle," Eisenberg, Germany

[b] Chair of Materials Science, Otto Schott Institute of Materials Research, Friedrich Schiller University Jena, Germany

[c] Jena Center for Soft Matter (JCSM), Friedrich Schiller University Jena, Germany

[d] Jena School for Microbial Communication (JSMC), Friedrich Schiller University Jena, Germany

[e] BIOPHARM GmbH, Heidelberg, Germany

*Corresponding author: Raimund W. Kinne; Experimental Rheumatology Unit, Department of Orthopedics, Jena University Hospital, Waldkrankenhaus "Rudolf Elle", Klosterlausnitzer Str. 81, 07607 Eisenberg; Germany. E-Mail: raimund.w.kinne@med.uni-jena.de, phone: 0049 (0) 36691 81228, fax: 0049 (0) 36691 81226.

1. Introduction

Calcium phosphate cement (CPC), first described in the 1980s [1, 2], represents a promising alternative to polymethylmethacrylate for the surgical treatment of osteoporotic vertebral compression fractures, due to its biodegradability, fast setting ability and osteointegrative capacity [3]. Own studies have recently demonstrated that the inclusion of fibers in a brushite-forming CPC on one hand considerably improves its mechanical strength and fracture toughness [4], and on the other hand enhances bone formation upon in vivo application [5].

To further stimulate bone formation, the CPC can be used as a carrier system for osteoinductive growth factors such as bone morphogenetic proteins (BMPs; [6-9]). BMPs belong to the 33 member superfamily of Transforming Growth Factor-ß (TGF-ß) proteins [10]. Their activity was first described around 1970, when their capacity to induce ectopic bone formation in adult animals was discovered [11, 12]. After cloning and further characterization until the 1990s [13, 14], the central role of BMPs in bone and cartilage formation, as well as osteogenic cell differentiation has been well documented [15].

Several BMPs have been tested for their therapeutic efficacy in animal models of osteopenia. Local or systemic administration of BMP-2 was shown to improve bone structure or bone formation in mice [16], rats [17], goats [18], and sheep [19], and BMP-2 is regarded as a very promising molecule for lumbar spine fusion [20]. Also, systemic administration of rhBMP-6 increased bone volume and mechanical stability of bone in aged, ovariectomized rats [21], and local delivery of rhBMP-7 to vertebral bodies in osteopenic sheep improved bone mechanical strength and histomorphometric parameters [22]. This has led to the approval of several clinical products containing rhBMP-2 or rhBMP-7 for either fracture treatment or spinal fusion in the 2000s, however with growing safety concerns [23].

Recently, GDF-5 (also known as BMP-14) has shown positive effects in a sheep model of lumbar osteopenia by enhancing middle to long-term bone formation via changes in bone structure, formation, resorption, and compressive strength [7]. A mutant GDF5 protein called BB-1, which carries two point mutations (methionine to valine at positions 453 and 456) in the BMP type1 receptor (BMPR-I) binding site of GDF-5 (and thus shows increased affinity to the subunit BMP receptor type 1A (BMPR-IA) [24]), also significantly enhanced the bone formation induced by a poly (l-lactide-co-glycolide) acid (PLGA) fiber-reinforced CPC in sheep lumbar osteopenia for at least 3 months after a single therapeutic application [9]. However, despite encouraging in vivo effects of GDF5 and BB-1 [7, 9], little is known on the quantity and bioactivity of these BMPs released from CPC or other bone replacement materials.

Most of the published in vitro release studies were focused on the BMP-2 release from surface-coated CPC [25], modified CPC [18, 26] or other carrier such as chitosan scaffolds [27, 28] or collagen-based CP composites [29]. Only two studies have so far investigated the release of GDF5, however only

from collagen membranes [30] or hydrogels [31]), and not from CPC. Finally, to our knowledge there is no published study on the release of BB-1 from bone replacement materials.

On the basis of the encouraging effects of GDF5, BB-1, and BMP-2 in sheep lumbar osteopenia models [7-9], the present study thus aimed at analyzing the quantity and bioactivity of BMPs released from a biodegradable, brushite-forming CPC in vitro.

2. Materials and Methods

2.1 Fabrication of PLGA fibers and PLGA fiber-reinforced cement

PLGA fibers were prepared from the granulate material PURASORB PLG 1017 (Purac, Gorinchem, Netherlands) using a mini extrusion system (RANDCASTLE EXTRUSION SYSTEMS INC, Cedar Grove, USA; resulting diameter: 25 µm) and cut to 1 mm length using a cutting mill PULVERISETTE 19 (FRITSCH GmbH, Idar-Oberstein, Germany) [4]. The commercially available brushite-forming CPC JectOS+ (Conformité Européenne (CE)-certified; Kasios, L'Union, France) was used. JectOS+ consisted of β-tricalcium phosphate (β-TCP, 98.5% w/w) and 1.5% w/w tetrasodium pyrophosphate and was mixed according to the manufacturer's instructions.

CPC powders with different fiber content [5 or 10% (w/w)] were produced by mixing defined amounts of fibers und CPC powder in pure isopropanol with a high shear stirrer. Afterwards, the isopropanol was removed by evaporation. The powder-to-liquid ratio was 2.2 for all experiments.

2.2 Production of recombinant GDF5, BB-1, and BMP-2

The recombinant human (rh) growth factors GDF5, BB-1, and BMP-2 were produced in E. coli by the company BIOPHARM (GDF5, BB-1) and the Hans-Knöll-Institut in Jena (BMP-2) using patented procedures. The material was analyzed for endotoxin and total DNA content using established procedures (LAL test; [32]). The results revealed very low contamination for endotoxin (rhBMP-2: endotoxin < 0.11 IU/mg; rhGDF5: endotoxin < 0.17 IU/mg) and DNA content (rhBMP-2: DNA-content < 0.01 pg/µg), both well below the threshold values for therapeutic products (https://www.fda.gov/downloads/drugs/guidances/ucm310098). The GDF5 mutant BB-1 was produced via site-directed mutagenesis, as previously described [24].

2.3 BMP release from CPC loaded with low-dose GDF5 and BB-1

CPC was used to obtain cement discs with a radius and a height of 2.0 mm, and a corresponding volume of 25.12 µl (mm^3). To prepare the growth factor-loaded cement, 2 µg/ml and 10 µg/ml of the lyophilized growth factors GDF5 and BB-1 were dissolved in the liquid and then added to the cement powder. These dosages were chosen because they reflect the low-dose BMP groups in our published sheep in vivo experiments (1 and 5 µg in 500 µl each; [7-9]). The discs were initially pre-washed 6 times in DPBS to remove harmful components [33], and subsequently incubated at 37°C in 1 ml of either PBS or cell culture medium (alpha-MEM; Gibco™, Life Technologies, Darmstadt, Germany) containing 10% fetal calf serum (FCS; Gibco™, Life Technologies). The release of GDF5 and BB-1 from non-ground (control) or ground cement discs was measured at 1 hour, as well as 1, 2, 3, 6, 8, 10, 13, 15, 17, 20, 22, 28 and 30 or 31 days using an ELISA assay developed by the company Biopharm GmbH (Heidelberg, Germany), in which the specific anti-GDF5 and anti-BB-1 antibodies recognize only correctly folded, presumably bioactive proteins.

2.4 BMP release from CPC loaded with high-dose GDF5 and BB-1

Cement cuboids (length 10 mm, height and width 5.0 mm) and a corresponding volume of 250 µl (mm^3) were prepared from JectOS CPC. During the preparation of the cement cuboids, 200 µg/ml and 1000 µg/ml of the growth factors GDF5 and BB-1 were loaded in the CPC formulation. These dosages are representative of the high-dose BMP groups in our published sheep in vivo experiments (100 and 500 µg in 500 µl each; [7-9]). The samples underwent the same pre-washing procedure described above and were then incubated at 37°C in 2 ml of either PBS or sheep serum. The release of GDF5 and BB-1 from non-ground (control) or ground cement cuboids was measured at 1 hour, as well as 1, 2, 5, 7, 9, 12, 14, 16, 19, 22, 27, and 30 days using an ELISA (see above).

2.5 Release of GDF5, BB-1, and BMP-2 from PLGA fiber-reinforced CPC

The PLGA fiber-reinforced CPC (5 and 10% fibers; w/w) was used to obtain discs with a radius of 4 mm, a height of 0.5 mm, and a corresponding volume of 25.12 µl (mm^3), which were loaded with an intermediate high dose of 400 µg/ml GDF5, BB-1, and BMP-2.

Samples consisting of pure CPC (controls) or CPC ± PLGA fibers were also pre-washed as above and then incubated at 37°C in 1 ml of sheep serum. The release of GDF5, BB-1, and BMP-2 from non-ground (control) or ground cement discs was measured at 1 hour, as well as 1, 3, 7, and 14 days using a self-developed ELISA (see above) for GDF5 and BB-1, and a commercial ELISA for BMP-2 (Quantikine, R&D Systems, Minneapolis, MN, USA).

2.6 Alkaline phosphatase (ALP) activity of the C2C12, C2C12BRIb, MCHT -1/26, and ATDC-5 cell lines following exposure to the extracts of BMP-loaded, PLGA fiber-reinforced CPC

PLGA fiber-reinforced CPC discs (geometry as described in section 2.5) were loaded with 400 µg/ml GDF5, BB-1 or BMP-2 and ground. BMPs were extracted at 37°C in 1 ml of sheep serum for 3 days. Then 100 µl of the extracts were added to 200 µl of culture medium [DMEM + 10% FCS, Gold (Seraglob, Schaffhausen, Switzerland) + L-Glutamin for C2C12 and C2C12BRIb (with overexpressed BMP-receptor-1b); DMEM + 10% FCS, Gold for MCHT-1/26; DMEM/F12 10% FCS, Gold for ATDC-5]. The four cell lines were then cultured for 3 days in the modified media in 48-well plates at 37°C, 5% CO_2, and a density of 4.5 x 10^3 cells/well.

To investigate the osteogenic activity of the extracts, the cells were washed once with PBS and lysed [1% (v/v) Nonidet 40 (Sigma, Taufkirchen, Germany); 0.1 M glycine; 1 mM $MgCl_2$]. A substrate solution was prepared containing 4 ml of diethanolamine substrate buffer (5%; v/v), 0.148 g/10 ml p-nitrophenyl phosphate (pNPP; both Thermo Scientific, Rockford, USA), and 6 ml of destilled water. Seventy µl of the cell lysate and 70 µl of the substrate solution were applied to each well (96-well plate). The ALP activity in each sample was measured at different time points with an ELISA reader at

405 nm (Tecan, Switzerland, Männedorf). For each cell line, the control group was represented by cells cultured with the extracts of growth factor-free CPC.

2.7 Statistical analysis

The data were expressed as means ± SEM. Significance was tested using the non-parametric Kruskal-Wallis and Mann-Whitney U tests and the IBM SPSS Statistics 21 program. Differences were considered statistically significant for $p \leq 0.05$.

3 Results

3.1 *In vitro* release of GDF5 from the CPC

There was almost no GDF5 release from either the non-ground CPC (in PBS or medium with 10% FCS/sheep serum) or from the ground CPC in PBS for any of the analyzed GDF5 doses (below the detection limit; data not shown).

In the case of CPC discs loaded with the lowest dose **(2 µg/ml)** and incubated in cell culture medium with 10% FCS, the release of GDF5 from the **ground material** showed a typical kinetics, with a burst/peak release of 10.2 ng/ml GDF5 at the 3 day time point (Fig. 1A). Subsequently, the GDF5 release rapidly dropped and reached levels below 1.0 ng/ml at day 6 and below 0.25 ng/ml at day 8 and thereafter (Fig. 1A).

The cumulative release increased to 16.5 ng within 3 days and thereafter reached a plateau with a final value of 17.3 ng at day 30 (Fig. 1B).

Within the first 3 days, 31% of the initial dose of GDF5 was released (Fig. 1C), resulting in a retention of 69% (Fig. 1D). Thereafter, the cumulative release only marginally increased to 34% of the initial dose at day 30 (retention of 66%; Figs. 1C, D), which suggests a continuous, long-term release of the protein.

The **10 µg/ml** GDF5 dose showed a similar kinetics, with a burst/peak release of 16.5 ng/ml GDF5 at day 1 (Fig. 1A). Subsequently, the GDF5 release again rapidly dropped and reached levels below 3.0 ng/ml at day 10 and below 1.0 ng/ml at day 13 and thereafter (Fig. 1A).

For this dose, the cumulative release increased to 43.8 ng and 55.6 ng at days 3 and 10, respectively, and thereafter slightly increased to a final value of 61.4 ng at day 30 (Fig. 1B).

Within the first 3 days, 18% of the initial dose of GDF5 was released (Fig. 1C), resulting in a retention of 82% (Fig. 1D). Thereafter, the cumulative release increased to 20% at day 6 and to a final value of 25% of the initial dose at day 30 (retention of 75%; Figs. 1C, D).

The dose of **200 µg/ml** of GDF5 was released from the **ground material** in 2 ml of sheep serum with an early burst/peak release of 1,536 ng/ml (Fig. 2A), and a subsequent, rapid decrease to levels below 500 ng/ml at day 12 and below 100 ng/ml at the last time point of day 30 (Fig. 2A).

The cumulative release increased to 4,620 ng within 14 days and then reached a plateau with a final value of 5,324 ng at day 30 (Fig. 2B).

Within the first 2 days, only 6% of the initial dose of GDF5 was released (Fig. 2C), resulting in a retention of 94% (Fig. 2D). Thereafter, the cumulative release slightly increased to 9% at day 9 and 11% of the initial dose at day 30 (retention of 89%; Figs. 2C, D).

The highest dose of **1,000 µg/ml** also showed an early burst/peak release of 7,425 ng/ml GDF5 at day 1 (Fig. 2A). Subsequently, the release dropped reaching levels below 2,000 ng/ml at day 12 and below 1,000 ng/ml at day 27 and thereafter (Fig. 2A).

For this dose, the cumulative release increased to 15,476 ng within 2 days and then progressively increased to a final value of 32,194 ng at day 30 (Fig. 2B).

Within 2 days, 7% of the initial dose of GDF5 was released (Fig. 2C), resulting in a retention percentage very close to the one observed with the 200 µg/ml dose (93%; Fig. 2D). Thereafter, the cumulative release increased to 10% at day 9 and to a final value of 13% of the initial dose at day 30 (retention of 87%; Figs. 2C, D).

3.2 *In vitro* release of BB-1 from the CPC

As in the case of GDF5, there was almost no BB-1 release from either the non-ground CPC (in PBS or medium with 10% FCS/sheep serum) or from the ground CPC in PBS for any of the analyzed BB-1 doses (below the detection limit; data not shown).

The lowest BB-1 dose of **2 µg/ml** was released from the **ground** CPC discs with an early burst release of 0.85 ng/ml at the 1 day time point (Fig. 1E). Subsequently, the BB-1 release rapidly dropped and reached levels below 0.5 ng/ml at day 2 and below 0.1 ng/ml at day 13 and thereafter (Fig. 1E).

The cumulative release increased to 2 ng within 3 days and thereafter reached a plateau with a final value of 2.7 ng at day 31 (Fig. 1F).

Within the first 3 days, 5% of the initial dose of BB-1 was released (Fig. 1G), resulting in a retention of 95% (Fig. 1H). Thereafter, the cumulative release only marginally increased to 6% of the initial dose at day 13 and thereafter (retention of 94%; Figs. 1G, H).

Similarly, the release of the **10 µg/ml** BB-1 dose showed an early burst/peak release of 9.6 ng/ml at day 1 (Fig. 1E). Subsequently, the BB-1 release again rapidly dropped and reached levels below 5.0 ng/ml at day 6 and below 1.0 ng/ml at day 15 and thereafter (Fig. 1E).

For this dose, the cumulative release rapidly increased to 29.0 ng at day 3 and thereafter progressively increased to a final value of 41.7 ng at day 31 (Fig. 1F).

Within the first 3 days, 12% of the initial dose of BB-1 was released (Fig. 1G), resulting in a retention of 88% (Fig. 1H). Thereafter, the cumulative release increased to a final value of 17% of the initial dose at day 31 (retention of 83%; Fig. 1G, H).

The dose of **200 µg/ml** BB-1 was released from the ground CPC with an early burst release of 719 ng/ml BB-1 (Fig. 2E), and a subsequent, rapid decrease to levels below 200 ng/ml at day 12 and below 100 ng/ml at days 27 and 30 (Fig. 2E).

The cumulative release increased to 1,248 ng at day 1 and then continued to increase to 2,142 ng at day 7 and to a final value of 3,441 ng at day 30 (Fig. 2F).

Within the first 2 days, 4% of the initial dose of BB-1 was released (Fig. 2G), resulting in a retention of 96% (Fig. 2H). Thereafter, the cumulative release slowly increased to 6% at day 19, reaching a final value of 7% of the initial dose at day 30 (retention of 93%; Fig. 2G, H).

The highest dose of **1,000 µg/ml** also showed an early burst/peak release of 5,122 ng/ml, after which the release dropped to levels below 1,000 ng/ml at day 22 and below 500 ng/ml at the last time point of 30 days (Fig. 2E).

For this BB-1 dose, the cumulative release reached 9,370 ng at day 1, and then continued to increase to 12,651 ng at day 7 and to 21,271 ng at day 30 (Fig. 2F).

Within the first 2 days, 4% of the initial dose of BB-1 was released (Fig. 2G), resulting in a retention of 96% (Fig. 2H). Thereafter, the cumulative release constantly increased up to 7% at day 14 reaching a final value of 9% at day 30 (retention of 91%; Figs. 2G, H).

3.3 Influence of PLGA fibers on the *in vitro* release of BMPs from the CPC

3.3.1 GDF5

The GDF5 dose of **400 µg/ml** was released from the ground pure CPC with an early burst release of 968 ng/ml at 1 h (Fig. 3A; Table 1). Subsequently, the GDF5 release rapidly dropped and reached levels below 100 ng/ml at day 7 and of approx. 50 ng/ml at day 14 (Fig. 3A). This release was increased by the presence of 5% PLGA fibers and, in particular, 10% PLGA fibers (peak release of 1,157 and 1,293 ng/ml, respectively; Fig. 3A; Table 1).

The augmentation of the GDF5 release by the presence of PLGA fibers was also visible in the increased cumulative release ($p \leq 0.05$ for 10% PLGA versus 0% PLGA at all time points; pure CPC: max. 1,764 ng; 5% fibers: 1,854 ng; 10% fibers: 2,259 ng; Fig. 3B) and increased % release within 14 days ($p \leq 0.05$ for 10% PLGA versus 0% PLGA at all time points; pure CPC: max. 18%; 5% fibers: 19%; 10% fibers: 23%; Fig. 3C; for the respective retention values see Fig. 3D).

3.3.2 BB-1

BB-1 (**400 µg/ml**) was released from the ground pure CPC with an early peak release of 536 ng/ml at 1 h (Fig. 3E; Table 1). The BB-1 release then rapidly dropped and reached levels below 50 ng/ml already at day 7 (Fig. 3E). This release was only marginally influenced by the presence of 5% or 10% PLGA fibers (peak release of 531 and 622 ng/ml, respectively; Fig. 3E; Table 1).

The marginal influence of the fibers on the BB-1 release was confirmed by the cumulative release (pure CPC: max. 1,129 ng/ml; 5% fibers: 1,071 ng/ml; 10% fibers: 1,381 ng/ml; Fig. 3F) and the % release at 14 days (pure CPC: max. 11%; 5% fibers: 11%; 10% fibers: 13%; Fig. 3G; for the respective retention values see Fig. 3H).

At selected time points, the BB-1 release from pure CPC and/or CPC ± PLGA fibers was significantly lower than the GDF5 release (see Table 1 for the absolute and % release; for both parameters $p \leq 0.05$ for pure CPC at 1 h and on days 3, 7, and 14; $p \leq 0.05$ for 5% PLGA at 1 h; $p \leq 0.05$ for 10% PLGA at 1 h and on days 1 and 14).

3.3.3 BMP-2

BMP-2 (400 µg/ml) was released from the ground pure CPC with an early burst/peak release of 842 ng/ml on day 1 (Fig. 3I; Table 1), which then less rapidly dropped to levels of 135 ng/ml at day 14 (Fig. 3I). This release was markedly increased by the presence of 5% PLGA fibers and, in pa
10% PLA fibers (peak release of 1,115 and 1,980 ng/ml, respectively; $p \leq 0.05$ for 10% PLGA versus pure CPC on day 1; Fig. 3I; Table 1).

This marked augmentation of the BMP-2 release by the presence of PLGA fibers was also reflected in the boosted cumulative release (pure CPC: max. 2,571 ng/ml; 5% fibers: 3,392 ng/ml; 10% fibers:

4,372 ng/ml; $p \leq 0.05$ for 5% PLGA versus pure CPC on days 1, 3, 7, and 14; $p \leq 0.05$ for 10% PLGA versus 5% PLGA at 1 h, versus pure CPC and 5% PLGA on days 1, 3, 7, and 14; Fig. 3J) and the increased % release within 14 days (pure CPC: max. 26%; 5% fibers: 34%; 10% fibers: 44%; significant differences as shown above for the cumulative release; Fig. 3K; for the respective retention values see Fig. 3L).

Except for the early time point 1 h (BMP-2 release < GDF5 release), the BMP-2 release from pure CPC and CPC ± PLGA fibers was always significantly higher than the release of GDF5 and BB-1 throughout the whole period of 14 days (see Table 1).

3.4 Bioactivity of the BMPs released from the CPC

3.4.1 Fold-change effects of GDF5, BB-1, and BMP-2 extracts on the cell line C2C12

Whereas the 3 day extracts of GDF5 or BMP-2-loaded CPC ± PLGA fibers did not induce any ALP activity in C2C12 cells, the extracts of BB-1-loaded CPC induced a higher ALP signal than the extracts of BB-1-free CPC (1.8-fold induction versus CPC without growth factor at 30 min; 2.3-fold at 60 min), an effect that was further enhanced by the presence of 10% PLGA fibers (to 11.9-fold at 30 min; Fig. 4).

3.4.2 Fold-change effects of GDF5, BB-1, and BMP-2 extracts on the cell line C2C12BRIb

In contrast to the effects on the cell line C2C12, the extracts of GDF5, BB-1, or BMP-2-loaded CPC ± PLGA fibers all induced an ALP activity in BMPR1B receptor-transfected C2C12BRIb cells (5.2-fold, 4.4-fold, and 4.8-fold, for GDF5, BB-1, or BMP-2, respectively, at 60 min; Fig. 5). Whereas this effect was further enhanced by the presence of 10% PLGA fibers in the case of GDF5 and BB-1 extracts (to 10.3-fold and 18.3-fold, respectively at 30 min), there was no further enhancement in the case of BMP-2 extracts (Fig. 5).

3.4.3 Fold-change effects of GDF5, BB-1, and BMP-2 extracts on the cell line MCHT-1/26

Also in MCHT-1/26 cells, GDF5, BB-1, or BMP-2-loaded CPC ± PLGA fibers all induced an ALP activity (9.3-fold at 60 min for GDF5, 46.3-fold at 30 min for BB-1, and 1.2-fold at 60 min for BMP-2; Fig. 6). This effect was further enhanced by the presence of 10% PLGA fibers in the case of BMP-2 extracts (to 2.5-fold at 60 min; Fig. 6).

3.4.4 Fold-change effects of GDF5, BB-1, and BMP-2 extracts on the cell line ATDC5

In ATDC5 cells, finally, GDF5, BB-1, or BMP-2-loaded CPC ± PLGA fibers all induced an ALP activity (7.9-fold at 5 min for GDF5, 68-fold at 10 min for BB-1, and 1.4-fold at 5 min for BMP-2; Fig. 7). This effect was further enhanced by the presence of 10% PLGA fibers in the case of BMP-2 extracts (to 2.2-fold at 5 min; Fig. 7).

4 Discussion

The main goal of the study was to analyze the quantity and, in particular, the bioactivity of BMPs released from a biodegradable, brushite-forming CPC in vitro. The results were consistent in indicating the following aspects: i) the cumulative release in medium+FCS/sheep serum from the body of the CPC within 30/31 days reached a maximum of 34% of the applied dosage for GDF5 and 17% for BB-1 (BMP-2: maximal release of 25.7% within 14 days); ii) the addition of 5% and, in particular, 10% PLGA fibers significantly augmented the BMP release within 14 days (maximal release of BMP-2 43.7%); and iii) the BMPs released from the CPC within 3 days were bioactive, as demonstrated by an increased ALP activity in comparison to negative controls in one or several cell lines. In selected cases, the ALP activity was further augmented by the addition of 10% PLGA fibers.

Considerable amounts of the different BMPs were thus released in a bioactive configuration from the CPC, and this release was augmented by the presence of PLGA fibers. These data suggest an active contribution of bioactive BMPs to the healing of bone defects after therapy with BMP-loaded CPC in large animal models [7-9], and may qualify the CPC as a suitable drug delivery system for BMPs in bone pathology [6].

Despite considerable differences among the current and published studies concerning experimental design and CPC formulations, two studies [18, 26] have also applied modified CPC to measure the release of comparable dosages of BMP-2 (in the second study in comparison to TGF-β1, another member of the TGF-beta superfamily). Using a composite CPC system, in which 100 µg/ml BMP-2 was either added to the liquid component of the CPC or incorporated into gelatin microspheres, a release of 14.7% ± 1.9% of BMP-2 was observed within 28 days from the pure CPC, which was further enhanced to 37.8% ± 2.3%, if the BMP-2 was loaded into gelatin microspheres [18]. In the second study from the same group, in contrast, approx. 30% of the BMP-2 (dose: 0.35 µg/ml) was released within 42 days from pure CPC and less than 20% from CPC with BMP-2-loaded gelatin microspheres. Although these studies remain only partially comparable with the present study, a similar broad range of the percentages of BMP release was observed.

Kinetics of BMP release

The release of all three BMPs from the pure CPC and/or CPC ± PLGA fibers followed a typical kinetics, with a burst release usually at 1 day, which in some experiments was followed by a second release peak between day 6 and day 9 (especially for the higher doses of the BMPs). These release kinetics are very similar to a study in which BMP-2 was mixed with demineralized bone putty (DBM) and showed a burst release over the first 4 days [34]. In another study, however, such a burst release of BMP-2 was only observed when the BMP-2 was surface-adsorbed onto a preset CPC, but not when incorporated into the CPC by adding it to the liquid component of the CPC [26]. These differences are likely due to the features of the carrier material, i.e., DBM versus CPCs with different CaP-compositions [26, 34]. Similar to the release from the DBM, the release kinetics of the current CPC appear to consist of an early bulk release from a “loose” compartment within the first 2-3 days,

followed by slower, long-term release from a more tightly packed second compartment [6, 25, 34-36]; own unpublished data). For higher BMP doses (≥ 200 µg/ml), the cumulative release of the three different BMPs from the CPC reached levels > 500 ng already after 1 day, i.e., levels sufficient to stimulate osteoblastic differentiation and proliferation of mesenchymal stem cell lines in vitro [37], and thus potentially relevant for the induction of bone healing in vivo [7-9].

Differences among the three BMPs

The present study confirms that there are considerable differences concerning the release of different members of the TGF-beta superfamily or other growth factors, indicating that the features of each protein strongly influence its binding to the CPC and the subsequent release [18, 26, 30, 31, 35, 38].

In particular, BMP-2 shows a very high affinity for calcium phosphates, which appears to be driven by chemical interactions between the hydroxyl, amine, and carboxyl groups in BMP-2 and the divalent Ca^{+2} ions present in the carrier [6, 35, 39, 40]. Another important factor for the specific interactions between growth factor and carrier is the 3D arrangement of the BMP molecule, potentially also including the regions responsible for its binding to BMP-receptors [41-43]. In terms of a therapeutic application, therefore, the carrier, dose, and route of administration need to be carefully established for every BMP and validated in vitro or by in vivo pharmacokinetics studies [41].

On the other hand, the release of different BMPs depends on the particular properties of the carrier material, such as the individual composition and/or spatial organization of their CP components and their physicochemical features (e.g., surface coating with soluble, bioactive or nanocrystalline CPs; local pH; microporosity [25, 33, 38, 39]). The porosity of the JectOS+ cement used in the present study is 40%, with a major proportion of small pores (pore diameter approx. 1 µm) and a low proportion of large pores (diameter approx. 200 µm; Kasios, technical file), as also confirmed by micro-CT analysis (own unpublished data). While there are differential effects of the macropores and micropores on cell immigration and angiogenesis versus nutrient transport and bone integration [44], their influence on the differential release of the 3 BMPs is presently unclear.

There are only two studies directly addressing the release of GDF5 from bone replacement materials, in this case from collagen membranes [30] or from photo-cured hyaluronic acid hydrogels [31]. While in the first study the release of GDF5 was not quantified, the release of GDF5 from photo-cured hyaluronic acid hydrogels over a period of 28 days was always > 70% for doses between 10 and 1000 ng/ml. Due to the completely different character of the carrier material, however, these results are difficult to compare with the present GDF5 release data. Finally, to our knowledge there is no published study on the release of BB-1 from bone replacement materials.

Augmentation of the BMP release by the presence of PLGA fibers

The addition of 5% and, in particular, 10% PLGA fibers to the CPC significantly augmented the BMP release within 14 days, especially in the case of GDF5 (max. increase by 5%) and BMP-2 (max. increase by 18%; see Table 1). This indicates a strong and differential influence of the presence of PLGA fibers on the release of BMPs from the CPC. Potential reasons for these effects include a high

solubility of the PLGA fibers in physiological fluids and an increased affinity of the BMPs for the fibers [6, 28, 45, 46], although there are currently no data on the BMP release from CPC-PLGA fiber composites. The enhancement of the BMP release is thus another interesting feature of PLGA fibers, in addition to their known effects on the mechanical stability [4], degradability [47], and increased osteoconductivity of the CPC in a sheep lumbar vertebroplasty model [5].

Bioactivity of the released BMPs

Although the CPC used in the present study (brushite-forming JectOS+) reaches pH values below 2.0 for a few minutes during the curing process and then continues to harden at a pH of approx. 4.0 (Kasios, technical file), the BMPs released from the CPC remained at least partially osteogenic for four different marker cell lines. When comparing the amounts of BMP released within 3 days from the CPC (see Table 1) to the standard dilution curve of the BMPs in ALP bioactivity assays, maximal recovery rates of 31.8%, 36.0%, and 12.3% were estimated for bioactive GDF5, BB1, and BMP-2, respectively (data not shown). This suggests that a considerable proportion of the BMP released from the CPC is bioactive.

This is in agreement with the known stability of BMPs in mildly acidic buffers and calcifying matrix vesicles, in which there is abundant release of protons during hydroxyapatite formation [48-50]. Because of the low BMP-2 solubility at pH values above 6 [51, 52], these mildly acidic conditions (pH of 4.5) are also used for the formulation of marketed BMP-2 products like INFUSE®.

On the other hand, BMPs are unstable at highly acidic conditions [53] and there are even previous reports on a limited, time-dependent stability of BMPs released in cell culture medium or PBS from different CPs, solvent-dehydrated human bone or demineralized bone matrix [34, 35]. Thus the exact percentage of bioactive BMP released from the CPC still needs to be specifically addressed.

To our knowledge, so far only one other study [45] has shown that bioactive BMPs can be released from a CPC, further supporting the suitability of CPC as a drug delivery system.

The different BMPs analyzed in the present study showed a highly differential induction of ALP activity in individual marker cell lines, i.e., GDF5 and BMP-2 reacted with all cell lines except for C2C12, whereas the GDF5 mutant BB-1 reacted with all cell lines. In addition, further augmentation of the ALP activity of the different BMPs by the presence of 10% PLGA fibers was only detectable in selected cell lines. Possible explanations for these differences include differential type I BMPR expression (for example C2C12 and ATDC5 cells exclusively carry the BMPR-IA; [54-58]) with functional importance for their osteogenic differentiation [59-62], differential affinity of a given BMP for individual type I or type II BMPR [63], and differential functional sensitivity to PLGA itself or to PLGA breakdown products [62, 64]. The present findings underline that combinations of individual biomarker cell lines have to be selected for each given BMP and experimental question.

Long-term retention of a depot of therapeutically applied BMP

Despite quantitative differences among the different BMPs, the current CPC formulation, i.e., BMP incorporation into the body of the carrier, presumably leads to a homogeneous distribution throughout

the CPC [6], with limited immediate release of BMP from the superficial loose compartment and long-term retention of therapeutic BMP for at least 30 days [41, 47]. This may represent an advantage of the current CPC, since this in vivo "depot" guarantees sustained local release of BMP despite a one-time surgical application, with potential long-term beneficial effects on bone regeneration [7-9].

Limitations of the present study

One limitation regards the exact percentage of bioactive BMP released from the CPC, which currently can only be approximated by comparing the amounts of released BMP to the concentrations estimated from the ALP bioactivity assays. Although the current ELISA systems for GDF5 and BB-1 were already designed to only recognize correctly folded protein (data not shown), marker cells transfected with BMP-reactive reporter gene constructs or receptor-ligand ELISAs to assess the binding of correctly folded BMP to its receptor(s) may provide such information.

A second limitation regards the long-term release of (bioactive) BMPs from the CPC. Depending on the respective BMP and CPC formulation (± 5% or 10% PLGA fibers), between 56% and 94% of the BMP were retained as a drug "depot" in the CPC for time periods as long as 30 days. This is in clear contrast to the lower retention of GDF5 in photo-cured hyaluronic acid hydrogels (max. 27%; 28 days; [31]) or on BMP-coated hydroxyapatite particles (max. 24%; 14 days; unpublished data). Long-term experiments over several months will thus be required to address the final quantity and bioactivity of the BMPs releasable from the second, more tightly packed "depot" compartment of the CPC.

A third, general, limitation is the transferability of in vitro results to the in vivo situation. The BMP concentrations in the present release experiments were deliberately designed to reflect the low-dose and high-dose BMP groups in our published sheep in vivo studies [7-9]. However, such experiments can never reflect the full range of cellular, enzymatic, and physicochemical factors acting at the local tissue level, and therefore the results will have to be validated by in vivo pharmacokinetics studies.

Conclusion

The present study showed that: i) a considerable proportion of BMPs was released in medium+FCS/ sheep serum from the body of the CPC within 30/31 days; ii) addition of PLGA fibers significantly augmented the BMP release within 14 days; and iii) the BMPs released within 3 days demonstrated bioactivity, in selected cases again augmented by the addition of 10% PLGA fibers. Thus, PLGA fiber-reinforced CPC may qualify as a drug delivery system, with a potential contribution of bioactive BMPs to bone defect healing after application of BMP-loaded CPC in large animal models [7-9].

Figure legends

Fig. 1: *In vitro* release of 2 and 10 µg/ml GDF5 and BB-1 from CPC. Cement discs (r = 2.0 mm, h = 2.0 mm, V = 25.12 µl) were loaded with 2 or 10 µg/ml GDF5 and BB-1 and incubated at 37°C in 1 ml of either PBS or cell culture medium+10% FCS. After 1 hour, as well as 1, 2, 3, 6, 8, 10, 13, 15, 17, 20, 22, 28 and 31 days, the release of GDF5 (A) and BB-1 (E) from non-ground (control) or ground cement discs was measured by ELISA and used for the calculation of cumulative release (B and F), % release (C and G), and retention (D and H). Data are expressed as means ± SEM (n = 2).

Fig. 2: *In vitro* release of 200 and 1000 µg/ml GDF5 and BB-1 from CPC. Cement cuboids (l = 10 mm, h = 5.0 mm, w = 5.0 mm, V = 250 µl) were loaded with 200 or 1000 µg/ml GDF5 and BB-1 and incubated at 37°C in 1 ml of either PBS or cell culture medium+10% FCS. After 1 hour, as well as 1, 2, 5, 7, 9, 12, 14, 16, 19, 22, 27, 30 days, the release of GDF5 (A) and BB-1 (E) from non-ground (control) or ground cement discs was measured by ELISA and used for the calculation of cumulative release (B and F), % release (C and G), and retention (D and H; n = 1).

Fig. 3: Release of GDF5, BB-1, and BMP-2 from PLGA fiber-reinforced CPC. Discs consisting of PLGA fiber-reinforced CPC (r = 4.0 mm, h = 0.5 mm, V = 25.12 µl) were loaded with 400 µg/ml GDF5, BB-1, and BMP-2 and incubated at 37°C in 1 ml of sheep serum. After 1 hour, as well as 1, 3, 7, and 14 days, the release of GDF5 (A), BB-1 (E), and BMP-2 (I) from non-ground (control) or ground cement discs was measured by ELISA and used for the calculation of cumulative release (B, F and J), % release (C, G and K), and retention (D, H and L). Data are expressed as means ± SEM (n = 3). * $p \leq 0.05$ Mann-Whitney *U* test vs. pure CPC. + $p \leq 0.05$ Mann-Whitney *U* test vs. 5% fibers.

Fig. 4: Alkaline phosphatase (ALP) activity in C2C12 cells. C2C12 cells were cultivated for 3 days in diluted extracts of GDF5, BB-1, or BMP-2-containing pure CPC or PLGA fiber-reinforced CPC. Thereafter, the ALP activity was measured using an ALP assay and the data were expressed as fold-change induction compared to the CPC without growth factor; n.d. = not determined; a.u. = arbitrary units.

Fig. 5: Alkaline phosphatase (ALP) activity in C2C12BRIb cells. C2C12BRIb cells were cultivated for 3 days in diluted extracts of GDF5, BB-1, or BMP-2-containing pure CPC or PLGA fiber-reinforced CPC. Thereafter, the ALP activity was measured using an ALP assay and the data were expressed as fold-change induction compared to the CPC without growth factor; n.d. = not determined; a.u. = arbitrary units.

Fig. 6: Alkaline phosphatase (ALP) activity in MCHT-1/26 cells. MCHT-1/26 cells were cultivated for 3 days in diluted extracts of GDF5, BB-1, or BMP-2-containing pure CPC or PLGA fiber-reinforced CPC. Thereafter, the ALP activity was measured using an ALP assay and the data were expressed as fold-change induction compared to the CPC without growth factor; n.d. = not determined; a.u. = arbitrary units.

Fig. 7: Alkaline phosphatase (ALP) activity in ATDC5 cells. ATDC5 cells were cultivated for 3 days in diluted extracts of GDF5, BB-1, or BMP-2-containing pure CPC or PLGA fiber-reinforced CPC. Thereafter, the ALP activity was measured using an ALP assay and the data were expressed as fold-change induction compared to the CPC without growth factor; n.d. = not determined; a.u. = arbitrary units.

References

[1] LeGeros RZ, Chohayeb A, Shulman A. Apatite calcium phosphates: possible dental restorative materials. Journal of Dental research. 1982;61:343.

[2] Brown WE, Chow LC. A new calcium-phosphate setting cement. J Dent Res. 1983;62:672.

[3] Zhang J, Liu W, Schnitzler V, Tancret F, Bouler JM. Calcium phosphate cements for bone substitution: chemistry, handling and mechanical properties. Acta biomaterialia. 2014;10:1035-49.

[4] Maenz S, Kunisch E, Muhlstadt M, Bohm A, Kopsch V, Bossert J, et al. Enhanced mechanical properties of a novel, injectable, fiber-reinforced brushite cement. Journal of the mechanical behavior of biomedical materials. 2014;39:328-38.

[5] Maenz S, Brinkmann O, Kunisch E, Horbert V, Gunnella F, Bischoff S, et al. Enhanced bone formation in sheep vertebral bodies after minimally invasive treatment with a novel, PLGA fiber-reinforced brushite cement. The spine journal : official journal of the North American Spine Society. 2017;17:709-19.

[6] Begam H, Nandi SK, Kundu B, Chanda A. Strategies for delivering bone morphogenetic protein for bone healing. Materials science & engineering C, Materials for biological applications. 2017;70:856-69.

[7] Bungartz M, Kunisch E, Maenz S, Horbert V, Xin L, Gunnella F, et al. GDF5 significantly augments the bone formation induced by an injectable, PLGA fiber-reinforced, brushite-forming cement in a sheep defect model of lumbar osteopenia. The spine journal : official journal of the North American Spine Society. 2017;17:1685-98.

[8] Gunnella F, Kunisch E, Bungartz M, Maenz S, Horbert V, Xin L, et al. Low-dose BMP-2 is sufficient to enhance the bone formation induced by an injectable, PLGA fiber-reinforced, brushite-forming cement in a sheep defect model of lumbar osteopenia. The spine journal : official journal of the North American Spine Society. 2017;17:1699-711.

[9] Gunnella F, Kunisch E, Maenz S, Horbert V, Xin L, Mika J, et al. The GDF5 mutant BB-1 enhances the bone formation induced by an injectable, poly(l-lactide-co-glycolide) acid (PLGA) fiber-reinforced, brushite-forming cement in a sheep defect model of lumbar osteopenia. The spine journal : official journal of the North American Spine Society. 2018;18:357-369.

[10] Kwiatkowski W, Gray PC, Choe S. Engineering TGF-beta superfamily ligands for clinical applications. Trends in pharmacological sciences. 2014;35:648-57.

[11] Urist MR. Bone: formation by autoinduction. Science. 1965;150:893-9.

[12] Reddi AH, Huggins C. Biochemical sequences in the transformation of normal fibroblasts in adolescent rats. Proc Natl Acad Sci U S A. 1972;69:1601-5.

[13] Wozney JM, Rosen V, Celeste AJ, Mitsock LM, Whitters MJ, Kriz RW, et al. Novel regulators of bone formation: molecular clones and activities. Science. 1988;242:1528-34.

[14] Rosen V, Wozney JM, Wang EA, Cordes P, Celeste A, McQuaid D, et al. Purification and molecular cloning of a novel group of BMPs and localization of BMP mRNA in developing bone. Connect Tissue Res. 1989;20:313-9.

[15] Scarfi S. Use of bone morphogenetic proteins in mesenchymal stem cell stimulation of cartilage and bone repair. World journal of stem cells. 2016;8:1-12.

[16] Turgeman G, Zilberman Y, Zhou S, Kelly P, Moutsatsos IK, Kharode YP, et al. Systemically administered rhBMP-2 promotes MSC activity and reverses bone and cartilage loss in osteopenic mice. Journal of cellular biochemistry. 2002;86:461-74.

[17] Sarban S, Senkoylu A, Isikan UE, Korkusuz P, Korkusuz F. Can rhBMP-2 containing collagen sponges enhance bone repair in ovariectomized rats?: a preliminary study. Clinical orthopaedics and related research. 2009;467:3113-20.

[18] Li M, Liu X, Liu X, Ge B. Calcium phosphate cement with BMP-2-loaded gelatin microspheres enhances bone healing in osteoporosis: a pilot study. Clinical orthopaedics and related research. 2010;468:1978-85.

[19] Egermann M, Baltzer AW, Adamaszek S, Evans C, Robbins P, Schneider E, et al. Direct adenoviral transfer of bone morphogenetic protein-2 cDNA enhances fracture healing in osteoporotic sheep. Human gene therapy. 2006;17:507-17.

[20] Pobloth AM, Duda GN, Giesecke MT, Dienelt A, Schwabe P. High-dose recombinant human bone morphogenetic protein-2 impacts histological and biomechanical properties of a cervical spine fusion segment: results from a sheep model. Journal of tissue engineering and regenerative medicine. 2017;11:1514-23.

[21] Simic P, Culej JB, Orlic I, Grgurevic L, Draca N, Spaventi R, et al. Systemically administered bone morphogenetic protein-6 restores bone in aged ovariectomized rats by increasing bone formation and suppressing bone resorption. The Journal of biological chemistry. 2006;281:25509-21.

[22] Hustedt JW, Blizzard DJ. The controversy surrounding bone morphogenetic proteins in the spine: a review of current research. Yale J Biol Med. 2014;87:549-61.

[23] Carragee EJ, Hurwitz EL, Weiner BK. A critical review of recombinant human bone morphogenetic protein-2 trials in spinal surgery: emerging safety concerns and lessons learned. The spine journal : official journal of the North American Spine Society. 2011;11:471-91.

[24] Kasten P, Beyen I, Bormann D, Luginbuhl R, Ploger F, Richter W. The effect of two point mutations in GDF-5 on ectopic bone formation in a beta-tricalciumphosphate scaffold. Biomaterials. 2010;31:3878-84.
[25] Ruhe PQ, Boerman OC, Russel FG, Mikos AG, Spauwen PH, Jansen JA. In vivo release of rhBMP-2 loaded porous calcium phosphate cement pretreated with albumin. Journal of materials science Materials in medicine. 2006;17:919-27.
[26] Habraken WJ, Boerman OC, Wolke JG, Mikos AG, Jansen JA. In vitro growth factor release from injectable calcium phosphate cements containing gelatin microspheres. Journal of biomedical materials research Part A. 2009;91:614-22.
[27] Chen Y, Liu X, Liu R, Gong Y, Wang M, Huang Q, et al. Zero-order controlled release of BMP2-derived peptide P24 from the chitosan scaffold by chemical grafting modification technique for promotion of osteogenesis in vitro and enhancement of bone repair in vivo. Theranostics. 2017;7:1072-87.
[28] Kong X, Wang J, Cao L, Yu Y, Liu C. Enhanced osteogenesis of bone morphology protein-2 in 2-N,6-O-sulfated chitosan immobilized PLGA scaffolds. Colloids and surfaces B, Biointerfaces. 2014;122:359-67.
[29] Lee EU, Lim HC, Hong JY, Lee JS, Jung UW, Choi SH. Bone regenerative efficacy of biphasic calcium phosphate collagen composite as a carrier of rhBMP-2. Clinical oral implants research. 2016;27:e91-e9.
[30] Yamano S, Haku K, Yamanaka T, Dai J, Takayama T, Shohara R, et al. The effect of a bioactive collagen membrane releasing PDGF or GDF-5 on bone regeneration. Biomaterials. 2014;35:2446-53.
[31] Bae MS, Ohe JY, Lee JB, Heo DN, Byun W, Bae H, et al. Photo-cured hyaluronic acid-based hydrogels containing growth and differentiation factor 5 (GDF-5) for bone tissue regeneration. Bone. 2014;59:189-98.
[32] Tsuji K, Martin PA, Bussey DM. Automation of chromogenic substrate Limulus amebocyte lysate assay method for endotoxin by robotic system. Applied and environmental microbiology. 1984;48:550-5.
[33] Kunisch E, Maenz S, Knoblich M, Ploeger F, Jandt KD, Bossert J, et al. Short-time pre-washing of brushite-forming calcium phosphate cement improves its in vitro cytocompatibility. Tissue & cell. 2017;49:697-710.
[34] Huber E, Pobloth AM, Bormann N, Kolarczik N, Schmidt-Bleek K, Schell H, et al. (*) Demineralized Bone Matrix as a Carrier for Bone Morphogenetic Protein-2: Burst Release Combined with Long-Term Binding and Osteoinductive Activity Evaluated In Vitro and In Vivo. Tissue engineering Part A. 2017;23:1321-30.
[35] Ziegler JM-W, U.; Kessler, S.; Breitig, D.; Günther, K.-P. Adsorption and release properties of growth factors from biodegradable implants. Journal of Biomedical Materials Research. 2001;59:422-8.
[36] Pietrzak WS, Dow M, Gomez J, Soulvie M, Tsiagalis G. The in vitro elution of BMP-7 from demineralized bone matrix. Cell and tissue banking. 2012;13:653-61.
[37] Zhang X, Guo J, Zhou Y, Wu G. The roles of bone morphogenetic proteins and their signaling in the osteogenesis of adipose-derived stem cells. Tissue engineering Part B, Reviews. 2014;20:84-92.
[38] Ziegler J, Anger D, Krummenauer F, Breitig D, Fickert S, Guenther KP. Biological activity of recombinant human growth factors released from biocompatible bone implants. Journal of biomedical materials research Part A. 2008;86:89-97.
[39] Autefage H, Briand-Mesange F, Cazalbou S, Drouet C, Fourmy D, Goncalves S, et al. Adsorption and release of BMP-2 on nanocrystalline apatite-coated and uncoated hydroxyapatite/beta-tricalcium phosphate porous ceramics. Journal of biomedical materials research Part B, Applied biomaterials. 2009;91:706-15.
[40] Li RH, Bouxsein ML, Blake CA, D'Augusta D, Kim H, Li XJ, et al. rhBMP-2 injected in a calcium phosphate paste (alpha-BSM) accelerates healing in the rabbit ulnar osteotomy model. Journal of orthopaedic research : official publication of the Orthopaedic Research Society. 2003;21:997-1004.
[41] Vo TN, Kasper FK, Mikos AG. Strategies for controlled delivery of growth factors and cells for bone regeneration. Advanced drug delivery reviews. 2012;64:1292-309.
[42] Nickel J, Kotzsch A, Sebald W, Mueller TD. A single residue of GDF-5 defines binding specificity to BMP receptor IB. Journal of molecular biology. 2005;349:933-47.
[43] Kotzsch A, Nickel, J., Seher, A., Sebald, W. and Müller, D.T. Crystal structure analysis reveals a spring-loaded latch as molecular mechanism for GDF-5-type I receptor specificity. EMBO J. 2009;28:937-47.
[44] Kissling S, Seidenstuecker M, Pilz IH, Suedkamp NP, Mayr HO, Bernstein A. Sustained release of rhBMP-2 from microporous tricalciumphosphate using hydrogels as a carrier. BMC biotechnology. 2016;16:44.
[45] Zhang HX, Zhang XP, Xiao GY, Hou Y, Cheng L, Si M, et al. In vitro and in vivo evaluation of calcium phosphate composite scaffolds containing BMP-VEGF loaded PLGA microspheres for the treatment of avascular necrosis of the femoral head. Materials science & engineering C, Materials for biological applications. 2016;60:298-307.
[46] Azimi B, et al. Poly (lactide-co-glycolide) Fiber: An Overview. Journal of Engineered Fibers and Fabrics. 2014;9:47-66.
[47] Lo KW, Ulery BD, Ashe KM, Laurencin CT. Studies of bone morphogenetic protein-based surgical repair. Advanced drug delivery reviews. 2012;64:1277-91.
[48] Nahar NN, Missana LR, Garimella R, Tague SE, Anderson HC. Matrix vesicles are carriers of bone morphogenetic proteins (BMPs), vascular endothelial growth factor (VEGF), and noncollagenous matrix proteins. Journal of bone and mineral metabolism. 2008;26:514-9.

[49] Bonucci E. Calcification in Biological Systems. CRC Press, Inc., Boca Raton, Florida, USA; 1992, pp.77-79.
[50] Mundy GR, Martin T.J. Physiology and Pharmacology of Bone: Springer-Verlag Berlin Heidelberg, Germany; 1993, pp. 267-271.
[51] Vallejo LF, Rinas U. Optimized procedure for renaturation of recombinant human bone morphogenetic protein-2 at high protein concentration. Biotechnology and bioengineering. 2004;85:601-9.
[52] Ruppert R, Hoffmann E, Sebald W. Human bone morphogenetic protein 2 contains a heparin-binding site which modifies its biological activity. European journal of biochemistry. 1996;237:295-302.
[53] El Bialy I, Jiskoot W, Reza Nejadnik M. Formulation, Delivery and Stability of Bone Morphogenetic Proteins for Effective Bone Regeneration. Pharmaceutical research. 2017;34:1152-70.
[54] Namiki M, Akiyama S, Katagiri T, Suzuki A, Ueno N, Yamaji N, et al. A kinase domain-truncated type I receptor blocks bone morphogenetic protein-2-induced signal transduction in C2C12 myoblasts. The Journal of biological chemistry. 1997;272:22046-52.
[55] Ebisawa T, Tada K, Kitajima I, Tojo K, Sampath TK, Kawabata M, et al. Characterization of bone morphogenetic protein-6 signaling pathways in osteoblast differentiation. Journal of cell science. 1999;112 (Pt 20):3519-27.
[56] Akiyama H, Shukunami C, Nakamura T, Hiraki Y. Differential expressions of BMP family genes during chondrogenic differentiation of mouse ATDC5 cells. Cell structure and function. 2000;25:195-204.
[57] Seemann P, Schwappacher R, Kjaer KW, Krakow D, Lehmann K, Dawson K, et al. Activating and deactivating mutations in the receptor interaction site of GDF5 cause symphalangism or brachydactyly type A2. The Journal of clinical investigation. 2005;115:2373-81.
[58] Osyczka AM, Diefenderfer DL, Bhargave G, Leboy PS. Different effects of BMP-2 on marrow stromal cells from human and rat bone. Cells, tissues, organs. 2004;176:109-19.
[59] Gruber R, Graninger W, Bobacz K, Watzek G, Erlacher L. BMP-6-induced osteogenic differentiation of mesenchymal cell lines is not modulated by sex steroids and resveratrol. Cytokine. 2003;23:133-7.
[60] Katagiri T, Yamaguchi A, Komaki M, Abe E, Takahashi N, Ikeda T, et al. Bone morphogenetic protein-2 converts the differentiation pathway of C2C12 myoblasts into the osteoblast lineage. The Journal of cell biology. 1994;127:1755-66.
[61] Ploger F, Seemann P, Schmidt-von Kegler M, Lehmann K, Seidel J, Kjaer KW, et al. Brachydactyly type A2 associated with a defect in proGDF5 processing. Human molecular genetics. 2008;17:1222-33.
[62] Ruijtenberg S, van den Heuvel S. Coordinating cell proliferation and differentiation: Antagonism between cell cycle regulators and cell type-specific gene expression. Cell cycle (Georgetown, Tex). 2016;15:196-212.
[63] Nishitoh H, Ichijo H, Kimura M, Matsumoto T, Makishima F, Yamaguchi A, et al. Identification of type I and type II serine/threonine kinase receptors for growth/differentiation factor-5. The Journal of biological chemistry. 1996;271:21345-52.
[64] Sonomoto K, Yamaoka K, Kaneko H, Yamagata K, Sakata K, Zhang X, et al. Spontaneous Differentiation of Human Mesenchymal Stem Cells on Poly-Lactic-Co-Glycolic Acid Nano-Fiber Scaffold. PloS one. 2016;11:e0153231.

Table(s) in MS Word

Table 1: Differences among the release of the different BMPs from pure CPC and CPC ± PLGA fibers (GDF5, BB-1, BMP-2; n = 3 experiments each); # $p \leq 0.05$ vs. GDF5; § $p \leq 0.05$ vs. BB-1; note: differences among the different release time points are only shown in Fig. 3.

		GDF5					BB-1					BMP-2				
Time point (days)		**1 h**	**1**	**3**	**7**	**14**	**1 h**	**1**	**3**	**7**	**14**	**1 h**	**1**	**3**	**7**	**14**
Release (ng/ml)	Pure CPC	968.21	445.87	225.50	73.90	50.84	535.58#	383.70	135.57#	39.17#	35.67#	542.95#	841.53#§	724.80#§	326.84#§	135.20#§
	CPC + 5% fibers	1157.43	488.07	142.64	36.64	29.30	530.47#	369.27	112.37	32.16	26.89	478.83#	1115.30#§	979.73#§	590.00#§	228.97#§
	CPC + 10% fibers	1293.16	705.91	189.64	43.64	26.90	621.76#	464.14#	172.40	38.41	21.42#	626.51#	1979.53#§	1017.47#§	511.34#§	237.37#§

		GDF5					BB-1					BMP-2				
Time point (days)		**1 h**	**1**	**3**	**7**	**14**	**1 h**	**1**	**3**	**7**	**14**	**1 h**	**1**	**3**	**7**	**14**
Release (%)	Pure CPC	9.68	14.14	16.39	17.13	17.64	5.35#	9.19	10.54#	10.94#	11.29#	5.42#	13.84#§	21.09#§	24.36#§	25.71#§
	CPC + 5% fibers	11.57	16.45	17.88	18.24	18.54	5.30#	8.99	10.12	10.44	10.71	4.78#	15.94#§	25.73#§	31.63#§	33.92#§
	CPC + 10% fibers	12.93	19.99	21.88	22.32	22.59	6.21#	10.85#	12.58	12.96	13.18#	6.26#	26.06#§	36.23#§	41.34#§	43.72#§

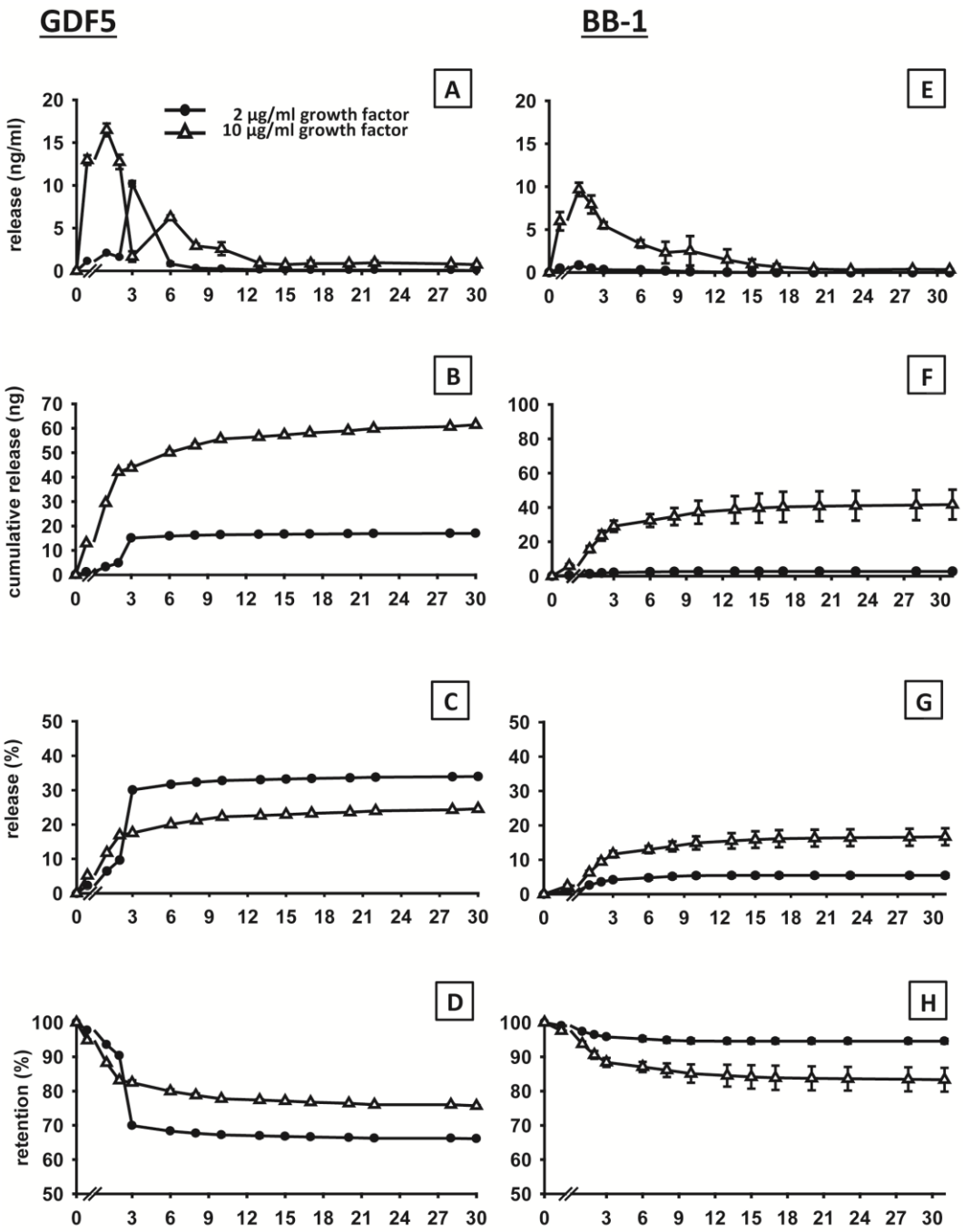
GDF5
BB-1
A
E
B
F
C
G
D
H
2 µg/ml growth factor
10 µg/ml growth factor
release (ng/ml)
cumulative release (ng)
release (%)
retention (%)
days

Fig. 1

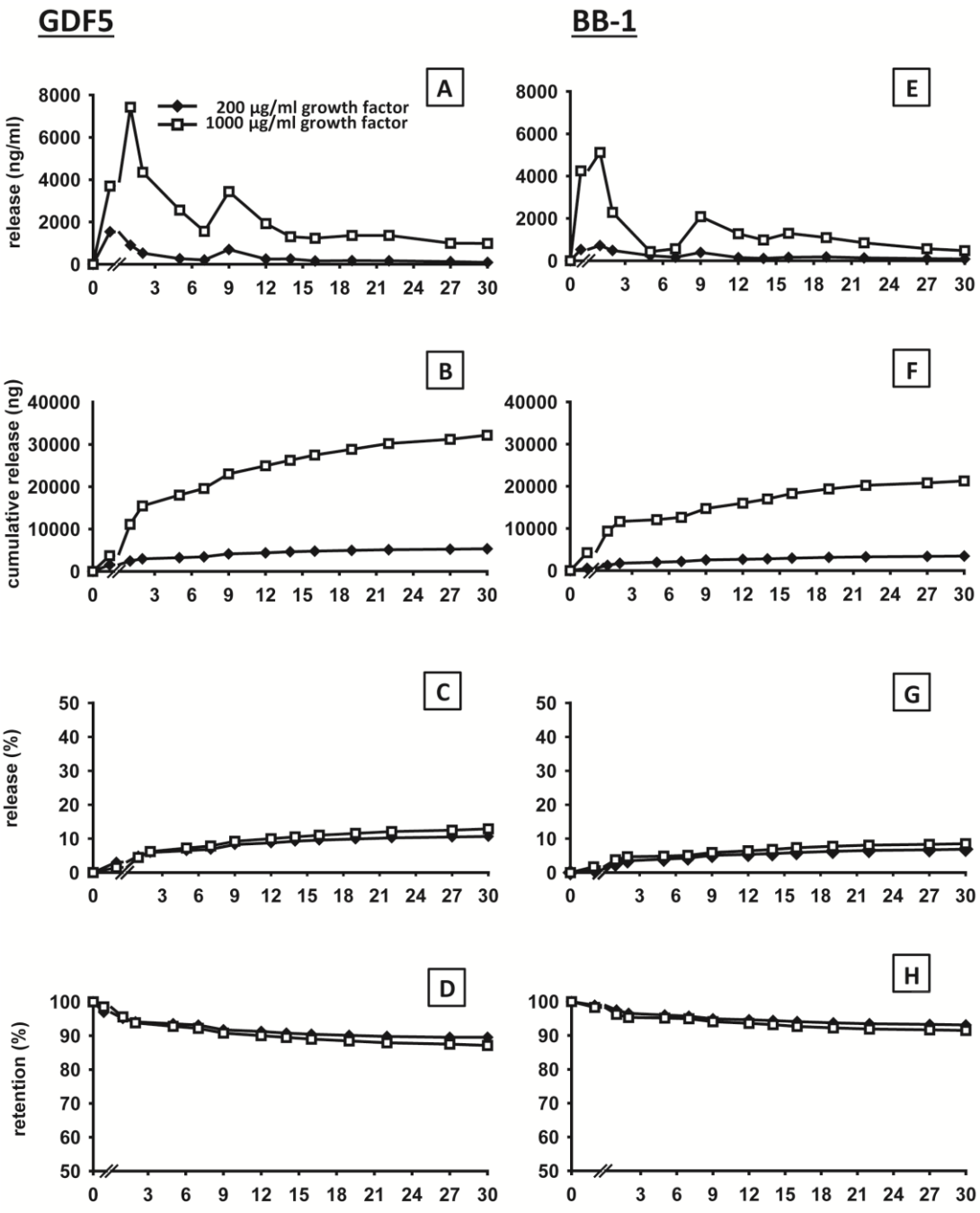
GDF5
BB-1
A
E
B
F
C
G
D
H
200 µg/ml growth factor
1000 µg/ml growth factor
release (ng/ml)
cumulative release (ng)
release (%)
retention (%)
days

Fig. 2

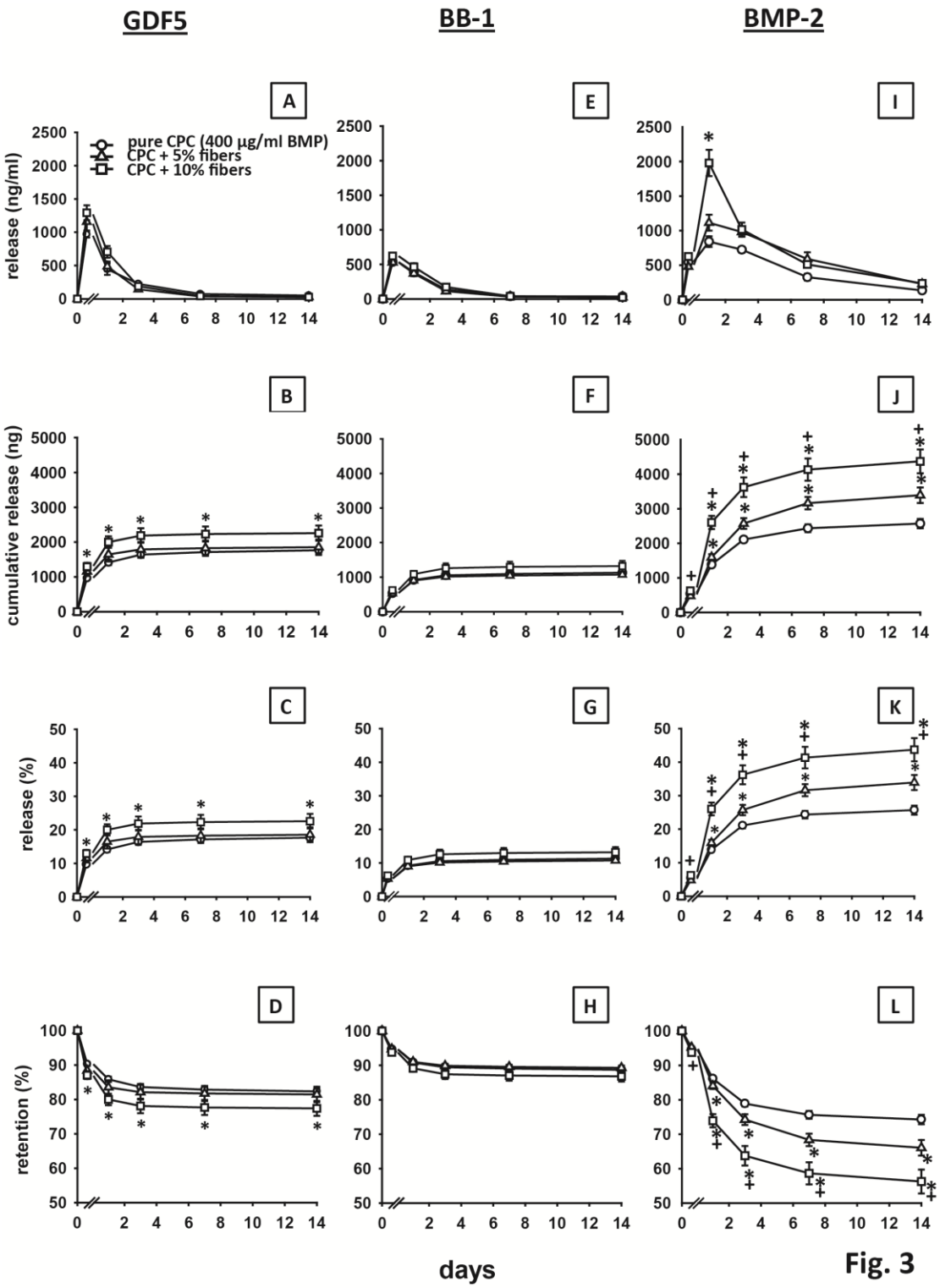
GDF5
BB-1
BMP-2
A
E
I
B
F
J
C
G
K
D
H
L
pure CPC (400 µg/ml BMP)
CPC + 5% fibers
CPC + 10% fibers
release (ng/ml)
cumulative release (ng)
release (%)
retention (%)
days

Fig. 3

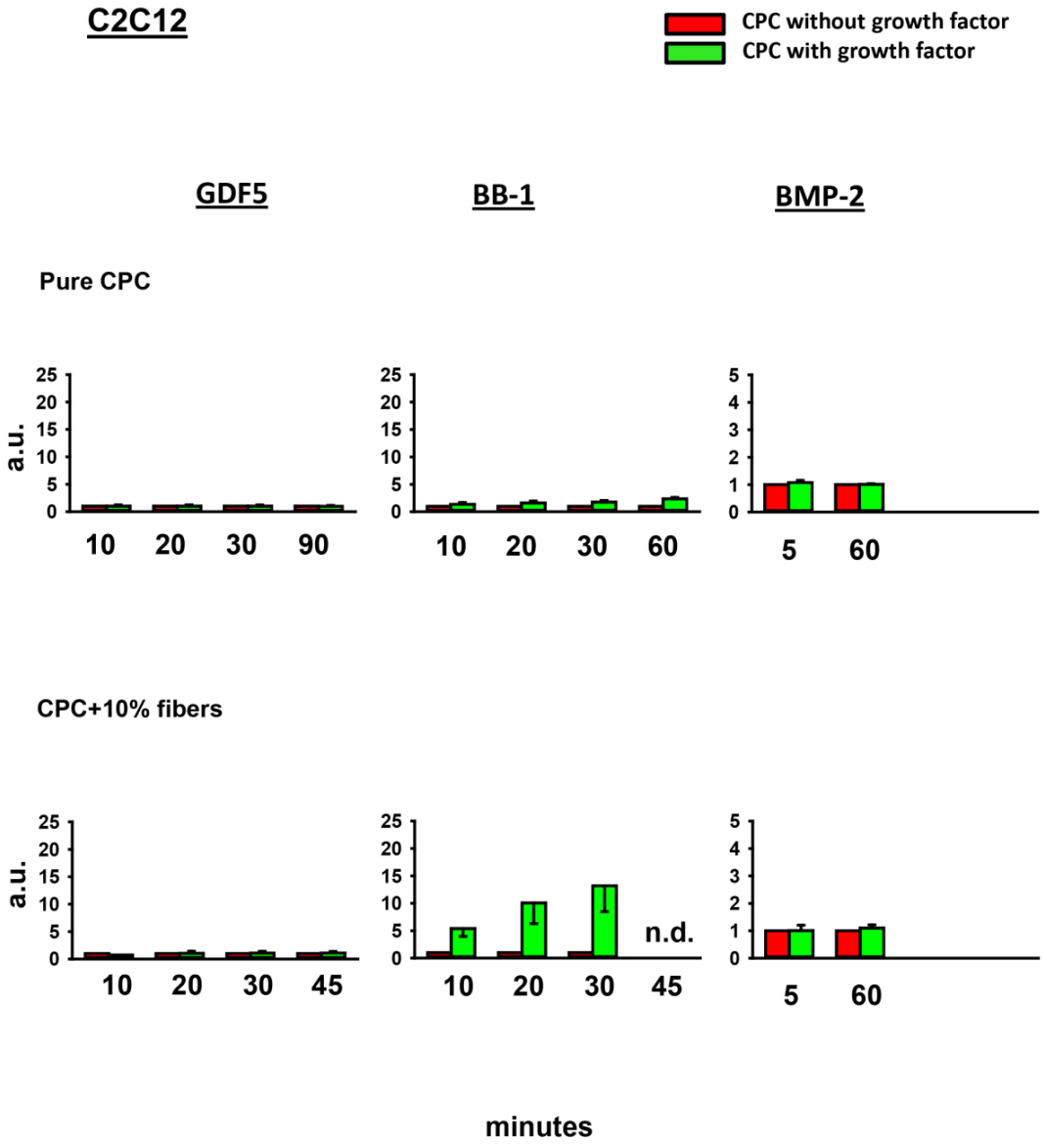
C2C12
CPC without growth factor
CPC with growth factor
GDF5
BB-1
BMP-2
Pure CPC
a.u.
25
20
15
10
5
0
10
20
30
90
60
5
4
3
2
1
CPC+10% fibers
45
n.d.
minutes

Fig. 4

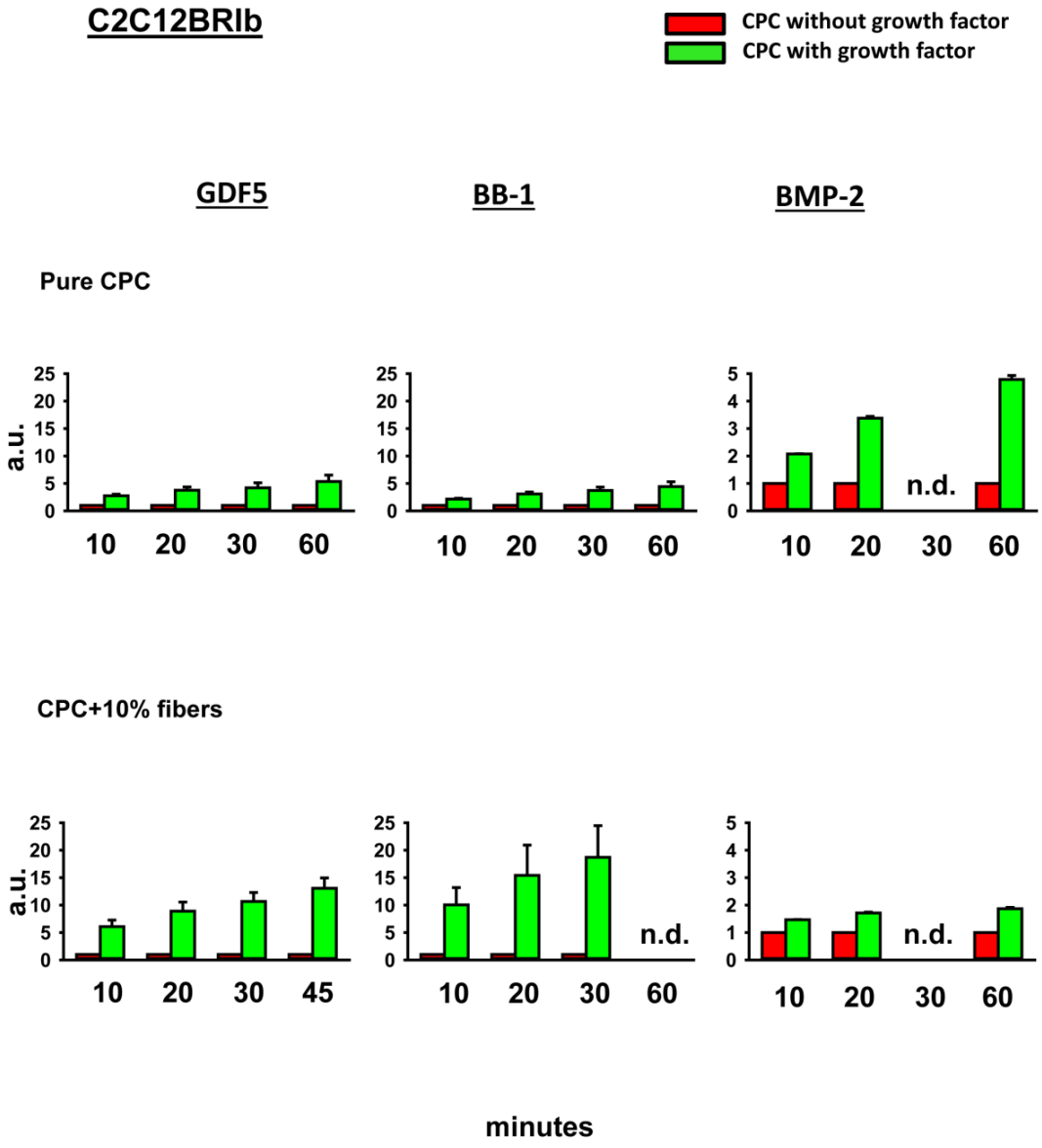
C2C12BRIb
CPC without growth factor
CPC with growth factor
GDF5
BB-1
BMP-2
Pure CPC
a.u.
n.d.
CPC+10% fibers
n.d.
n.d.
10 20 30 60
10 20 30 60
10 20 30 60
10 20 30 45
10 20 30 60
10 20 30 60
minutes

Fig. 5

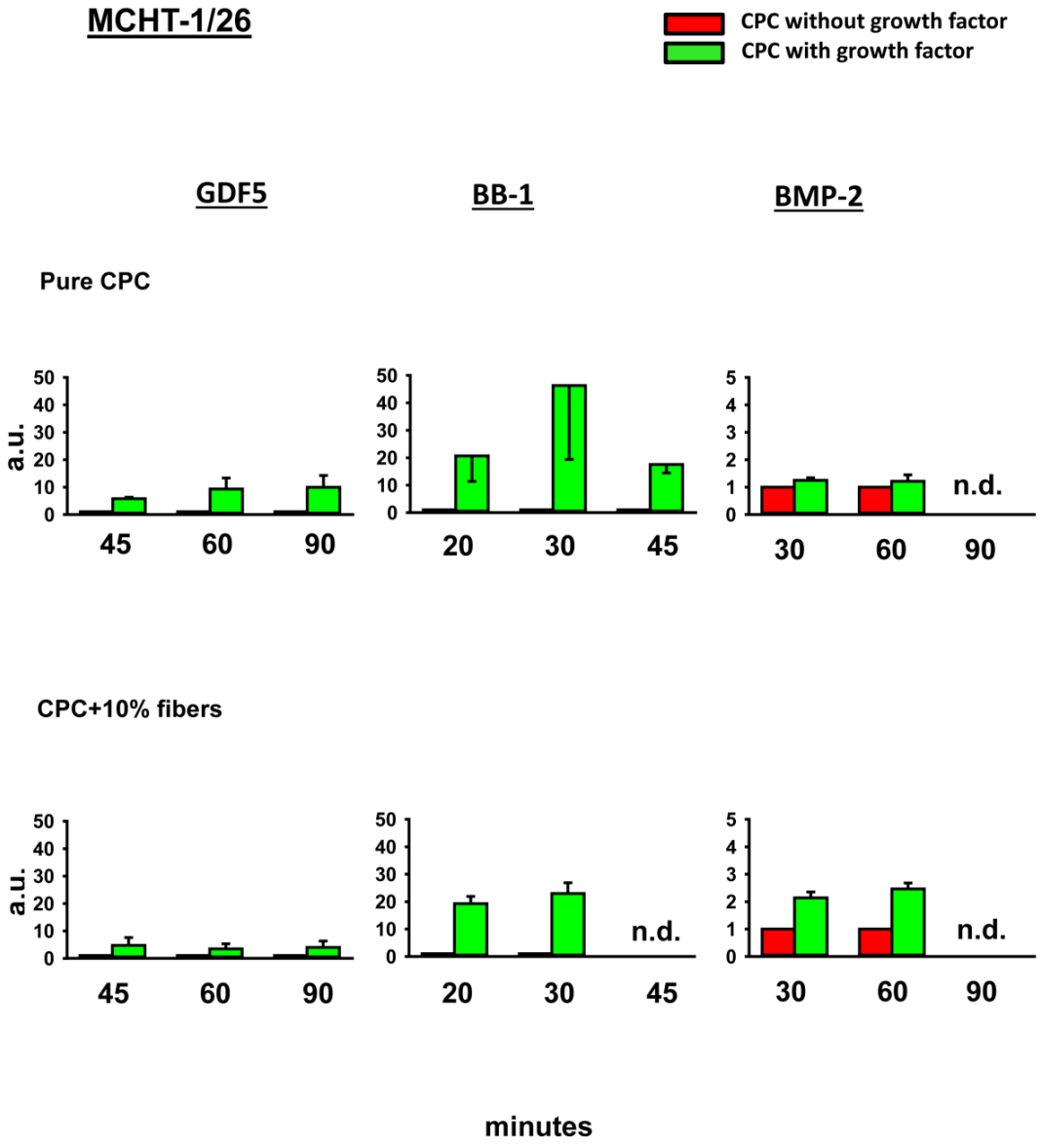
MCHT-1/26
CPC without growth factor
CPC with growth factor
GDF5
BB-1
BMP-2
Pure CPC
a.u.
50
40
30
20
10
0
45
60
90
20
30
45
5
4
3
2
1
n.d.
30
60
90
CPC+10% fibers
minutes

Fig. 6

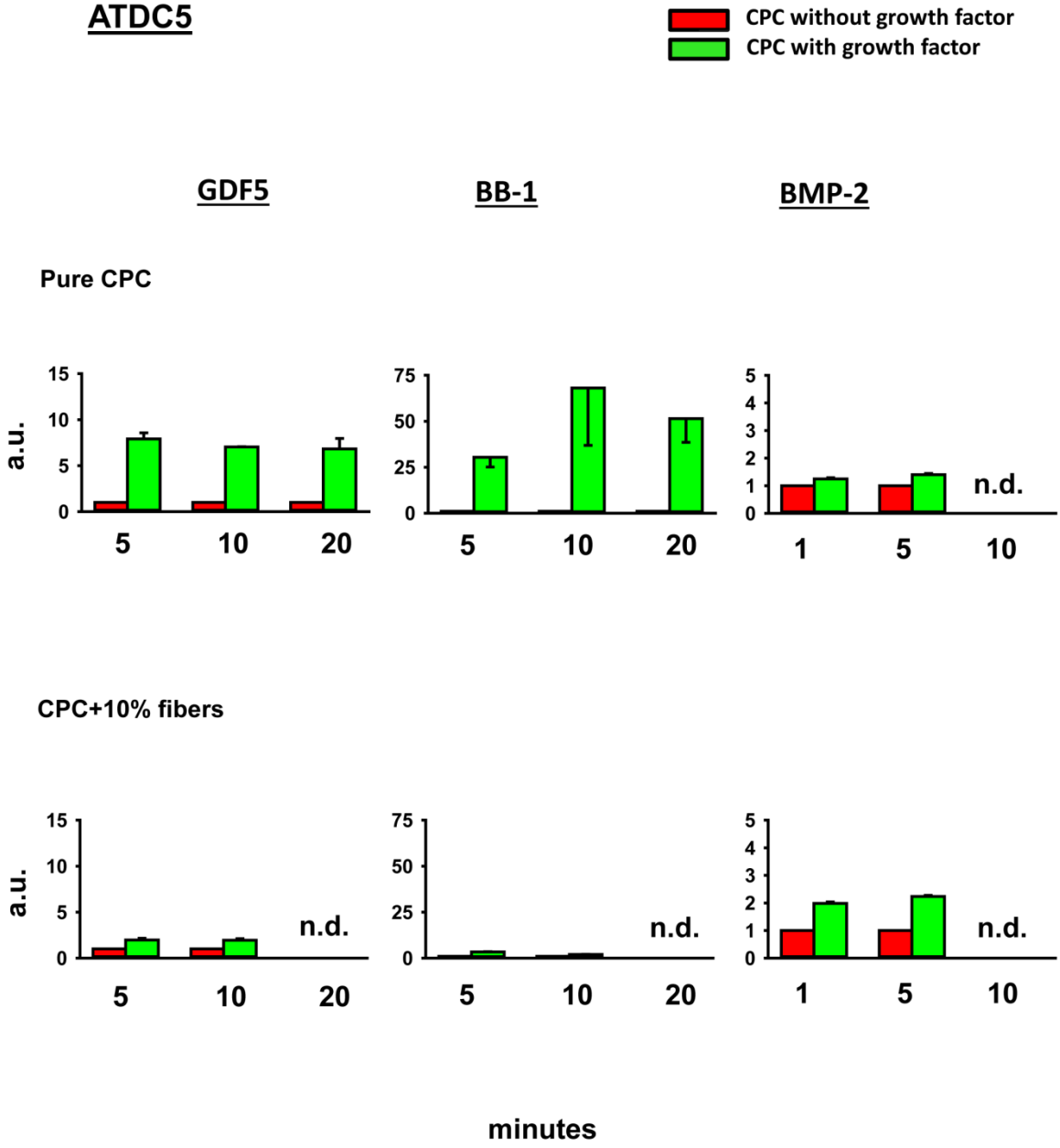
ATDC5
CPC without growth factor
CPC with growth factor
GDF5
BB-1
BMP-2
Pure CPC
a.u.
15
10
5
0
5
10
20
75
50
25
0
5
4
3
2
1
0
n.d.
1
CPC+10% fibers
minutes

Fig. 7

4. First-time systematic postoperative clinical assessment of a minimally invasive approach for lumbar ventrolateral vertebroplasty in the large animal model sheep

Bungartz M, Maenz S, Kunisch E, Horbert V, Xin L, **Gunnella F**, Mika J, Borowski J, Bischoff S, Schubert H, Sachse A, Illerhaus B, Günster J, Bossert J, Jandt KD, Kinne RW, Brinkmann O.

The Spine Journal 2016;16(10):1263-1275.
doi: 10.1016/j.spinee.2016.06.015. Epub 2016 Jun 23

Preface

As already discussed (Paragraph 1.5; pp. 23-24), large animal models are highly recommended for meaningful pre-clinical studies. In particular, in the case of experiments regarding the optimization of cement augmentation for vertebral body defects, the sheep spine may be a useful model due to its anatomic and biomechanical similarities with the human spine. To date, most of the studies in sheep were executed using "open surgery" and only a small number used minimally invasive techniques (Verron, Pissonnier et al. 2014). The aim of the study described in the current chapter was to develop a minimally invasive in vivo sheep model for lumbar ventrolateral vertebroplasty, including detailed analysis of intraoperative performance, trauma and functional impairment, reproducibility, resulting bone defects/cement filling, as well as defect healing and functional augmentation.

The Spine Journal 16 (2016) 1263–1275

THE SPINE JOURNAL

Basic Science

First-time systematic postoperative clinical assessment of a minimally invasive approach for lumbar ventrolateral vertebroplasty in the large animal model sheep

Matthias Bungartz[a,b,*], Stefan Maenz[c,d], Elke Kunisch[b], Victoria Horbert[b], Long Xin[b], Francesca Gunnella[b], Joerg Mika[b,1,2], Juliane Borowski[b], Sabine Bischoff[e], Harald Schubert[e], Andre Sachse[a], Bernhard Illerhaus[f], Jens Günster[f], Jörg Bossert[c], Klaus D. Jandt[c,d,g], Raimund W. Kinne[b], Olaf Brinkmann[a,b]

[a]*Chair of Orthopedics, Department of Orthopedics, Jena University Hospital, Waldkrankenhaus "Rudolf Elle," Klosterlausnitzer Str 81, D-07607 Eisenberg, Germany*

[b]*Experimental Rheumatology Unit, Department of Orthopedics, Jena University Hospital, Waldkrankenhaus "Rudolf Elle", Klosterlausnitzer Str 81, D-07607 Eisenberg, Germany*

[c]*Chair of Materials Science, Otto Schott Institute of Materials Research, Friedrich Schiller University Jena, Löbdergraben 32, D-07743 Jena, Germany*

[d]*Jena School for Microbial Communication (JSMC), Friedrich Schiller University Jena, Neugasse 23, D-07743 Jena, Germany*

[e]*Institute of Laboratory Animal Sciences and Welfare, Jena University Hospital, Dornburger Str. 23, D-07743 Jena, Germany*

[f]*BAM Bundesanstalt für Materialforschung und – prüfung (BAM), Unter den Eichen 87, D-12205 Berlin, Germany*

[g]*Jena Center for Soft Matter (JCSM), Friedrich Schiller University Jena, Humboldstr. 10, D-07743 Jena, Germany*

Received 28 January 2016; revised 20 May 2016; accepted 21 June 2016

Abstract

BACKGROUND CONTEXT: Large animal models are highly recommended for meaningful preclinical studies, including the optimization of cement augmentation for vertebral body defects by vertebroplasty/kyphoplasty.

PURPOSE: The aim of this study was to perform a systematic characterization of a strictly minimally invasive in vivo large animal model for lumbar ventrolateral vertebroplasty.

STUDY DESIGN/ SETTING: This is a prospective experimental animal study.

METHODS: Lumbar defects (diameter 5 mm; depth approximately 14 mm) were created by a ventrolateral percutaneous approach in aged, osteopenic, female sheep (40 Merino sheep; 6–9 years; 68–110 kg). L1 remained untouched, L2 was left with an empty defect, and L3 carried a defect injected with a brushite-forming calcium phosphate cement (CPC). Trauma/functional impairment, surgical techniques (including drill sleeve and working canula with stop), reproducibility, bone defects, cement filling, and functional cement augmentation were documented by intraoperative incision-to-suture time and X-ray, postoperative trauma/impairment scores, and ex vivo osteodensitometry, microcomputed tomography (CT), histology, static/fluorescence histomorphometry, and biomechanical testing.

FDA device/drug status: Not applicable.

Author disclosures: ***MB:*** Nothing to disclose. ***SM:*** Grant: Carl Zeiss Foundation (D, PhD scholarship), German Federal Ministry of Education and Research (F, Paid to the institution), pertaining to submitted manuscript; ***EK:*** Grant: German Federal Ministry of Education and Research (FKZ 03577D, 0316205B, and 13N12601; H, Paid to the institution), pertaining to submitted manuscript. ***VH:*** Grant: German Federal Ministry of Education and Research (H, Paid to the institution), pertaining to submitted manuscript. ***LX:*** Grant: German Federal Ministry of Education and Research (H, Paid to the institution), pertaining to submitted manuscript, Grant: Department of Health of Zhejiang Province, Hangzhou, China (D, Research scholarship). ***FG:*** Grant: German Federal Ministry of Education and Research (H, Paid to the institution), pertaining to submitted manuscript. ***JM:*** Nothing to disclose. ***JuB:*** Nothing to disclose. ***SB:*** Nothing to disclose. ***HS:*** Nothing to disclose. ***AS:*** Nothing to disclose. ***BI:*** Nothing to disclose. ***JG:*** Nothing to disclose. ***JöB:*** Grant: German Federal Ministry of Education and Research (FKZ 0316205C; F, Paid to the institution), pertaining to submitted manuscript. ***KDJ:*** Grant: German Federal Ministry of Education and Research (F, Paid to the institution), pertaining to submitted manuscript. ***RWK:*** Grant: German Federal Ministry of Education and Research (H, Paid to the institution), pertaining to submitted manuscript. ***OB:*** Nothing to disclose.

The disclosure key can be found on the Table of Contents and at www.TheSpineJournalOnline.com.

* Corresponding author. Chair of Orthopedics, Department of Orthopedics, Jena University Hospital, Waldkrankenhaus "Rudolf Elle", Klosterlausnitzer Str. 81, D-07607 Eisenberg, Germany. Tel.: +49 (0) 36691-81556; fax: +49 (0) 36691-81807.

E-mail address: m.bungartz@krankenhaus-eisenberg.de (M. Bungartz)

[1] Current address: Laboratory of Experimental Trauma Surgery, Justus-Liebig-University Giessen, 35394 Giessen, Germany.

[2] Current address: Department of Trauma, Hand and Reconstructive Surgery Giessen, University Hospital Giessen-Marburg, Campus Giessen, Rudolf-Buchheim-Str. 7, 35385 Giessen, Germany.

http://dx.doi.org/10.1016/j.spinee.2016.06.015

RESULTS: Minimally invasive vertebroplasty resulted in short operation times (28±2 minutes; mean±standard error of the mean) and X-ray exposure (1.59±0.12 minutes), very limited local trauma (score 0.00±0.00 at 24 hours), short postoperative recovery (2.95±0.29 hours), and rapid decrease of the postoperative impairment score to 0 (3.28±0.36 hours). Reproducible defect creation and cement filling were documented by intraoperative X-ray and ex vivo conventional/micro-CT. Vertebral cement augmentation and osteoconductivity of the CPC was verified by osteodensitometry (CPC>control), micro-CT (CPC>control and empty defect), histology/static histomorphometry (CPC>control and empty defect), fluorescence histomorphometry (CPC>control; all $p<.05$ for 3 and 9 months), and compressive strength measurements (CPC numerically higher than control; 102% for 3 months and 110% for 9 months).

CONCLUSIONS: This first-time systematic clinical assessment of a minimally invasive, ventrolateral, lumbar vertebroplasty model in aged, osteopenic sheep resulted in short operation times, rapid postoperative recovery, and high experimental reproducibility. This model represents an optimal basis for standardized evaluation of future studies on vertebral augmentation with resorbable and osteoconductive CPC.

Keywords: Calcium phosphate cement; Large animal model; Minimal-invasive; Sheep; Ventrolateral; Vertebroplasty; Void defect

Introduction

Despite successful results of the percutaneous, minimally invasive vertebro- and kyphoplasty with injectable cements for the treatment of osteoporotic vertebral body fractures, various problems concerning in particular the composition of the applied cement remain a matter of debate. For example, injectable poly(methyl methacrylate) (PMMA) cements, most frequently used in load-bearing areas such as the spine, lack bioactivity and biodegradability and, due to their supraphysiological strength and Young's modulus, may lead to critical loads and subsequent fractures in adjacent vertebral bodies [1–4]. In this context, calcium phosphate cements (CPCs) may be a promising alternative because they are biodegradable, have a Young's modulus comparable with that of cancellous bone, and are equally efficacious in generating pain relief upon therapy of osteoporotic vertebral fractures [5–11].

Large animal models are highly recommended for meaningful preclinical studies because they approach most closely the situation in humans; are suitable for more invasive testing than possible in humans [12,13]; and possibly show a better homogeneity than human specimens when selected for breed, gender, age, and weight [13–17]. In addition, Wilke et al [13] showed that, due to a similar structure of the thoracic and lumbar spine, the sheep spine may be a useful model for experiments regarding the optimization of cement augmentation for vertebral body defects.

However, there is currently only little information on minimally invasive large animal models for vertebroplasty/kyphoplasty with injectable CPCs. Published data differ from those of the present study concerning either the surgical approach (dorsolateral, medial, or ventrolateral), the duration of the postoperative study period, and/or the less detailed evaluation of reproducibility and postoperative trauma/recovery [18–20]. Therefore, the aim of the present study was to develop a minimally invasive in vivo large animal model for lumbar ventrolateral vertebroplasty, including detailed analysis of intraoperative performance, trauma and functional impairment, reproducibility, resulting bone defects/cement filling, as well as defect healing and functional augmentation.

Materials and methods

Animals

Aged, osteopenic, female sheep (40 Merino animals; 6–9 years old [7.56±0.12 years, mean±standard error of the mean]; 68–110 kg body weight [90.98±1.61 kg]) were used. Permission for the animal experiments was obtained from the governmental commission for animal protection, Free State of Thuringia, Germany (registration number: 02–036/11).

Anesthesia and surgical technique

First, the right lateral back of the animals was shaved under sedation (Ketamine hydrochloride, 2 mg/kg body weight, Zoetis Deutschland GmbH, Berlin, Germany; 0.1–0.3 mg/kg Midazolam-hydrochloride, Hameln Pharmaceuticals GmbH, Hameln, Germany; both intramuscular). Following intubation, an inhalation anesthesia was induced (isoflurane, 1.5–1.8 vol%, AbbVie, Ludwigshafen, Germany; Propofol 0.2 mg/kg/h iv, Fresenius Kabi Deutschland GmbH, Bad Homburg, Germany). Perioperative analgesia was induced by a one-time intravenous (iv) injection of 0.1 mg/kg Fentanyl before the operation (Rotexmedica, Trittau, Germany), as soon as a venous catheter was available. Volume substitution was performed by iv supply of 6% hydroxyethyl starch in isotonic saline (125 mL per operation, Fresenius Kabi Deutschland GmbH) and Ringer-lactate solution (10 mL/kg/h, Fresenius Kabi Deutschland GmbH).

The sheep was optimally positioned on its left side under X-ray control of the exact lateral and anterior-posterior plane using a mobile, radiological image converter (Ziehm Imaging GmbH, Nuremberg, Germany; Fig. 1A). The operation situs

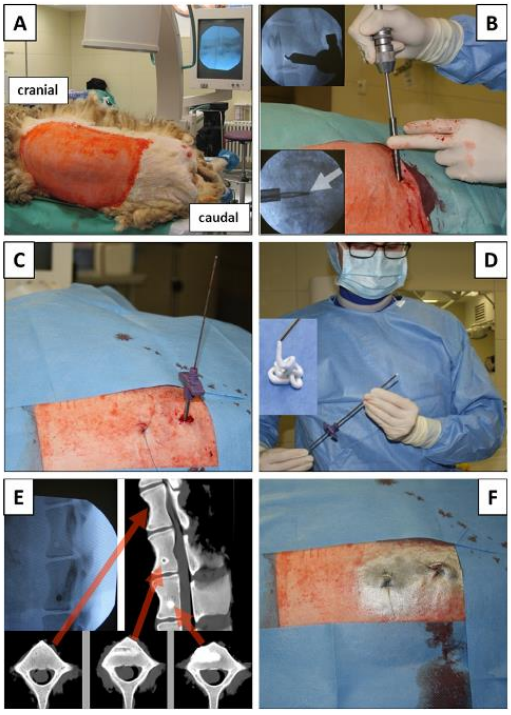

Fig. 1. Surgical technique. (A) Optimal positioning of the sheep on its left side under X-ray control of the exact lateral and anterior-posterior plane; (B) definition of the exact entrance point for the drill canal on the lower third of the vertebral body under X-ray and tactile control (upper insert) and advancement of the drill (5 mm diameter in a T-handle) in a drill sleeve toward the center of the vertebral body under continuous X-ray control in two planes (lateral/anterior-posterior; final depth of the drill channel up to the contralateral delimitation of the respective spinous process; lower insert); (C) placement of a 12.5-cm long working canula with a stop collar over the guide wire in the drill hole (following removal of the drill from the drill sleeve, insertion of a blunt guide wire through the drill sleeve into the defect, and removal of the drill sleeve; see also Fig. 2); (D) preparation and injection of the calcium phosphate cement (CPC) through a separate bone filler/pestle system under radiolucent control (after removal of the guide wire); (E) control of the CPC placement by intraoperative X-ray (upper left panel), as well as conventional computed tomography (CT) (upper right and three lower panels); (F) operation situs following exclusion of bleeding, closure of the incisions with skin sutures, and covering of the wound with aluminum dispersion.

was disinfected fourfold with disinfection solution (50% of 2-Propanol, 1% Povidone-Iodine in aqua destillata; Braun, Melsungen, Germany), and sterile surgical drapes were used to create an operating field of approximately 15×25 cm on the right lateral back. The lower third of the third lumbar vertebral body (L3) was identified by X-ray (lateral plane) for correct longitudinal placement of the first 1-cm stab incision on the right lateral side of the animal, followed by careful blunt dissection of the muscular layers toward the ventral facet of the processus transversus. Its ventral aspect was then used as a bony guide bar to approach the lateral wall of the vertebral body. An exact entrance point for the drill canal was defined on the lower third of the vertebral body under X-ray and tactile control, and the drill (5 mm diameter; Stryker, Freiburg, Germany) was fixed in a T-handle (Heraeus, Wehrheim, Germany) and advanced in a drill sleeve toward the center of the vertebral body under continuous X-ray control in two planes (lateral/anterior-posterior; Figs. 1B and 2A, B). The final depth of the drill channel was defined by the contralateral delimitation of the respective processus spinosus (Figs. 1B, lower insert, and 2B).

The drill was removed from the drill sleeve (Fig. 2C), a blunt guide wire was inserted through the drill sleeve into the defect (Fig. 2D), and the drill sleeve was removed. Subsequently, a 12.5-cm long working canula (Osteo Introducer, Medtronic, Meerbusch, Germany; gray; Fig. 2J) with a stop collar for reliable fixation was placed over the guide wire into the drill hole (Fig. 1C; Fig. 2E–H). After removal of the guide wire (Fig. 2F), the cement (FDA-approved, brushite-forming CPC JectOS+; kindly provided by Kasios, L'Union, France) was injected through a separate bone filler/pestle system (Medtronic) under radiolucent control (Figs. 1D, E and 2G–I). All respective system components were then removed, the situs checked to exclude bleeding and the skin incisions closed with skin sutures. In addition, the wound was then covered with aluminum dispersion (33 mg of aluminum/g spray; CP-Pharma, Burgdorf, Germany; Fig. 1F).

The same procedure, but without inserting a guide wire or working cannula, was repeated for the vertebral body L2 using a separate skin incision and access channel (Figs. 1C, E, F and 2A–C). This defect was left without cement and served as an empty defect control. L1 was left untouched and served as a normal control (Figs. 1C, E, F).

After the completion of surgery, animals were housed in separate pens for 1–2 weeks and then returned to long-care paddocks for 3 (short term) or 9 months (long term). Postoperative medication included antibiotic protection (Ampicillin-sodium, twice daily 10 mg/kg body weight for 4 days, Ratiopharm GmbH, Ulm, Germany; Enrofloxacin, once daily 2.5 mg/kg for 4 days, Bayer, Leverkusen, Germany), as well as antiphlogistic therapy (Metamizol-Sodium, twice daily 2 mg/kg for 4 days, Wirtschaftsgenossenschaft Deutscher Tierärzte—WdT, Garbsen, Germany; Carprofen, twice daily 2 mg/kg for 2.5 days, Pfizer Animal Health, Berlin, Germany).

To determine dynamic histomorphometric indices, sheep were given alternate intramuscular injections of oxytetracycline (20 mg/kg body weight and 10 mg of lidocaine) and alizarin red (12 mg/kg body weight; both Sigma, Deisenhofen, Germany) at equal 3 months distance. Short-term animals thus received a total of two injections (oxytetracycline 10 days postoperatively and alizarin red 10 days before sacrifice), long-term animals instead received a total of four injections (oxytetracycline 10 days and 6 months postoperatively, and alizarin red 3 months postoperatively and 10 days before sacrifice).

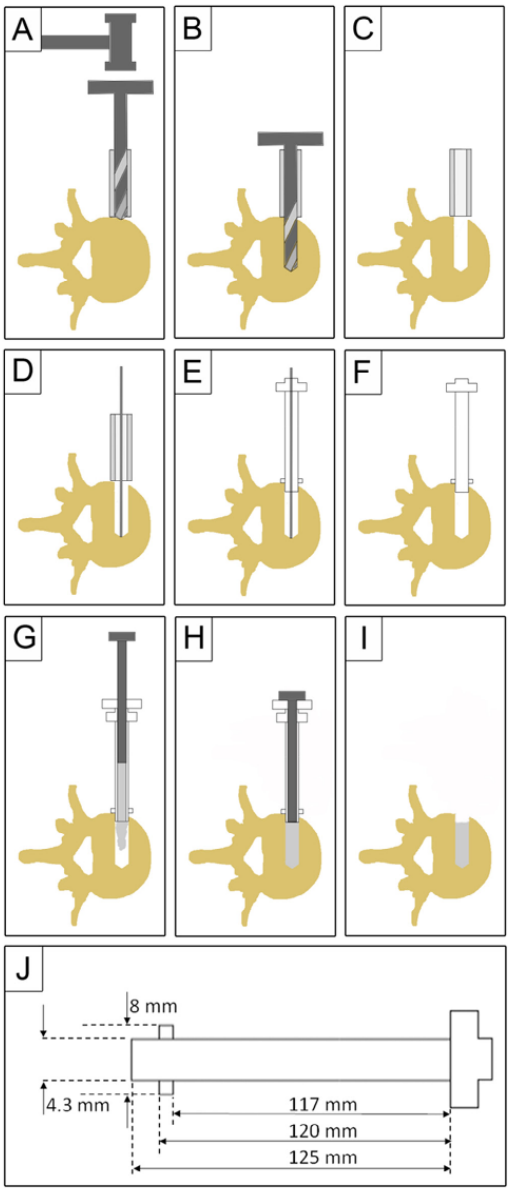

Fig. 2. Schematic depiction of the surgical technique. (A) Following positioning of the sheep under X-ray control, disinfection of the operation situs, and sterile surgical draping, the exact entrance point for the drill canal was identified on the lower third of the vertebral body by X-ray (lateral plane) and tactile control and accessed by careful blunt dissection of the muscular layers toward the processus transversus, using its ventral aspect as a bony guide bar to approach the lateral wall of the vertebral body; (B) advancement of the drill (5 mm diameter in a T-handle) in a drill sleeve toward the center of the vertebral body under continuous X-ray control in two planes (lateral/anterior-posterior; final depth of the drill channel up to the contralateral delimitation of the respective spinous process); (C) removal of the drill from the drill sleeve; (D) insertion of a blunt guide wire through the drill sleeve into the defect; (E) removal of the drill sleeve and placement of working canula with a stop collar over the guide wire into the drill hole; (F) removal of the guide wire; (G–I) injection of the calcium phosphate cement (CPC) through a separate bone filler/pestle system under radiolucent control; (J) dimensions of the custom-designed working canula with a stop collar (compare with E–H).

Assessment of operating time, X-ray exposure, and postoperative recovery

The operating time (incision-to-suture) and X-ray exposure duration were noted and averaged over all 40 animals. Postoperatively (24 hours), a wound score was determined, which consisted of five levels (0=no macroscopic signs of wound secretion, swelling, or infection; 1=macroscopic signs of wound secretion; 2=macroscopic signs of wound swelling; 3=macroscopic signs of wound secretion and swelling; 4=macroscopic signs of wound secretion, swelling, or infection). In addition, the times to complete stand without having to lie down again and until the animals reached an impairment score of 0 were registered. The impairment score also consisted of five levels with 0=animal stands and walks normally; 1=standing normal, mild lameness while walking; 2=standing normal, severe lameness while walking; 3=abnormal posture while standing, severe lameness while walking; and 4=no weight bearing/paralysis of lower limb(s).

Excision of the samples

The animals were sacrificed by iv injection of overdosed barbiturate (Pentobarbital, Essex Pharma GmbH, Munich, Germany) and subsequent application of magnesium sulfate ($MgSO_4$). The lumbar spine was removed using an oscillating bone saw, analyzed by computer tomography (CT; Bright Speed Performix 1.6 SI; General Electric Healthcare, Munich, Germany; spiral CT; standard spine program; raw data resolution 0.625 mm; final resolution 1 mm) and kept frozen until further use.

Digital osteodensitometric investigations

Osteodensitometry was conducted using a software-guided digital bone density measuring instrument (DEXA QDR 4,500 Elite; Hologic, Waltham, MA, USA [21,22];). To allow for an artifact-free osteodensitometry, the lumbar spine was sawn into individual vertebrae (L1=untouched normal control; L2=empty defect control; L3=CPC); the spinous and transverse processes, as well as the base and upper plates, were removed (final height in each case 15 mm) and the central, spongeous area of the vertebral bodies was imaged longitudinally. The high-density area of the injected cement was excluded from quantification, and a rectangular region of

interest in a transversal orientation with a defined size of 9×11 mm served as a measuring field.

High-resolution microcomputed tomography (μCT)

For the acquisition of three-dimensional (3D) images, an X-RAY WorX 225 kV tube μCT system with a minimal spot size below 5 μm and a flat panel detector (PerkinElmer 1,621; CsJ as scintillator; 2,048×2,048 pixel) were used. The following settings were used: 100 kV, 380 μA, and a prefilter of 0.5 mm copper. The distance between source and detector was 1,169.59 mm, and the distance between source and sample center was 389.37 mm. The shadow image had a size of 1,951×1,813 pixels, and 3,600 images were recorded for a full 360° turn (duration 6 seconds; average of 3×2 seconds). A total of eight frozen samples were analyzed under dry ice within 6 hours, resulting in a voxel size of 66.6 μm after reconstruction with the original Feldkamp code.

Quantitative analysis of the μCT data was carried out using the 3D software VGStudio MAX 2.2 (Volume Graphics GmbH, Heidelberg, Germany) and applying half-cylinders with a radius of 2.5, 3, 3.5, 4, 4.5, and 5 mm. The longitudinal axis and length of the half cylinders for each individual vertebral body were defined based on the respective parameters of the drill channel. The exact 3D position of the half cylinders (eg, rotation and depth) was chosen to exclude cortical bone. Bone volume (BV), cement volume (CV), the sum of the two values (BV+CV), and the total volume (TV) were separately determined in the drill channel (maximal radius of 2.5 mm) and the adjacent half-cylinder segments by global threshold determination (principle of onion shell). For this purpose, the respective maxima of the gray values for soft tissue, bone tissue, and cement were determined, and the mean values between the maxima were used as thresholds for the volume determination of the three individual components.

The depth of the drill channel, the width of the vertebral body, and the % cement filling of the drill channel at this transversal sectional plane were also determined in the μCT images.

Histological and static/dynamic histomorphometrical measurements

After cutting the lumbar vertebral bodies in two parts directly along the axis of the cement injection channel, the analyses were carried out using two different types of histological sections: (i) decalcified paraffin sections stained by hematoxylin-eosin [23,24]; or (ii) plastic-embedded sections obtained by fixation in acetone and dehydration in ascending alcohol series without demineralization. Static/dynamic histomorphometry of the lumbar vertebral bodies (L1–L3) was performed as previously published [25–30]. For this purpose, the samples were embedded in Technovit 9,100 according to the instructions of the supplier (Heraeus Kulzer, Wehrheim, Germany [31]). Sections were then cut to a thickness of approximately 7 μm. For static histomorphometry, the sections were stained with trichrome stain according to Masson-Goldner [23]; for dynamic histomorphometry, the sections were left unstained.

For static histomorphometry, the respective parameters were determined according to published procedures [25–30]. For dynamic histomorphometry, bone induction was assessed in 10 fields of each individual vertebral body by determining the histomorphometric parameters in the vicinity of the injection channel using a standard microscope (Axiovert 200 M, Carl Zeiss, Microimaging GmbH, Oberkochem, Germany), 100-fold magnification, and the corresponding software (Axioversion 3.1, Carl Zeiss). Total bone surface, labeled surface (single and double fluorescence lines), and interlabel distance were quantified using the ImageJ program

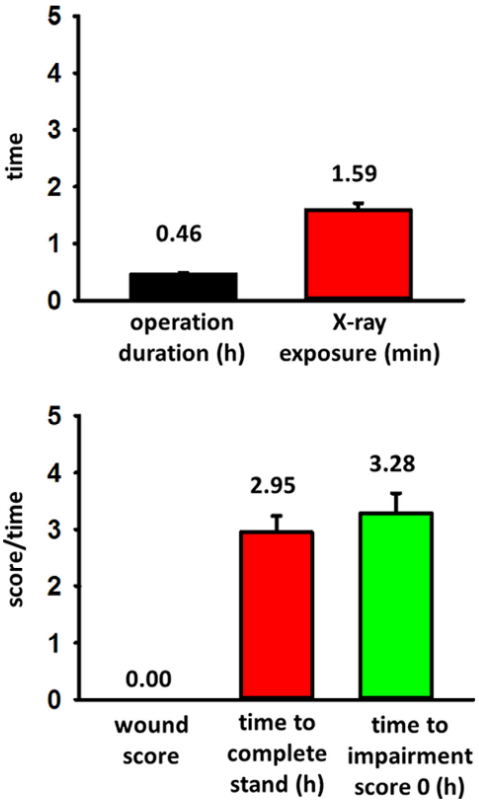

Fig. 3. Assessment of operating time, X-ray exposure, and postoperative recovery. Assessment of operation duration and X-ray exposure (Top), as well as postoperative wound score, time to complete stand without having to lie down again, and time to impairment score of 0 (Bottom); data represent means±standard error of the mean from n=9–40 animals.

(imagej.nih.gov). These parameters were then used to calculate the mineralizing surface per bone surface, mineral apposition rate, and bone formation rate surface based [29].

Biomechanical testing (compressive strength)

Biomechanical compressive strength measurements were conducted using a universal material testing machine (FPG 7/20-010, Kögel, Leipzig, Germany) and the corresponding software (FRK Quicktest 2,004.01, Kögel, Leipzig, Germany). For biomechanical testing, frozen cancellous bone cylinders (10 mm diameter×15 mm height) were obtained from the central part of the vertebral bodies (L1–L3; n=20 animals each from the short-term and long-term groups) using a surgical diamond hollow milling cutter (Ø 10 mm). After a defined thawing time of exactly 30 minutes, samples were semiconfined in two semilunar clamps (minimal inner diameter of 10.1 mm and length of 9.8 mm) and then compressed along their longitudinal axis until fracturing. This axis was chosen because it represents the main loading axis in humans and is therefore of major interest for future clinical application.

Statistical methods

All results were expressed as means±standard error of the mean. The Wilcoxon test was used for the comparison of paired samples. Significance was accepted at $p \leq .05$.

Results

Surgical technique

Vertebroplasty was successfully established in the large animal sheep model with percutaneous 1-cm stab incisions, channel drilling, and cement injection under X-ray control, as well as wound closure by suturing (Figs. 1A–F; 2A–I). It was a rapid surgical procedure, as demonstrated by a limited duration of operation (28±2 minutes; ie, 0.46 hours) and X-ray exposure (1.59±0.12 minutes; Fig. 3, Top). Vertebroplasty was minimally invasive, as shown by a postoperative wound score of 0 (0.00±0.00), as well as very short postoperative recovery times to complete stand of the animals (2.95±0.29 hours) and until reaching a postoperative impairment score of 0 (3.28±0.36 hours; Fig. 3, Bottom).

Surgical complications included cement leakage into the spinal canal (two animals sacrificed postoperatively), unrelated premature death before the end of the experiment (one short-term 7-year-old animal lost at 2 months), X-ray detectable, but limited paravertebral cement leakage (most vertebral bodies), moderate to severe bleeding from the paravertebral venous plexus (11 animals; likely less than 750 mL because no changes of heart rate or arterial blood pressure were observed; data not shown), and breaking of the drill (two vertebral bodies), in the latter three cases without any influence on the experimental course or any notable impairment for the animals.

The technique allowed reproducible defect creation (channel depth 13.9±0.3 mm, ie, 56.2±1.7% of the vertebral body width) and cement filling (68±5% of the fillable defect volume), as shown by intraoperative X-ray (Fig. 1B) and ex vivo conventional/micro-CT (Figs. 4 and 5).

Cement augmentation

Vertebral cement augmentation and osteoconductivity of the CPC was verified by osteodensitometry (CPC>control; 3 and 9 months; Fig. 6), micro-CT (CPC>control and empty defect in the injection channel and up to a distance of *2.5 mm* from the its edge; 3 and 9 months; Fig. 5), static histomorphometry (BV/TV; CPC>control and empty

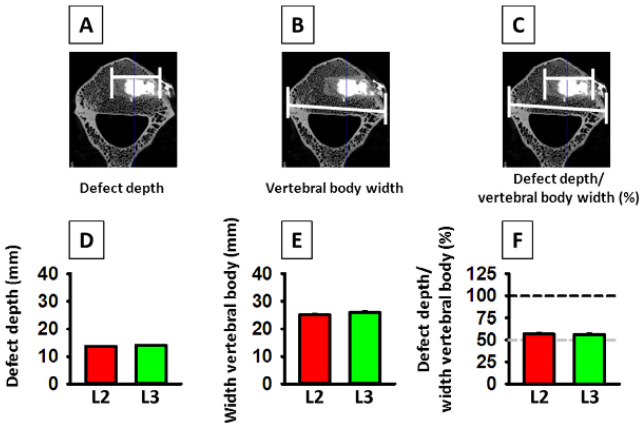

Fig. 4. Assessment of defect depth. Assessment of the depth of the drill channel (A, D), vertebral body width (B, E), and the relationship between the two values in % (C, F), as determined in microcomputed tomography (CT) images of the lumbar vertebral body 2 (L2; empty defect) and L3 (calcium phosphate cement [CPC]); data represent means±standard error of the mean from n=40 animals.

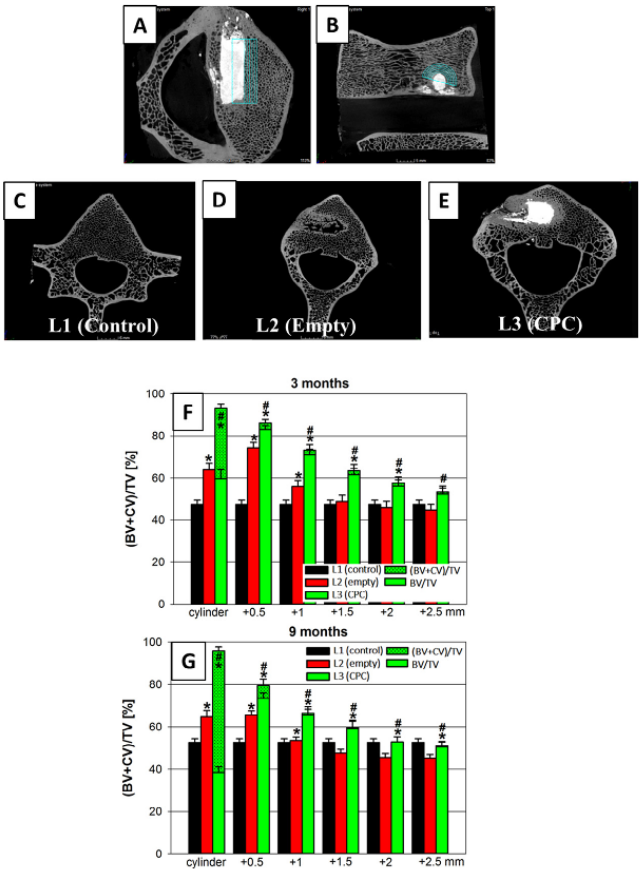

Fig. 5. Assessment of bone volume+cement volume/total volume (BV+CV/TV). Assessment of BV+CV/TV in 3 months (F) and 9 months animals (G; n=20 each), as determined by software evaluation of microcomputed tomography (CT) images of the drill channel and onion-shell 5 mm half-cylinders (A, B) around the drill channel in lumbar vertebral body 1 (L1; untouched; C), L2 (empty defect; D), and L3 (CPC; E); data represent means±standard error of the mean. * p<.05 vs. L1; # p<.05 vs. L2.

defect; 3 and 9 months; Fig. 7), dynamic fluorescence histomorphometry (CPC>control; 3 and 9 months; Figs. 8 and 9; all p≤.05), and compressive strength measurements (CPC numerically higher than control; 102% for 3 months and 110% for 9 months; Fig. 10).

Interestingly, stabilization and osteoinduction was also observed in the case of the empty drill defect, as shown by osteodensitometry (empty defect>control; 3 and 9 months; Fig. 6), micro-CT (empty>control in the drill channel and up to a distance of *1.0 mm* from its edge; 3 and 9 months; Fig. 5), static histomorphometry (BV/TV; empty defect>control; 3 and 9 months; Fig. 7), dynamic fluorescence histomorphometry (empty defect>control; 3 and 9 months; Figs. 8 and 9: all p≤.05), and compressive strength measurements (empty defect numerically higher than control; 103% for 3 months and 106% for 9 months; Fig. 10).

Discussion

The present study describes a new, strictly minimally invasive sheep model for lumbar ventrolateral vertebroplasty in aged, osteopenic sheep with new instruments (drill sleeve, working canula with stop), which guarantees short operation and postoperative recovery times with very limited local trauma, as well as high experimental reproducibility. It proved well suited to demonstrate vertebral cement augmentation and osteoconductivity of an FDA-approved, resorbable, brushite-forming CPC in short-term (3 months) and long-term animals (9 months), as shown by osteodensitometry, micro-CT, histology/static or dynamic fluorescence histomorphometry, and compressive strength measurements.

In addition, the present study for the first time provides a systematic clinical assessment of this vertebroplasty model

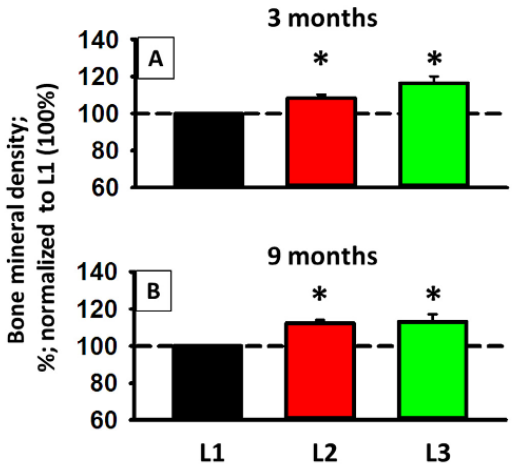

Fig. 6. Assessment of bone mineral density. Assessment of the bone mineral density in 3 months (A) and 9 months animals (B; n=20 each), as determined by osteodensitometry in lumbar vertebral body 1 (L1; untouched), L2 (empty defect), and L3 (CPC); data represent means±standard error of the mean. * p<.05 vs. L1.

and illustrates that it may serve as an optimal basis for future studies on vertebral augmentation with resorbable and osteoconductive CPC.

Surgical technique/animal model

There are only three other published studies describing sheep models for lumbar vertebroplasty [18–20]; the Table). Although in two of these studies, no specific information was given, a minimally invasive approach can be assumed in all studies including our own. However, there are several differences concerning the choice of the animals, the surgical procedure, and/or the applied cement.

The present study used relatively old sheep (age 6–9 years), which have been previously shown by our group to represent a suitable model for selective, age-dependent osteopenia with significantly altered parameters of bone structure (total BV and osteoid volume are less than in young animals aged ≤4 years), bone formation (osteoid surface and osteoid thickness are less than in young animals), and bone resorption (osteoclast surface is higher than in young animals; unpublished data). In addition, the spongiosa in the vertebral bodies of the old sheep used in the present study showed a significantly lower compressive strength than that in young animals of 2–4 years of age. Our model may thus be the only one addressing the effects of vertebral bone defects and their therapy with CPC cement in old, osteopenic animals and may thus be more representative for vertebral fractures in human osteoporosis of the aging population. Alternatively, an ovine model with induced osteoporosis in young animals can be used, which, however, requires long-term and costly preparation of the animals [20].

Except for one study, which used the ventral recumbency also used for lumbar vertebroplasty/kyphoplasty in humans, three studies preferred a lateral position, which may be more suitable for a minimally invasive approach because of the complex anatomic architecture of the sheep lumbar spine (Ref. [18] and references therein; the Table). In addition, the first study used a dorsolateral, para- to transpedicular access to the vertebral body, whereas the three other studies preferred a ventrolateral, extrapedicular access. In our hands, this lateral approach allows rapid and, in conjunction with the drill sleeve and the working canula with stop collar, secure positioning of the drill on the lateral vertebral wall (see also operation duration), as well as reproducible drilling of the defect hole and filling with cement, and thus appears well suitable for the vertebroplasty model. This is in good agreement with the successful use of para- or extrapedicular approaches for thoracolumbar osteoporotic vertebral fractures or vertebral tumor ablation in humans [32–34].

All studies have used the vertebral bodies L1 to L3/L6 for their analyses. Several studies have demonstrated the similarities between the sheep and the human spines concerning size and anatomy, biomechanical behavior, and, to some degree, bone mineral density [13,21,35–41]. This may make the sheep lumbar vertebrae suitable for cement augmentation studies because of similar instrumentation, clinical time course, and bone formation parameters, although this

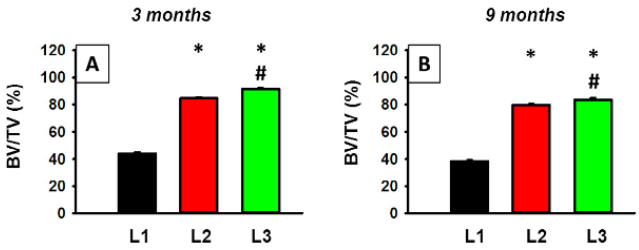

Fig. 7. Assessment of bone volume/total volume (BV/TV). Assessment of BV/TV in 3 months (A) and 9 months animals (B; n=20 each), as determined by static histomorphometry in lumbar vertebral body 1 (L1; untouched), L2 (empty defect), and L3 (calcium phosphate cement [CPC]); data represent means±standard error of the mean. * p<.05 vs. L1; # p<.05 vs. L2.

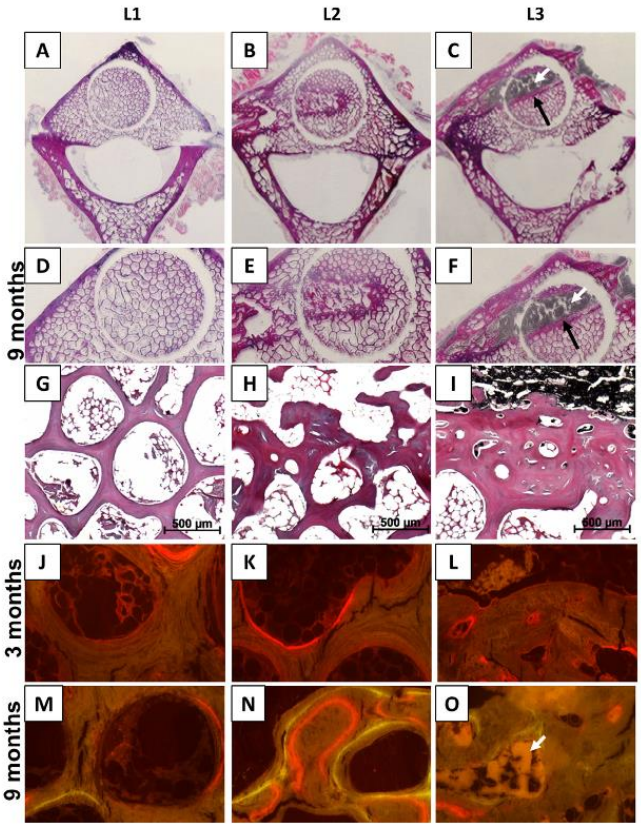

Fig. 8. Treatment of a lumbar vertebral body defect and reactive spongiosa thickening (black arrows) in the large animal model sheep 9 months after injection of a calcium phosphate cement (L3; white arrows). Controls were untouched vertebral bodies (L1) and vertebral bodies with empty defects without cement injection (L2). The stimulation of bone formation after cement injection was documented by histology (upper three rows in different magnifications) or via incorporation of injected fluorescence dyes with a high affinity for newly formed bone (lower two rows).

suitability has also been questioned on the basis of the disadvantageous, hour-glass shape of the vertebral bodies and the incomplete cement filling upon minimally invasive vertebroplasty [20,42]. In our anatomic studies, L6 in sheep shows a substantially flatter shape with a considerably lower anterior-posterior diameter of the spongiosa than L1–L5 and may thus be of limited suitability for comparative analyses.

Due to the hour-glass shape of the sheep vertebral bodies [42], the cement injection site may be of critical importance. Although two studies used the central third of the sheep vertebrae (the Table [19,20]), only one of which specifically discussed the disadvantages of this location [20], the cranial and/or caudal third of the sheep vertebrae may be considerably more suitable for cement augmentation studies than their central part.

Only two of the four studies mentioned in the Table have used a critical size defect for the vertebroplasty model, ranging from 5.0 to 6.0 mm in diameter, and showing 14–15 mm depth (the Table [19]; the present study). In both studies, the critical size empty control defect had only been partially filled with newly formed bone up to a period of 9 months maximum, clearly showing that a defect with a diameter of 5.0 mm and a depth of 14 mm is sufficiently large to serve as a defect model for vertebral cement augmentation.

Pulmonary and/or cardiovascular complications similar to those observed in human vertebroplasty/kyphoplasty have also been reported for vertebroplasty with PMMA or CPC cements in sheep models [18,43–51], including significant decreases of heart rate and arterial pressure, an increase of the venous pressure, the appearance of showers of echogenic material in the pulmonary artery, and transient changes of blood pH and pCO_2. However, there were no indications of such complications in the present study, as indicated by the absence of significant changes in heart rate and arterial or venous blood pressure following injection of the CPC cement into L3 (data not shown). This is probably due to the fact that in the present

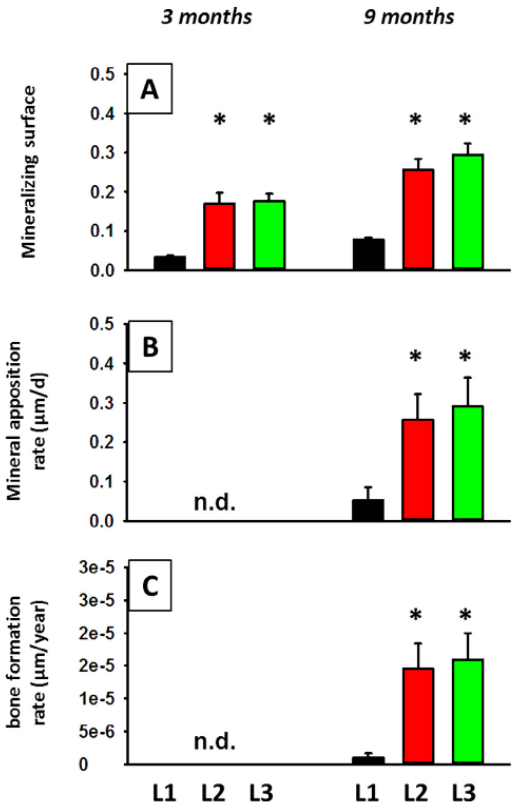

Fig. 9. Assessment of mineralizing surface, mineral apposition rate, and bone formation rate. Assessment of mineralizing surface (A), mineral apposition rate (B), and bone formation rate (C) in 3 months and 9 months animals (n=20 each), as determined by dynamic static histomorphometry in lumbar vertebral body 1 (L1; untouched), L2 (empty defect), and L3 (CPC); data represent means±standard error of the mean. * p<.05 vs. L1.

study, the CPC was applied with limited pressure via a separate bone filler/pestle system into a pre-drilled injection channel, since our preliminary studies had indicated that kyphoplasty in the sheep spine required very high, non-physiological pressures of up to 20 bar, in agreement with previous reports [18,20,42,46,52]. For this reason, direct kyphoplasty was not further pursued in the present animal model, but was replaced by the low-pressure injection of the CPC via a bone filler/pestle system into a pre-formed space, in analogy to the cement injection in humans following generation of a pre-formed intravertebral space by balloon expansion during kyphoplasty. Consequently, there were no signs of an expansion of the vertebral bodies or a decrease in kyphosis following cement injection (data not shown).

The duration of the operation (28 minutes; incision to suture) and the X-ray exposure (approximately 1.6 minutes), which was for the first time systematically assessed in the present study, was shorter or remained well within the range of previous reports in animal models of vertebroplasty and femoral/tibial bone augmentation [18,42] or vertebroplasty in human [53]. Also, the wound trauma score (0 of maximum 4), as well as the times to complete stand (approximately 3 hours) and until reaching a postoperative impairment score of 0 (3.3 hours; see Fig. 3, Right) were comparable with other animal studies, although, due to the fact that the time to a complete stand without having to lie down again was assessed, the recovery time was judged somewhat longer than previously [18,42]. These findings demonstrate that the vertebral surgery in the present study is well tolerated by the animals, with an acceptable rate of severe complications due to cement leakage into the spinal canal (current study 5%; in subsequent studies decreased to 3.75%) and a very limited pain burden. Finally, the depth of the drill channel and particularly the ratio defect depth/vertebral body width was highly standardized, underlining the reproducibility and technical reliability of the present animal model. Further modifications of the surgical procedure such as neuromonitoring or the use of light-guided endoscopes were deemed unnecessary and were thus omitted to preserve the short duration and the minimally invasive character of the intervention.

To our knowledge, there is currently only one model that completely reproduces osteoporotic compression fractures [54,55]. This model, however, requires ovariectomy (operation 1), steroid therapy for 5.5 months, and surgical generation of the fracture in one vertebral body (L2; operation 2) of adult, young sheep. In addition to the time- and resource-consuming

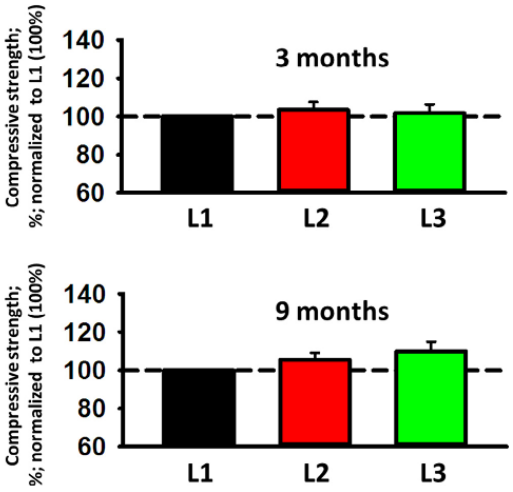

Fig. 10. Assessment of compressive strength. Assessment of compressive strength in 3 months (Top) and 9 months animals (Bottom; n=20 each), as determined by biomechanical testing of spongiosa cylinders (see Materials and methods) from lumbar vertebral body 1 (L1; untouched), L2 (empty defect), and L3 (CPC); data represent means±standard error of the mean.

Table
Comparison of the sheep large animal models for lumbar vertebroplasty

	Benneker et al [18]	Zhu et al [19]	Galovich et al [20]	The present study
Sheep; gender; age	Race (n.d.); female; 3.4±0.9 y	Race (n.d.); female; 2–3 y	Merino; female; 4–6 y	Merino; female; 6–9 y (aged)
Bone status (spine)	Normal	Normal	Normal; osteoporotic	Osteopenic
Position	Ventral recumbency	Lateral position?	Lateral position	Lateral position
Invasiveness	Minimally invasive	No information	No information	Minimally invasive
Vertebral access	Dorsolateral (para- to transpedicular)	Ventrolateral (extrapedicular)	Ventrolateral (extrapedicular)	Ventrolateral (extrapedicular)
Vertebral bodies	L1–L5	L2–L5	L1–L6	L1–L3
Defect size	Diameter: 4.2 mm (drill 3.2 mm)	Diameter: 6.0 mm	Diameter: 5.0 mm	Diameter: 5.0 mm
	Depth: n.d.	Depth: 15.0 mm	Depth: n.d.	Depth: 14.0 mm
Critical size empty defect	No (acute study)	Yes	No (?)	Yes
Specific tools	Drill (3.2 mm); Filling cannula (4.2 mm)	Drill with stop	Drill; drill guide	Drill: drill sleeve; Working canula with stop
Cement injection site	Cranial/caudal third	Central third ("Center")	Central third	Caudal third
Cement	PMMA-based (55% ceramic/45% PMMA; Vertecem, Synthes Inc., Oberdorf, Switzerland)	CPC (Rebone Biomaterials Co. Ltd., Shanghai, China; amorphous hydroxyapatite-forming CPC)	PMMA (Osteopal V, Biomet, Varsaw, IN, USA); CPC (Calcibon, Biomet; amorphous hydroxyapatite-forming CPC)	CPC (JectOS, Kasios, L'Union, France; brushite-forming CPC)
Operation duration; X-ray exposure	7–21 min (instrumentation time only); not determined	Not determined	Not determined	28 min; 1.6 min
Wound score (24 h)	Not applicable (acute)	Not determined (no indication of inflammation at 2 weeks)	Not determined	0.0 (of maximum 4)
Time to complete stand	Not applicable (acute)	Not determined	Not determined (all animals but one recovered well with normal locomotion)	1.6 h
Standing time (weeks)	0 (acute)	2, 24	0, 13, 26, 52 (0, 3, 6, 12 months)	13, 39 (3, 9 months)

Note: PMMA, poly(methyl methacrylate); CPC, calcium phosphate cement; n.d., not determined.

procedure, which also puts a considerable burden on the animals, it only allows the assessment of therapeutic effects in one vertebral body and thus strongly increases the number of animals, if different treatment modalities are to be compared. We therefore strongly believe that our current model in aged sheep may at least be a physiological, simple, and suitable alternative to the above model or other ovine models with long-term and costly induction of osteoporosis in young animals [20].

Cement augmentation

Vertebral cement augmentation (with limited extrusion of CPC into the spongiosa, detailed data not shown) and osteoconductivity of the CPC was verified by osteodensitometry, micro-CT, static or dynamic fluorescence histomorphometry, and, at least numerically, by compressive strength measurements. The limited effects on the compressive strength were likely due to the fact that the injected cement core accounted for only approximately 1.65% of the total vertebral body volume. Nevertheless, the cement core was sufficiently stabile to be extruded out of the spongiosa without semiconfinement by the two semilunar clamps, which led to the test set-up applied in the present study. The present results are in line with the known osteoconductivity of CPC for bone substitution in animals and humans [19,20,56,57] and again confirm the suitability of the present large animal model to validate or confirm optimized vertebral augmentation with resorbable CPC.

Interestingly, stabilization and osteoinduction was also observed in the case of the empty drill defect, as shown by osteodensitometry, micro-CT, static and dynamic histomorphometry, and compressive strength measurements. However, the significant increase of the BV/TV observed by micro-CT in the case of the empty drill defect was limited to a distance of *1.0 mm* from its edge, showing that the effects of the bone injury on reactive bone formation/healing are less marked than in the case of the injection of the CPC.

Conclusions

The new, minimally invasive sheep model for lumbar ventrolateral vertebroplasty allows short operation and postoperative recovery times with very limited local trauma, as well as high experimental reproducibility. This model represents an optimal basis for standardized evaluation of future studies on vertebral augmentation with resorbable and osteoconductive CPC, using osteodensitometry, micro-CT, histology, static and dynamic histomorphometry, and compressive strength measurements. Due to anatomical and functional differences between sheep and humans, however, further studies on sheep and human cadaver vertebrae will be needed to confirm the applicability of the current results to human patients.

Acknowledgment

We gratefully acknowledge the financial support by the Carl Zeiss Foundation (doctoral candidate scholarship to S.M.) and by the German Federal Ministry of Education and Research (BMBF FKZ 0316205C to J.B and K.D.J.; BMBF FKZ 035577D, 0316205B, and 13N12601 to R.W.K). We gratefully acknowledge E. Mark for performing the osteodensitometry analyses, and G. Grunert and S. Födisch for their excellent technical assistance. Nicolas Guéna and Alain Lerch (Kasios, L'UNION, France) are gratefully acknowledged for providing the FDA-approved, brushite-forming CPC JectOS+.

References

[1] Hulme PA, Krebs J, Ferguson SJ, Berlemann U. Vertebroplasty and kyphoplasty: a systematic review of 69 clinical studies. Spine 2006;31:1983–2001.
[2] Nouda S, Tomita S, Kin A, Kawahara K, Kinoshita M. Adjacent vertebral body fracture following vertebroplasty with polymethylmethacrylate or calcium phosphate cement: biomechanical evaluation of the cadaveric spine. Spine 2009;34:2613–18.
[3] Trout AT, Kallmes DF, Kaufmann TJ. New fractures after vertebroplasty: adjacent fractures occur significantly sooner. AJNR Am J Neuroradiol 2006;27:217–23.
[4] Uppin AA, Hirsch JA, Centenera LV, Pfiefer BA, Pazianos AG, Choi IS. Occurrence of new vertebral body fracture after percutaneous vertebroplasty in patients with osteoporosis. Radiology 2003;226:119–24.
[5] Blattert TR, Jestaedt L, Weckbach A. Suitability of a calcium phosphate cement in osteoporotic vertebral body fracture augmentation: a controlled, randomized, clinical trial of balloon kyphoplasty comparing calcium phosphate versus polymethylmethacrylate. Spine 2009;34:108–14.
[6] Burguera EF, Xu HH, Weir MD. Injectable and rapid-setting calcium phosphate bone cement with dicalcium phosphate dihydrate. J Biomed Mater Res B Appl Biomater 2006;77:126–34.
[7] Wilke HJ, Mehnert U, Claes LE, Bierschneider MM, Jaksche H, Boszczyk BM. Biomechanical evaluation of vertebroplasty and kyphoplasty with polymethyl methacrylate or calcium phosphate cement under cyclic loading. Spine 2006;31:2934–41.
[8] Brown WE, Chow LC. A new calcium-phosphate setting cement. J Dent Res 1983;62:672.
[9] LeGeros RZ, Chohayeb A, Shulman A. Apatite calcium phosphates: possible dental restorative materials. J Dent Res 1982;61:343.
[10] Grafe IA, Baier M, Noldge G, et al. Calcium-phosphate and polymethylmethacrylate cement in long-term outcome after kyphoplasty of painful osteoporotic vertebral fractures. Spine 2008;33:1284–90.
[11] Ryu KS, Shim JH, Heo HY, Park CK. Therapeutic efficacy of injectable calcium phosphate cement in osteoporotic vertebral compression fractures: prospective nonrandomized controlled study at 6-month follow-up. World Neurosurg 2010;73:408–11.
[12] Turner RT, Maran A, Lotinun S, et al. Animal models for osteoporosis. Rev Endocr Metab Disord 2001;2:117–27.
[13] Wilke HJ, Kettler A, Wenger KH, Claes LE. Anatomy of the sheep spine and its comparison to the human spine. Anat Rec 1997;247:542–55.
[14] Eggli S, Schlapfer F, Angst M, Witschger P, Aebi M. Biomechanical testing of three newly developed transpedicular multisegmental fixation systems. Eur Spine J 1992;1:109–16.
[15] Gurwitz GS, Dawson JM, McNamara MJ, Federspiel CF, Spengler DM. Biomechanical analysis of three surgical approaches for lumbar burst fractures using short-segment instrumentation. Spine 1993;18:977–82.
[16] Committee for Advanced Therapies EMA. Reflection paper on in-vitro cultured chondrocyte containing products for cartilage repair of the knee. Doc Ref EMEA/CAT/CPWP/288934/2009. 2009:1–8.
[17] Edmonston SJ, Singer KP, Day RE, Breidahl PD, Price RI. Formalin fixation effects on vertebral bone density and failure mechanics: a study of human and sheep vertebrae. Eur Spine J 1994;1:175–9.
[18] Benneker LM, Gisep A, Krebs J, Boger A, Heini PF, Boner V. Development of an in vivo experimental model for percutaneous vertebroplasty in sheep. Vet Comp Orthop Traumatol 2012;25:173–7.
[19] Zhu XS, Zhang ZM, Mao HQ, et al. A novel sheep vertebral bone defect model for injectable bioactive vertebral augmentation materials. J Mater Sci Mater Med 2011;22:159–64.
[20] Galovich LA, Perez-Higueras A, Altonaga JR, Orden JM, Barba ML, Morillo MT. Biomechanical, histological and histomorphometric analyses of calcium phosphate cement compared to PMMA for vertebral augmentation in a validated animal model. Eur Spine J 2011;20(Suppl. 3):376–82.
[21] Turner AS. The sheep as a model for osteoporosis in humans. Vet J 2002;163:232–9.
[22] Syed Z, Khan A. Bone densitometry: applications and limitations. J Obstet Gynaecol Can 2002;24:476–84.
[23] Plenck H. Untersuchung des Binde- und Stützgewebes (Trichrom-Färbung nach Goldner). In: Böck P, editor. Romeis—mikroskopische technik. Munich, Germany: Urban und Schwarzenberg Verlag; 1989. p. 499.
[24] Knutsen G, Engebretsen L, Ludvigsen TC, et al. Autologous chondrocyte implantation compared with microfracture in the knee. A randomized trial. J Bone Joint Surg Am 2004;86-A:455–64.
[25] Parfitt AM. Bone histomorphometry: standardization of nomenclature, symbols and units. Summary of proposed system. Bone Miner 1988;4:1–5.
[26] Parfitt AM. Bone histomorphometry: proposed system for standardization of nomenclature, symbols, and units. Calcif Tissue Int 1988;42:284–6.
[27] Parfitt AM, Drezner MK, Glorieux FH, et al. Bone histomorphometry: standardization of nomenclature, symbols, and units. Report of the ASBMR Histomorphometry Nomenclature Committee. J Bone Miner Res 1987;2:595–610.
[28] Delling G. Endokrine Osteopathien. Stuttgart, Germany: Gustav Fischer Verlag; 1975.
[29] Dempster DW, Compston JE, Drezner MK, et al. Standardized nomenclature, symbols, and units for bone histomorphometry: a 2012 update of the report of the ASBMR Histomorphometry Nomenclature Committee. J Bone Miner Res 2013;28:2–17.
[30] Protze A. Einschätzung der Knochenqualität am proximalen Femur bei fortgeschrittener Koxarthrose und deren Einfluss auf die postoperative periprothetische Knochenmineraldichteänderung [Thesis] Jena 2004.
[31] Donath K, Breuner G. A method for the study of undecalcified bones and teeth with attached soft tissues. The Sage-Schliff (sawing and grinding) technique. J Oral Pathol 1982;11:318–26.
[32] Beall DP, Braswell JJ, Martin HD, Stapp AM, Puckett TA, Stechison MT. Technical strategies and anatomic considerations for parapedicular access to thoracic and lumbar vertebral bodies. Skeletal Radiol 2007;36:47–52.
[33] Erkan S, Wu C, Mehbod AA, Cho W, Transfeldt EE. Biomechanical comparison of transpedicular versus extrapedicular vertebroplasty using polymethylmethacrylate. J Spinal Disord Tech 2010;23:180–5.
[34] Cianfoni A, Massari F, Ewing S, Persenaire M, Rumboldt Z, Bonaldi G. Combining percutaneous pedicular and extrapedicular access for tumor ablation in a thoracic vertebral body. Interv Neuroradiol 2014;20:603–8.
[35] Cotterill PC, Kostuik JP, D'Angelo G, Fernie GR, Maki BE. An anatomical comparison of the human and bovine thoracolumbar spine. J Orthop Res 1986;4:298–303.
[36] Wilke HJ, Kettler A, Claes LE. Are sheep spines a valid biomechanical model for human spines? Spine 1997;22:2365–74.

[37] Newton BI, Cooper RC, Gilbert JA, Johnson RB, Zardiackas LD. The ovariectomized sheep as a model for human bone loss. J Comp Pathol 2004;130:323–6.
[38] Egermann M, Goldhahn J, Schneider E. Animal models for fracture treatment in osteoporosis. Osteoporos Int 2005;16(Suppl. 2):S129–38.
[39] Lill CA, Gerlach UV, Eckhardt C, Goldhahn J, Schneider E. Bone changes due to glucocorticoid application in an ovariectomized animal model for fracture treatment in osteoporosis. Osteoporos Int 2002;13:407–14.
[40] Turner AS, Alvis M, Myers W, Stevens ML, Lundy MW. Changes in bone mineral density and bone-specific alkaline phosphatase in ovariectomized ewes. Bone 1995;17(Suppl. 4):395S–402S.
[41] Smit TH. The use of a quadruped as an in vivo model for the study of the spine—biomechanical considerations. Eur Spine J 2002;11:137–44.
[42] Klein K, Zamparo E, Kronen PW, et al. Bone augmentation for cancellous bone- development of a new animal model. BMC Musculoskelet Disord 2013;14:200.
[43] Krebs J, Ferguson SJ, Nuss K, et al. Plasma levels of endothelin-1 after a pulmonary embolism of bone marrow fat. Acta Anaesthesiol Scand 2007;51:1107–14.
[44] Krebs J, Ferguson SJ, Hoerstrup SP, Goss BG, Haeberli A, Aebli N. Influence of bone marrow fat embolism on coagulation activation in an ovine model of vertebroplasty. J Bone Joint Surg Am 2008;90:349–56.
[45] Aebli N, Krebs J, Davis G, Walton M, Williams MJ, Theis JC. Fat embolism and acute hypotension during vertebroplasty: an experimental study in sheep. Spine 2002;27:460–6.
[46] Aebli N, Krebs J, Schwenke D, Davis G, Theis JC. Pressurization of vertebral bodies during vertebroplasty causes cardiovascular complications: an experimental study in sheep. Spine 2003;28:1513–19. discussion 9-20.
[47] Aebli N, Krebs J, Schwenke D, Davis G, Theis JC. Cardiovascular changes during multiple vertebroplasty with and without vent-hole: an experimental study in sheep. Spine 2003;28:1504–11. discussion 11-2.
[48] Aebli N, Schwenke D, Davis G, Hii T, Theis JC, Krebs J. Polymethylmethacrylate causes prolonged pulmonary hypertension during fat embolism: a study in sheep. Acta Orthop 2005;76:904–11.
[49] Koessler MJ, Aebli N, Pitto RP. Fat and bone marrow embolism during percutaneous vertebroplasty. Anesth Analg 2003;97:293. author reply 4.
[50] Krebs J, Aebli N, Goss BG, et al. Cardiovascular changes after pulmonary embolism from injecting calcium phosphate cement. J Biomed Mater Res B Appl Biomater 2007;82:526–32.
[51] Krebs J, Aebli N, Goss BG, Wilson K, Williams R, Ferguson SJ. Cardiovascular changes after pulmonary cement embolism: an experimental study in sheep. AJNR Am J Neuroradiol 2007;28:1046–50.
[52] Boger A, Benneker LM, Krebs J, Boner V, Heini PF, Gisep A. The effect of pulsed jet lavage in vertebroplasty on injection forces of PMMA bone cement: an animal study. Eur Spine J 2009;18:1957–62.
[53] Cannavale A, Salvatori FM, Wlderk A, Cirelli C, d'Adamo A, Fanelli F. Percutaneous vertebroplasty with the rotational fluoroscopy imaging technique. Skeletal Radiol 2014;43:1529–36.
[54] Eschler A, Ropenack P, Herlyn PK, et al. The standardized creation of a lumbar spine vertebral compression fracture in a sheep osteoporosis model induced by ovariectomy, corticosteroid therapy and calcium/phosphorus/vitamin D-deficient diet. Injury 2015;46(Suppl. 4):S17–23.
[55] Eschler A, Roepenack P, Roesner J, et al. Cementless titanium mesh fixation of osteoporotic burst fractures of the lumbar spine leads to bony healing: results of an experimental sheep model. Biomed Res Int 2016;2016:4094161.
[56] Zhang J, Liu W, Schnitzler V, Tancret F, Bouler JM. Calcium phosphate cements for bone substitution: chemistry, handling and mechanical properties. Acta Biomater 2014;10:1035–49.
[57] Bai B, Yin Z, Xu Q, et al. Histological changes of an injectable rhBMP-2/calcium phosphate cement in vertebroplasty of rhesus monkey. Spine 2009;34:1887–92.

5. Low-dose BMP-2 is sufficient to enhance the bone formation induced by an injectable, PLGA fiber-reinforced, brushite-forming cement in a sheep defect model of lumbar osteopenia

Gunnella F, Kunisch E, Bungartz M, Maenz S, Horbert V, Xin L, Mika J, Borowski J, Bischoff S, Schubert H, Hortschansky P, Sachse A, Illerhaus B, Günster J, Bossert J, Jandt KD, Plöger F, Kinne RW, Brinkmann O.

The Spine Journal 2017;17(11):1699-1711.
doi: 10.1016/j.spinee.2017.06.005. Epub 2017 Jun 12.

Preface

The minimally invasive vertebroplasty sheep model described in the previous chapter has proven suitable for future studies on the vertebral augmentation with resorbable and osteoconductive CPC. On the basis of the central role of BMP-2 in promoting bone repair, its extended clinical use, and the promising release data obtained in our previous study (Chapter 3; pp. 26-56), our minimally invasive lumbar osteopenia model was used to test an injectable, PLGA-fiber reinforced, brushite-forming cement (CPC) containing the bone morphogenetic protein BMP-2.

For the choice of the doses one important aspect was taken into consideration, i.e., the numerous serious adverse effects observed after the use of high doses between 1.95 and 40 mg of BMP-2 for spinal surgery, including back or leg pain, ectopic bone formation, wound complications, radiculitis, and retrograde ejaculation (Carragee, Hurwitz et al. 2011). For this reason, a fiber-reinforced CPC was developed with considerably lower doses of BMP-2 (between 1 and 500 µg) and tested in our sheep model of ventrolateral vertebroplasty.

ELSEVIER

CrossMark

The Spine Journal 17 (2017) 1699–1711

THE SPINE JOURNAL

Basic Science

Low-dose BMP-2 is sufficient to enhance the bone formation induced by an injectable, PLGA fiber-reinforced, brushite-forming cement in a sheep defect model of lumbar osteopenia

Francesca Gunnella[a], Elke Kunisch[a], Matthias Bungartz[a,b], Stefan Maenz[c,d], Victoria Horbert[a], Long Xin[a], Joerg Mika[a,1], Juliane Borowski[a], Sabine Bischoff[e], Harald Schubert[e], Peter Hortschansky[f], Andre Sachse[b], Bernhard Illerhaus[e], Jens Günster[g], Jörg Bossert[c], Klaus D. Jandt[c,d,h], Frank Plöger[i], Raimund W. Kinne[a,*], Olaf Brinkmann[a,b]

[a]*Experimental Rheumatology Unit, Department of Orthopedics, Jena University Hospital, Waldkrankenhaus "Rudolf Elle", Klosterlausnitzer Str. 81, 07607 Eisenberg, Germany*

[b]*Chair of Orthopedics, Department of Orthopedics, Jena University Hospital, Waldkrankenhaus "Rudolf Elle", Klosterlausnitzer Str. 81, 07607 Eisenberg, Germany*

[c]*Chair of Materials Science, Otto Schott Institute of Materials Research, Friedrich Schiller University Jena, Löbdergraben 32, 07743 Jena, Germany*

[d]*Jena Center for Soft Matter (JCSM), Friedrich Schiller University Jena, Humboldtstr. 10, 07743 Jena, Germany*

[e]*Institute of Laboratory Animal Sciences and Welfare, Jena University Hospital, Dornburger Straße 23, 07743 Jena, Germany*

[f]*Leibniz-Institute for Natural Products Research and Infection Biology – Hans-Knoell-Institute, Beutenbergstr. 11a, 07745 Jena, Germany*

[g]*BAM Bundesanstalt für Materialforschung und –prüfung (BAM), Unter den Eichen 44-46, 12203 Berlin; Germany*

[h]*Jena School for Microbial Communication (JSMC), Friedrich Schiller University Jena, Neugasse 23, 07743 Jena, Germany*

[i]*BIOPHARM GmbH, Handelsstrasse 15, 69214 Eppelheim, Germany*

Received 7 March 2017; revised 23 May 2017; accepted 8 June 2017

Abstract

BACKGROUND CONTEXT: Bioresorbable calcium phosphate cement (CPC) may be suitable for vertebroplasty/kyphoplasty of osteoporotic vertebral fractures. However, additional targeted delivery of osteoinductive bone morphogenetic proteins (BMPs) in the CPC may be required to counteract the augmented local bone catabolism and support complete bone regeneration.

PURPOSE: This study aimed at testing an injectable, poly (l-lactide-co-glycolide) acid (PLGA) fiber-reinforced, brushite-forming cement (CPC) containing low-dose bone morphogenetic protein BMP-2 in a sheep lumbar osteopenia model.

STUDY DESIGN/ SETTING: This is a prospective experimental animal study.

METHODS: Bone defects (diameter 5 mm) were generated in aged, osteopenic female sheep and filled with fiber-reinforced CPC alone (L4; CPC+fibers) or with CPC containing different dosages

FDA device/drug status: Not applicable.

Author disclosures: ***FG:*** Grant: German Federal Ministry of Education and Research (H, Paid to the institution), pertaining to submitted manuscript. ***EK:*** Grant: German Federal Ministry of Education and Research (FKZ 03577D, 0316205B, and 13N12601; H, Paid to the institution), pertaining to submitted manuscript. ***MB:*** Nothing to disclose. ***SM:*** Grant: Carl Zeiss Foundation (D, Paid directly to the author, PhD scholarship), German Federal Ministry of Education and Research (F, Paid to the institution), pertaining to submitted manuscript. ***VH:*** Grant: German Federal Ministry of Education and Research (H, Paid to the institution), pertaining to submitted manuscript. **LX:** Grant: German Federal Ministry of Education and Research (H, Paid to the institution), pertaining to submitted manuscript, Grant: Department of Health of Zhejiang Province, Hangzhou, China (D, Paid directly to the author, Research scholarship). ***JM:*** Nothing to disclose. ***JuB:*** Nothing to disclose. ***SB:*** Nothing to disclose. ***HS:*** Nothing to disclose. ***PH:*** Nothing to disclose. ***AS:*** Nothing to disclose. ***BI:*** Nothing to disclose. ***JG:*** Nothing to disclose. ***JöB:*** Grant: German Federal Ministry of Education and Research (FKZ 0316205C; F, Paid to the institution), pertaining to submitted manuscript. ***KDJ:*** Grant: German Federal Ministry of Education and Research (F, Paid to the institution), pertaining to submitted manuscript. ***FP:*** BMBF (FKZ 0316205A, G, Paid to the institution). ***RWK:*** Grant: German Federal Ministry of Education and Research (H, Paid to the institution), pertaining to submitted manuscript. ***OB:*** Nothing to disclose.

The disclosure key can be found on the Table of Contents and at www.TheSpineJournalOnline.com.

* Corresponding author. Experimental Rheumatology Unit, Department of Orthopedics, Jena University Hospital, Waldkrankenhaus "Rudolf Elle", Klosterlausnitzer Str. 81, 07607 Eisenberg, Germany. Tel.: 0049 (0) 36691 81228; fax: 0049 (0) 36691 81226.

E-mail address: raimund.w.kinne@med.uni-jena.de (R.W. Kinne)

[1] Current addresses: Laboratory of Experimental Trauma Surgery, Justus-Liebig-University Giessen, 35394 Giessen, Germany and Department of Trauma, Hand and Reconstructive Surgery Giessen, University Hospital Giessen-Marburg, Campus Giessen, Rudolf-Buchheim-Str. 7, 35385 Giessen, Germany.

https://doi.org/10.1016/j.spinee.2017.06.005

of BMP-2 (L5; CPC+fibers+BMP-2; 1, 5, 100, and 500 μg BMP-2; n=5 or 6 each). The results were compared with those of untouched controls (L1). Three and 9 months after the operation, structural and functional effects of the CPC (±BMP-2) were analyzed ex vivo by measuring (1) *bone mineral density* (BMD); (2) *bone structure*, that is, bone volume/total volume (assessed by micro-computed tomography [micro-CT] and histomorphometry), trabecular thickness, and trabecular number; (3) *bone formation*, that is, osteoid volume/bone volume, osteoid surface/bone surface, osteoid thickness, mineralizing surface/bone surface, mineral apposition rate, and bone formation rate/bone surface; (4) *bone resorption*, that is, eroded surface/bone surface; and (5) *compressive strength*.

RESULTS: Compared with untouched controls (L1), CPC+fibers (L4) and/or CPC+fibers+BMP-2 (L5) significantly improved all parameters of bone formation, bone resorption, and bone structure. These effects were observed at 3 and 9 months, but were less pronounced for some parameters at 9 months. Compared with CPC without BMP-2, additional significant effects of BMP-2 were demonstrated for bone structure (bone volume/total volume, trabecular thickness, trabecular number) and formation (osteoid surface/bone surface and mineralizing surface/bone surface), as well as for the compressive strength. The BMP-2 effects on bone formation at 3 and 9 months were dose-dependent, with 5–100 μg as the optimal dosage.

CONCLUSIONS: BMP-2 significantly enhanced the bone formation induced by a PLGA fiber-reinforced CPC in sheep lumbar osteopenia. A single local dose as low as ≤100 μg BMP-2 was sufficient to augment middle to long-term bone formation. The novel CPC+BMP-2 may thus represent an alternative to the bioinert, supraphysiologically stiff polymethylmethacrylate cement presently used to treat osteoporotic vertebral fractures by vertebroplasty/kyphoplasty.

Keywords: Bone morphogenetic protein 2; Bone regeneration; Calcium phosphate cement; Growth factor; Large animal model sheep; Osteoporotic vertebral fracture

Introduction

Osteoporosis is a systemic skeletal disease characterized by reduced bone mass and disruption of bone architecture, resulting in increased risk of fragility fractures. The fractures are associated with substantial pain, disability, or even death for the affected patients and substantial costs for the health care systems [1,2]. Osteoporotic vertebral body fractures account for approximately 45% of the fractures. At the age of 50 years, the remaining lifetime probability to suffer from an osteoporosis-associated fracture is 46% in women and 22% in men [1].

The estimated increase of osteoporotic vertebral body fractures from 2010 to 2025 in the European countries is 27% [1]. The disease is asymptomatic and often remains undetected until a fracture occurs. Innovative, minimally invasive methods such as vertebroplasty and kyphoplasty have increased in popularity because they offer a recognizable increase in quality of life in patients with an osteoporotic vertebral fracture by improving lumbar biomechanics and stability, and thus relieving pain [3,4]. Polymethylmethacrylate (PMMA) cement, currently the most widely used material for vertebroplasty and kyphoplasty, however, lacks bioactivity and biodegradability, and its supraphysiological strength and Young modulus may lead to critical loads and subsequent fractures in adjacent vertebral bodies [5–8]. Because of such safety concerns, calcium phosphate cements (CPCs) have recently been used as an alternative to PMMA based on the following aspects: (1) biodegradability and Young modulus comparable with those of cancellous bone; (2) excellent osteoconductivity for bone ingrowth and remodeling; and (3) setting reaction at body temperature [9–11], instead of highly unphysiological, tissue-damaging temperatures of approximately 60°C in the case of PMMA ([12] and references therein). On the other hand, the use of commercially available, injectable CPCs in load-bearing areas is limited by their low mechanical strength and low fracture toughness, leading to premature damage of the cement at the implant site [9,13]. One strategy to successfully overcome this limitation is the addition of fibers in the structure of the CPC [14–16]. For this reason, a poly (l-lactide-co-glycolide) acid (PLGA) fiber-reinforced CPC was used in the present study [17].

CPC can be used as a carrier system to apply osteoinductive molecules such as bone morphogenetic protein-2 (BMP-2 [18]). Bone morphogenetic proteins were first described as mediators of the osteoinductive activity of demineralized bone for ectopic bone formation in adult animals [19,20] and were later shown to play an important role in bone development, osteogenic cell differentiation, and fracture healing [21,22]. BMP-2 belongs to the superfamily of transforming growth factor-β (TGF-β) proteins, which comprises 33 members of ligands that activate the so-called type I and type II receptors of the TGF-β superfamily [22,23].

BMP-2 plays a central role in triggering osteogenesis via autocrine and paracrine regulatory mechanisms, as demonstrated by elegant in vitro and ex vivo studies [21]. BMP-2 also improves the in vivo parameters of bone structure or bone formation in models of osteopenia in mice [24], rats [25], rabbits [26], goats [27], and sheep [28], and is regarded as a very promising molecule for lumbar spine fusion [29], with additional applications in alveolar/dental surgery [30].

This has led to FDA marketing approval of several rhBMP-2 carrier systems (e.g., INFUSE_and *AMPLIFY* with 1.5 mg/mL and 2.0 mg/mL BMP-2, respectively), which are used for spinal fusion in place of autologous bone grafts and allow a reduction of operating time and blood loss during surgery, as well as a higher fusion rate [31]. However, numerous serious adverse effects have been reported using high doses between 1.95 and 40 mg of BMP-2 for spinal surgery, including back or leg pain, ectopic bone formation, wound complications, radiculitis, and retrograde ejaculation [31,32].

For this reason, a newly developed, fiber-reinforced CPC with considerably lower doses of BMP-2 (between 1 and 500 µg) was tested in a sheep model of ventrolateral vertebroplasty [33]. Aged, osteopenic female sheep were used (6–9 years; significantly lower bone volume/total volume in the central spongious region of lumbar vertebrae than young sheep aged 2–4 years; see figure S1 in References [34] and [35,36]). Interestingly, a local dose as low as ≤100 µg BMP-2 significantly enhanced the bone formation induced by a PLGA fiber-reinforced CPC.

Materials and methods

Bone defects placed in lumbar vertebrae of aged, osteopenic female sheep and treated with fiber-reinforced CPC alone (sacrifice: 3, 9 months) or with CPC containing 1, 5, 100, and 500 µg BMP-2 were compared with controls without a defect. Bone mineral density (BMD), bone structure, bone formation, bone resorption, and compressive strength were measured to assess structural and functional effects.

Fabrication of PLGA fibers and preparation of the injectable, PLGA fiber-reinforced, growth factor-loaded CPC

Poly (l-lactide-co-glycolide) acid (PLGA) fibers with a diameter of 25 µm were prepared and characterized as described recently [16]. In brief, PLGA fibers were extruded from the granulate material PURASORB PLG 1017 (Purac, Gorinchem, The Netherlands) using a mini extrusion system (Randcastle Extrusion Systems, Inc, Cedar Grove, NJ, USA). Fibers were then cut to a length of 597±362 µm using a cutting mill PULVERISETTE 19 (FRITSCH GmbH, Idar-Oberstein, Germany) with a 1mm sieve insert. CPC powder of a commercially available bone cement (Conformité Européenne (CE)-certified, brushite-forming CPC JectOS+; Kasios, L'Union, France) with 10% fiber content (w/w) and a fiber length of 1 mm was obtained by mixing defined amounts of fibers and CPC powder.

The different CPC samples were prepared during surgery, shortly before injection into the defect. For PLGA fiber-reinforced CPC, the cement powder was thoroughly mixed with the liquid compound of JectOS+ in a powder-to-liquid ratio of 2.2. Recombinant human BMP-2 was prepared as described previously [37]. To prepare the BMP-2-loaded, PLGA fiber-reinforced cement, the lyophilized growth factor was dissolved in the liquid and then added to the cement powder.

Animals

Aged, osteopenic, female sheep (44 Merino animals; 6–9 years old [7.56±0.80 years, mean±standard deviation]; 68–110 kg body weight [90.98±10.67 kg]) were used. Animals were allocated to the different experimental groups to achieve an equal mean age. The 3- and 9-month groups consisted of n=5 animals each for 1 and 5 µg (total n=20), and n=6 animals each for 100 and 500 µg BMP-2 (total n=24). Power analyses (G*power [38]) for dose-dependent differences among the various doses of BMP-2 for the structural parameter bone volume/total volume (BV/TV), as well as for the bone formation parameters osteoid volume/bone volume (OV/BV) and mineralizing surface/bone surface (MS/BS) confirmed that group sizes between 3 and 5 animals were sufficient to detect differences with an alpha error probability of .05, a power (1-β error probability) of .80, and an effect size between 2.10 and 3.75. Permission was obtained from the governmental commission for animal protection, Free State of Thuringia, Germany (registration number 02–036/11).

Anesthesia and surgical technique

The right lateral back of the animals was shaved under sedation (ketamine hydrochloride, 2 mg/kg body weight, Zoetis Deutschland GmbH, Berlin, Germany; 0.1–0.3 mg/kg Midazolam-hydrochloride, Hameln Pharmaceuticals GmbH, Hameln, Germany; both intramuscular). Following intubation, anesthesia was induced by inhalation of isoflurane (Isofluran, 1.5–1.8 vol%, AbbVie, Ludwigshafen, Germany; intravenous injection of Propofol 0.2 mg/kg/h, Fresenius Kabi Deutschland GmbH, Bad Homburg, Germany). Perioperative analgesia was induced by a one-time intravenous injection of 0.1 mg/kg Fentanyl before the operation (Rotexmedica, Trittau, Germany), as soon as a venous catheter was available. Volume substitution was performed by intravenous supply of 6% hydroxyethyl starch in isotonic saline (125 mL/operation, Fresenius Kabi Deutschland GmbH) and Ringer lactate solution (10 mL/kg/h, Fresenius Kabi Deutschland GmbH).

The surgical technique used in this study for the generation of the bone defects has been previously performed and described by our group as a minimally invasive ventrolateral vertebroplasty [33], in which lumbar defects (diameter 5 mm; depth approximately 14 mm) were created by a ventrolateral percutaneous approach and subsequently filled following a standardized protocol with a bone filler/pestle system (Medtronic, Minneapolis, MN, USA) under radiolucent control. L1 remained without a defect (untouched) and served as a normal control, the defects created in L4 were injected with CPC+fibers, and those in L5 with CPC+fibers+BMP-2. The localization of the untouched vertebral body and the cement

injections in the lumbar vertebral column was not randomized because previous investigations had shown that there were no statistically significant differences in structural bone parameters among different lumbar vertebra of young sheep (2–4 years; figure S3 in Reference [34]).

After the removal of all system components, the situs was checked to exclude bleeding, and the skin incisions were closed with skin sutures. In addition, the wound was then covered with aluminum dispersion (33 mg aluminum/g spray; CP-Pharma, Burgdorf, Germany).

The effects of CPC+fibers have been partially reported in previous publications [33,34]; thus, the current manuscript is focused on the comparison of L5 and L4 with the untouched control L1.

After the completion of surgery, animals were housed in separate pens for 1–2 weeks and then returned to long-care paddocks for 3 (short-term) or 9 months (long-term). Postoperative medication included antibiotic protection (ampicillin sodium, twice daily 10 mg/kg body weight for 4 days, Ratiopharm GmbH, Ulm, Germany; Enrofloxacin, once daily 2.5 mg/kg for 4 days, Bayer, Leverkusen, Germany), as well as antiphlogistic therapy (metamizole sodium, twice daily 2 mg/kg for 4 days, Wirtschaftsgenossenschaft Deutscher Tierärzte [WDT], Garbsen, Germany; carprofen, twice daily 2 mg/kg for 2.5 days, Pfizer Animal Health, Berlin, Germany).

To determine dynamic histomorphometric indices, sheep were given alternate intramuscular injections of oxytetracycline (20 mg/kg body weight and 10 mg lidocaine) and alizarin red (12 mg/kg body weight; both Sigma, Deisenhofen, Germany) at equal 3 months' interval. Short-term animals thus received a total of 2 injections (oxytetracycline 7 days postoperatively and alizarin red 10 days before sacrifice), long-term animals instead received a total of 4 injections (oxytetracycline 7 days and 6 months postoperatively; alizarin red 3 months postoperatively and 10 days before sacrifice).

Sample excision

The animals were sacrificed by intravenous injection of overdosed barbiturate (Pentobarbital, Essex Pharma GmbH, Munich, Germany) and subsequent application of magnesium sulfate ($MgSO_4$). The lumbar spine was removed using an oscillating bone saw and kept frozen until further use.

Measurement of bone mineral density (BMD) via digital osteodensitometry

Osteodensitometry was conducted using a software-guided digital bone density measuring instrument (DEXA QDR 4500 Elite, Hologic, Waltham, MA, USA [39,40]). To allow for an artifact-free osteodensitometry, the lumbar spine was sawn into individual vertebrae: L1, L4, and L5. The spinous and transverse processes, as well as the covering and base plates, were removed (final height in each case 15 mm) and the central, spongious area of the vertebral bodies was imaged longitudinally. The high-density injected cement was excluded from quantification by manually eliminating the respective pixel regions, and a rectangular region of interest in a transversal orientation served as a measuring field (size 9×11 mm; Fig. 1A). Osteodensitometric measurements were therefore limited to the central, spongious area of the vertebral bodies.

Analysis of bone structure via high-resolution microcomputed tomography (micro-CT)

An X-RAY WorX 225 kV tube micro-CT system with a minimal spot size below 5 µm and a flat panel detector were used for the acquisition of 3-D images (PerkinElmer 1621; CsJ as scintillator; 2,048×2,048 pixel). The following settings were used: 100 kV, 380 µA, and a prefilter of 0.5 mm copper. The distance between source and detector was 1,169.59 mm, and the distance between source and sample center was 389.37 mm. The shadow image had a size of 1,951×1,813 pixels and 3,600 images were recorded for a full 360° turn (duration 6 seconds; average of 3×2 seconds). A total of 8 frozen samples were analyzed under dry ice within 6 hours, resulting in a voxel size of 66.6 µm after reconstruction with the original Feldkamp code (Fig. 1A).

Quantitative analysis of the micro-CT data was carried out using the 3-D software VGSTUDIO MAX 2.2 (Volume Graphics GmbH, Heidelberg, Germany) and applying half-cylinders with a radius of 3.0, 4.0, and 5.0 mm. The longitudinal axis and length of the half cylinders for each individual vertebral body were defined on the basis of the respective parameters of the drill channel. The exact 3-D position of the half cylinders (e.g., rotation and depth) was chosen to exclude cortical bone. Bone volume (BV) and total volume (TV) were separately determined in the drill channel (maximal radius of 2.5 mm) and the adjacent half cylinder segments by global threshold determination (principle of onion shell). For this purpose, the respective maxima of the gray values for soft tissue, bone tissue, and cement were determined and the mean values between the maxima were used as thresholds for the volume determination of the individual components, thus excluding the consideration of the high-density injected cement.

Histologic and static/dynamic histomorphometrical measurements

After cutting the lumbar vertebral bodies in two parts directly along the axis of the cement injection channel, the analyses were carried out using two different types of histologic sections: (1) decalcified paraffin sections stained by hematoxylin and eosin [41,42] or (2) plastic-embedded sections obtained by fixation in acetone and dehydration in ascending alcohol series without demineralization. For this purpose, the samples were embedded in Technovit 9100 according to the instructions of the supplier (Heraeus Kulzer, Wehrheim, Germany [43]). Sections were then cut to a thickness of approximately 7 µm. For static histomorphometry, the

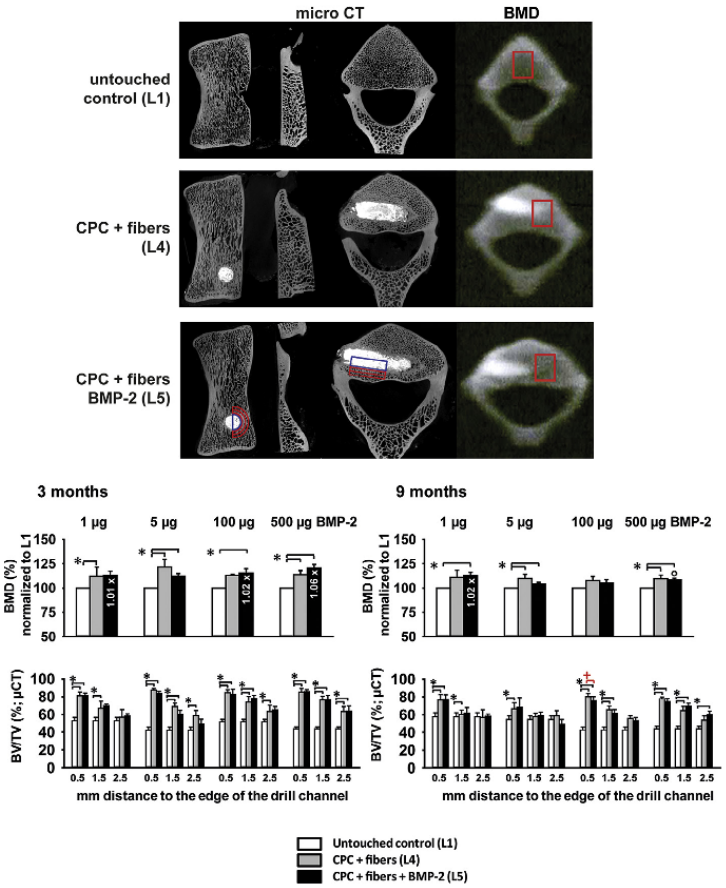

Fig. 1. (Top) Control of CPC placement by micro-CT (determination of BV/TV using onion shell regions as depicted in the two panels on the lower left); definition of region of interests (ROI) for osteodensitometry (BMD); (Middle) bone mineral density (BMD) 3 months and 9 months after surgery (n=5 for 1 and 5 µg BMP-2 group; n=6 for 100 and 500 µg BMP-2 group), as determined by osteodensitometry in differently treated lumbar vertebral bodies; (Bottom) bone volume/total volume (BV/TV) after 3 months and 9 months, as determined by micro-CT in differently treated lumbar vertebral bodies. * p≤.05 Wilcoxon test versus L1; + p ≤ .05 Wilcoxon test versus L4; ° p ≤ .05 Mann Whitney U test versus 3 months; data are expressed as means ± SEM; the fold-change in L5 (+BMP-2) versus L4 (–BMP-2) is indicated.

sections were stained with trichrome stain according to Masson-Goldner [41]; for dynamic histomorphometry the sections were left unstained (Fig. 2A).

Static histomorphometry of each individual vertebral body was performed in the immediate vicinity of the injection channel using a standard microscope (Axiovert 200 M, Carl Zeiss Microimaging GmbH, Oberkochen, Germany) with a 200-fold magnification. The respective parameters were determined according to published procedures [44–46], excluding the injected CPC from the analysis. For dynamic histomorphometry, bone induction was assessed in 10 fields of each individual vertebral body by determining the histomorphometric parameters using a standard microscope (Axiovert 200 M, Carl Zeiss Microimaging GmbH), 100-fold magnification, and the corresponding software (Axioversion 3.1, Carl Zeiss Microimaging GmbH). Total bone surface, labeled surface (single and double fluorescence lines), and interlabel distance were quantified using the ImageJ program (imagej.nih.gov). These parameters were then used to calculate the MS/BS, mineral apposition rate (MAR), and bone formation rate surface-based (BFR/BS [46]).

Biomechanical testing (compressive strength)

Biomechanical compressive strength measurements were conducted using a universal material testing machine (FPG

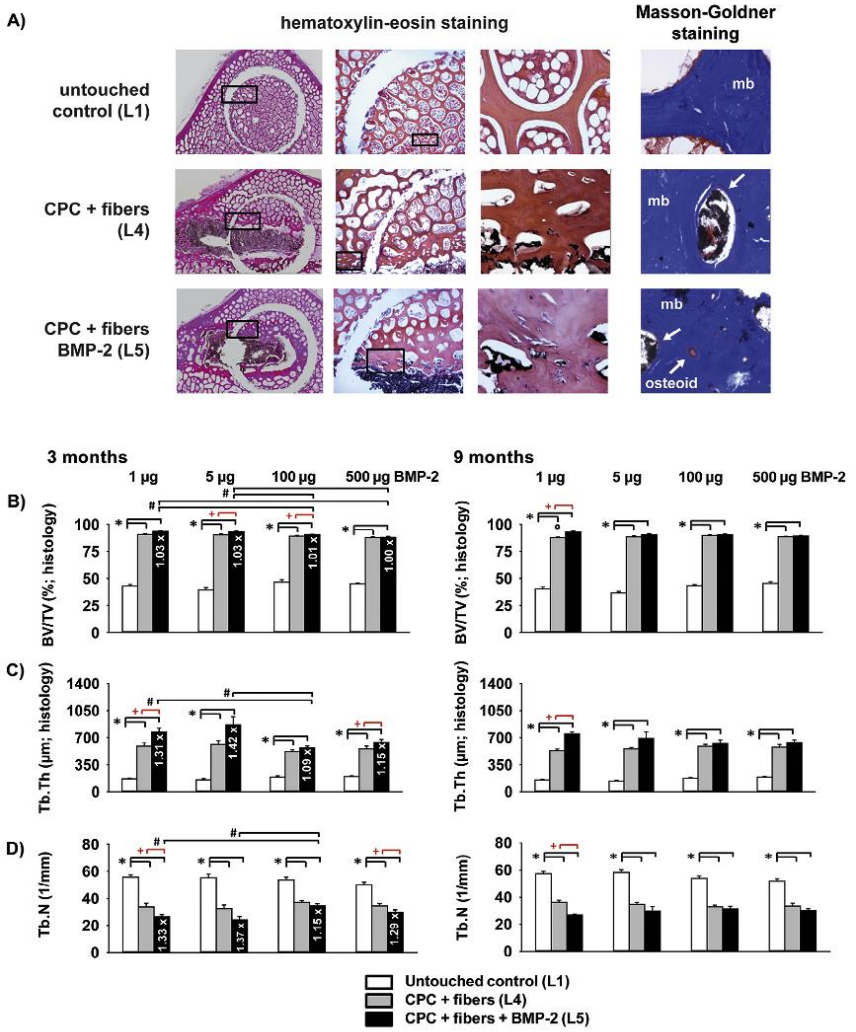

Fig. 2. (A) Representative histology images of differently treated lumbar vertebral bodies 9 months after surgery stained by hematoxylin-eosin (paraffin sections, second panel: 12.5x magnification; third panel 100x magnification) and Masson Goldner staining (plastic-embedded tissue sections, right panel: 200x magnification; white arrow: osteoid; mb: mineralized bone); untreated control (L1), CPC+fibers (L4), and CPC+fibers+BMP-2 (L5). (B—D) Structural bone parameters 3 months and 9 months after surgery (n=5 for 1 and 5 µg BMP-2 group; n=6 for 100 and 500 µg BMP-2 group), as determined by static histomorphometry in differently treated lumbar vertebral bodies: (B) bone volume/total volume (BV/TV); (C) trabecular thickness (Tb.Th); (D) trabecular number (Tb.N). * p≤.05 Wilcoxon test versus L1; + p ≤ .05 Wilcoxon test versus L4; ° p ≤ .05 Mann Whitney U test versus 3 months; # p ≤ .05 Mann Whitney U test versus indicated BMP-2 concentration; data are expressed as means ± SEM; the fold-change in L5 (+BMP-2) versus L4 (–BMP-2) is indicated.

7/20-010, Kögel, Leipzig, Germany) and the corresponding software (FRK Quicktest 2,004.01). For biomechanical testing, frozen cancellous bone cylinders (10 mm diameter × 15 mm height) were obtained from the central part of the vertebral bodies (L1, L4, L5) using a surgical diamond hollow milling cutter (diameter 10 mm). After defined thawing for exactly 30 minutes, samples were semi-confined in 2 semilunar clamps (minimal inner diameter of 10.1 mm; length 9.8 mm) and then

compressed along their longitudinal axis until fracturing. This axis was chosen because it is the main loading axis in humans and is thus of major interest for future clinical application.

Statistical methods

All results were expressed as means±SEM. Because the populations did not consistently show a normal distribution (as determined using the Shapiro-Wilk test), the non-parametric Wilcoxon signed-rank test was used for the comparison of dependent groups, and the Kruskall-Wallis multigroup and Mann-Whitney *U* tests for the comparison of independent groups. To address the problem of multiple testing and to reduce the number of individual statistical comparisons, only the parameters showing statistically significant differences among different doses of BMP-2 in the Kruskall-Wallis test were further analyzed for significant differences between individual groups. Significance was accepted at $p \leq .05$.

In addition, as all outcome parameters were expected to undergo the same direction of changes, the possibility of a type 1 error was expected to decrease.

Results

Bone densitometry

In contrast to a numerical or significant increase of the BMD in L4 (CPC+fibers) and L5 (CPC+fibers+BMP-2) compared with L1 (untouched control) in all groups, the 3-month and 9-month BMD values for L5 (+BMP-2) did not significantly differ from those for L4 (–BMP-2; Fig. 1B).

In general, the BMD values for both L4 and L5 decreased from 3 months to 9 months, with a significant difference for L5 at 500 µg BMP-2.

Upon comparison of the L5 vertebral bodies among the different dosage groups, there were no dose-dependent BMP-2 effects for this parameter at 3 or 9 months (Fig. 1B).

Micro-computed tomography (bone volume/total volume; BV/TV)

Numerical or significant increases of the BV/TV in L4 (CPC+fibers) and L5 (CPC+fibers+BMP-2) compared with L1 (untouched control) were observed in almost all groups and at all distances from the edge of the drill channel (0.5, 1.5, or 2.5 mm; with decreased effects at larger distances). However, significant differences between L5 (+BMP-2) and L4 (–BMP-2) were only observed at 9 months for 100 µg BMP-2 at the distance 0.5 mm (Fig. 1C).

The BV/TV values for both L4 and L5 decreased from 3 months to 9 months, however, without significant differences between the 2 time points (Fig. 1C).

As for the BMD, there were no dose-dependent BMP-2 effects at 3 or 9 months.

Histologic analysis

Bone volume/total volume (BV/TV)

In representative 9-month histology images of untouched controls (L1) and treated vertebral bodies (L4: CPC+fibers; L5: CPC+fibers+BMP-2), L4 and L5 showed a dense bony layer in the vicinity of the injection channel (Fig. 2A). Also, there was bone formation in the cement region of the vertebral bodies. There were no signs of inflammatory infiltration close to or distant from the injection channel in either L4 or L5 at any time point.

In parallel to a significant increase of the BV/TV in L4 (CPC+fibers) and L5 (CPC+fibers+BMP-2) compared with L1 (untouched control) in all groups, all BV/TV values for L5 (+BMP-2) were numerically higher than those for L4 (–BMP-2) for all doses of BMP-2. Significant differences between L5 and L4 were observed for 5 µg and 100 µg BMP-2 at 3 months, as well as for 1 µg at 9 months ($p<.05$; Fig. 2B).

The BV/TV values for both L4 and L5 only moderately decreased from 3 months to 9 months, with only one significant difference for L4 in the 1 µg BMP-2 group (Fig. 2B).

At 3 months, maximal BMP-2 effects were observed at 1 µg and 5 µg (with a significant decrease of the effects from 1 µg and 5 µg to 100 and 500 µg BMP-2; Fig. 2B).

Trabecular thickness (Tb.Th)

Concerning the significant increases in L4 and L5 versus L1, the results for the Tb.Th were identical to those for the BV/TV (compare Fig. 2C with Fig. 2B).

As for the BV/TV, all 3-month and 9-month Tb.Th values for L5 (+BMP-2) were higher than those for L4 (–BMP-2) for all doses of BMP-2 ($p<.05$ versus L4 for 1 µg and 500 µg BMP-2 at 3 months, as well as for 1 µg at 9 months; Fig. 2C). The highest fold-increases in the comparison between L5 and L4 were observed for 5 µg BMP-2 at 3 months (1.42-fold), as well as for 1 µg BMP-2 at 9 months (1.41-fold; not indicated).

There was no significant decrease of the Tb.Th values from 3 months to 9 months in any group (Fig. 2C).

Similar to the BV/TV, maximal BMP-2 effects at 3 months were observed for 5 µg (with a significant decrease from 1 µg and 5 µg to 100 µg BMP-2; Fig. 2C).

Trabecular number (Tb.N)

In contrast to the results for BV/TV and Tb.Th, there was a significant decrease of the Tb.N in L4 (CPC+fibers) and L5 (CPC+fibers+BMP-2) compared with L1 (untouched control) in all groups (Fig. 2D).

Also, the Tb.N for L5 (+BMP-2) was lower than for L4 (–BMP-2) in all groups ($p<.05$ versus L4 for 1 µg and 500 µg BMP-2 at 3 months, as well as for 1 µg BMP-2 at 9 months; Fig. 2D).

There were no significant changes of the Tb.N from 3 months to 9 months in any group (Fig. 2D).

As already noted for BV/TV and Tb.Th, maximal BMP-2 effects for the Tb.N at 3 months were observed at 5 µg (again

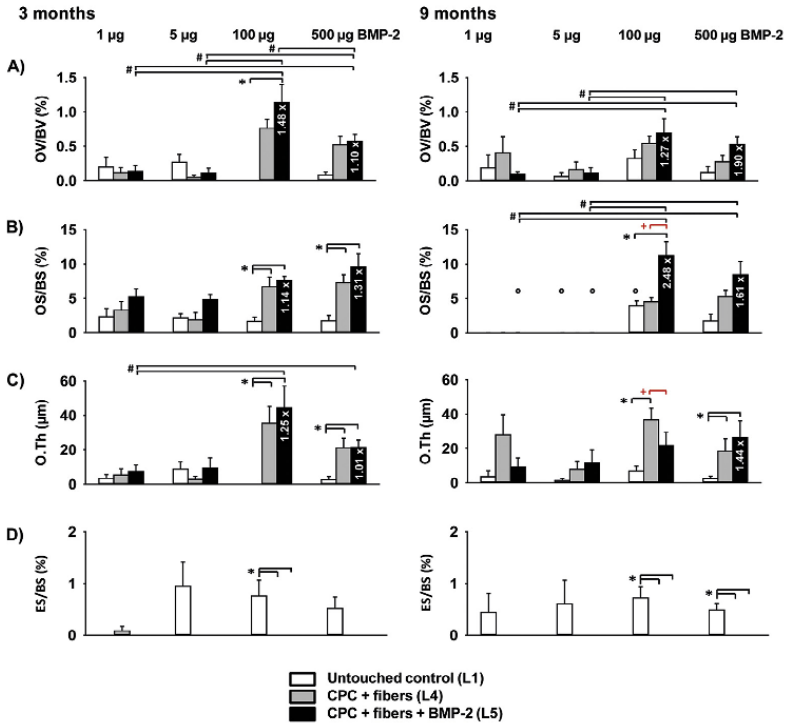

Fig. 3. (A–D) Bone formation and erosion parameters 3 months and 9 months after surgery (n=5 for 1 and 5 µg BMP-2 group; n=6 for 100 and 500 µg BMP-2 group), as determined by static histomorphometry in differently treated lumbar vertebral bodies: (A) osteoid volume (OV/BV); (B) osteoid surface (OS/BS); (C) osteoid thickness (O.Th); (D) eroded surface (ES/BS). * p≤.05 Wilcoxon test versus L1; ° p≤.05 Mann Whitney U test versus 3 months; # p≤.05 Mann Whitney U test versus indicated BMP-2 concentration; data are expressed as means±SEM; the fold-change in L5 (+BMP-2) versus L4 (–BMP-2) is indicated.

with a significant decrease from 1 µg and 5 µg to 100 µg BMP-2; Fig. 2D).

Osteoid volume/bone volume (OV/BV)

A significant increase of the OV/BV compared with L1 (untouched control) was only observed in the 3 month groups and only for L5 (CPC+fibers+BMP-2; 100 µg BMP-2). For this parameter, there were no significant differences between L5 (+BMP-2) and L4 (–BMP-2), or between 3 and 9 months in any group (Fig. 3A).

Maximal BMP-2 effects at 3 and 9 months were observed for 100 µg (with a significant increase at 3 months and 9 months from 1 and 5 µg to 100 µg and 500 µg BMP-2; Fig. 3A).

Osteoid surface/bone surface (OS/BS)

Significant increases of the OS/BS in comparison with L1 (untouched control) were observed for L4 (CPC+fibers) in the 100 and 500 µg BMP-2 group at 3 months and for L5 (CPC+fibers+BMP-2) in the 100 and 500 µg BMP-2 group at 3 months and the 100 µg BMP-2 group at 9 months (Fig. 3B). In the latter group, the OS/BS in L5 (+BMP-2) was also significantly higher than in L4 (–BMP-2; Fig. 3B).

For selected groups, especially in the low-dose BMP-2 range, there was a significant decrease of the OS/BS values from 3 months to 9 months (Fig. 3B).

As for the OV/BV, maximal BMP-2 effects were observed for 100 µg at 9 months (with a significant increase from 1 and 5 µg to 100 µg and 500 µg BMP-2; Fig. 3B).

Osteoid thickness (O.Th)

Similar to the OS/BS, the O.Th displayed significant increases in comparison to L1 (untouched control) for L4 (CPC+fibers) in the 100 and 500 µg BMP-2 group at 3 and 9 months and for L5 (CPC+fibers+BMP-2) in the 100 and 500 µg BMP-2 group at 3 months and the 500 µg BMP-2 group at 9 months (Fig. 3C). In the 100 µg BMP-2 group at 9 months, the O.Th in L5 (+BMP-2) was significantly lower than in L4 (–BMP-2; Fig. 3C).

There were no significant differences between the 3 and 9 months values in any group (Fig. 3C).

As described above for OV/BV at 3 and 9 months and for OS/BS at 9 months, maximal BMP-2 effects were observed for 100 µg at 3 months (with a significant increase from 1 µg to 100 µg and 500 µg BMP-2; Fig. 3C).

Eroded surface/bone surface (ES/BS)

Interestingly, significant decreases of the ES/BS compared with L1 (untouched control) were observed for both L4 (CPC+fibers) and L5 (CPC+fibers+BMP-2) in the 100 µg BMP-2 group at 3 months and the 100 and 500 µg BMP-2 group at 9 months (Fig. 3D).

For this parameter, there were no significant differences between L5 (+BMP-2) and L4 (–BMP-2), between the 3 and 9 months values, or among the different BMP-2 doses (Fig. 3D).

Mineralizing surface/bone surface (MS/BS)

In parallel to a significant increase of the MS/BS in L4 (CPC+fibers) and L5 (CPC+fibers+BMP-2) compared with L1 (untouched control) in all groups, the MS/BS in L5 (+BMP-2) for 100 µg BMP-2 at 3 months was also significantly higher than in L4 (–BMP-2; Fig. 4A).

The respective MS/BS values were stable over time or even increased from 3 to 9 months, with significant differences in selected L4 or L5 groups (Fig. 4A).

Maximal BMP-2 effects were observed for 100 µg at 3 months (with a significant increase from 1 and 5 µg to 100 µg and 500 µg BMP-2; Fig. 3A).

Mineral apposition rate (MAR) and bone formation rate surface based (BFR/BS)

In the 3 month groups, no double lines were observed, and the MAR and BFR/BS could therefore not be calculated. At 9 months, there was a significant increase of the MAR or BFR/BS compared with L1 (untouched control) for L4 (CPC+fibers) in the 1 µg and 500 µg BMP-2 groups and for L5 (CPC+fibers+BMP-2) in the 1 µg and 500 µg BMP-2 groups (Figs. 4B and 4C).

For these parameters, there were no significant differences between L5 (+BMP-2) and L4 (–BMP-2), or between the 3 and 9 months' values, but dose-dependent, significant increases of the BMP-2 effects for the BFR/BS from 1 µg and 5 µg to 500 µg BMP-2 (maximum effects for both parameters at 100 or 500 µg; Figs. 4B and 4C).

Compressive strength

Interestingly, at 3 months, L5 (+BMP-2) showed a significantly higher compressive strength compared with L1 (untouched control) for 500 µg BMP-2 and compared with L4 (–BMP-2) for 100 µg BMP-2 (1.15-fold increase; Fig. 5).

The values were stable or slightly decreased from 3 to 9 months (Fig. 5).

For this parameter, there were no dose-dependent BMP-2 effects at 3 or 9 months (Fig. 5).

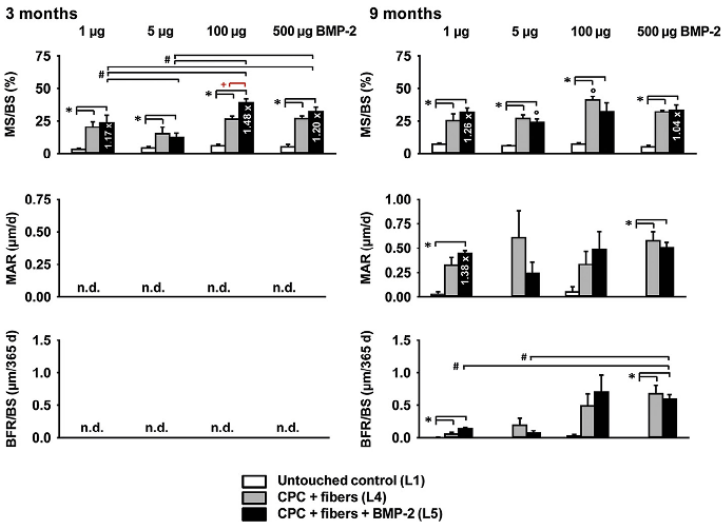

Fig. 4. (–Top to Bottom) Bone formation parameters 3 months and 9 months after surgery (n=5 for 1 and 5 µg BMP-2 group; n=6 for 100 and 500 µg BMP-2 group), as determined by dynamic histomorphometry in differently treated lumbar vertebral bodies; (Top) mineralizing surface/bone surface (MS/BS); (Middle) mineral apposition rate (MAR; n.d.: not detected); (Bottom) bone formation rate (BFR/BS; n.d.: not detected). * p≤.05 Wilcoxon test versus L1; + p ≤ .05 Wilcoxon test versus L4; # p ≤ .05 Mann Whitney U test versus indicated BMP-2 concentration; data are expressed as means ± SEM; the fold-change in L5 (+BMP-2) versus L4 (–BMP-2) is indicated.

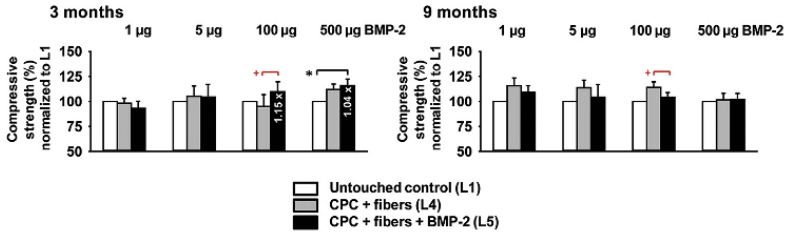

Fig. 5. Compressive strength of cancellous bone cylinders 3 months and 9 months after surgery (n=5 for 1 and 5 µg BMP-2 group; n=6 for 100 and 500 µg BMP-2 group) in differently treated lumbar vertebral bodies. * p≤.05 Wilcoxon test versus L1; + p ≤ .05 Wilcoxon test versus L4; data are expressed as means ± SEM; the fold-change in L5 (+BMP-2) versus L4 (–BMP-2) is indicated.

Discussion

On the basis of the extended clinical use of BMP-2 for the promotion of bone repair [22], the present study aimed at investigating the influence of loading BMP-2 into a PLGA fiber-reinforced CPC on bone regeneration in a sheep model of lumbar osteopenia.

The present results indicated the following aspects: (1) both BMP-2-free and BMP-2-loaded CPC significantly enhanced bone formation via changes in bone structure, formation, and resorption (e.g., BV/TV and Tb.Th; OS/BS and MS/BS; as well as ES/BS); (2) BMP-2-loaded CPC even significantly augmented bone formation in comparison to BMP-2-free CPC, with a subsequent, significant increase of the compressive strength at 3 months (maximum 1.15-fold); (3) BMP-2 effects showed a clear dose dependence, with maximal effects between 5 and 100 µg; (4) there were no signs of inflammatory infiltration after the use of BMP-2-free or BMP-2-loaded CPC, underlining the high biocompatibility of all its components [22]. The present study thus shows that the application of BMP-2 for the treatment of lumbar vertebral defects not only enhances bone formation and bone structure, but also at least temporarily strengthens the functionality of trabecular bone. It also confirms the suitability of the present physiological and convenient osteopenia model for the analysis of vertebral augmentation with resorbable and osteoconductive CPC [33], as well as for dose-response studies with BMP-2 [34,47]. Despite the considerably more time- and resource-consuming induction procedure, further support for the efficacy of doses as low as ≤100 µg BMP-2 to augment middle to long-term bone formation would be derived from the confirmation of the effects in models with induced osteoporosis and osteoporotic compression fractures [48,49].

Effects of the PLGA fiber-reinforced CPC

The enhancement of bone formation by PLGA fiber-reinforced CPC is in line with the known osteoconductive effects of CPC with different compositions [50–52], without any suppressive effect on bone formation [34,52].

Early versus late effects of BMP-2

Some of the parameters measured in the present study indicated exclusively early effects of BMP-2 (MS/BS) or exclusively late effects of BMP-2 (OS/BS and O.Th), whereas several parameters supported an inductive effect of BMP-2 at both the early and the late time point (BV/TV [histology], Tb.Th, Tb.N). The fact that bone formation parameters such as MS/BS showed a reaction already at the early time point of 3 months is consistent with the knowledge that bone healing initiates very rapidly after injury and leads to load-bearing fracture healing already after approximately 6 weeks ([53,54]; own unpublished work). On the other hand, several bone structure or bone formation parameters still showed significant effects of BMP-2 at 9 months, supporting a middle to long-term effect of BMP-2 after a single therapeutic application (in analogy to growth and differentiation factor-5 [GDF5] [55,56].

Dose-dependence of BMP-2 effects

Several parameters indicated a dose-dependence of the BMP-2 effects, with maximal effects of 5 µg for the bone structure parameters BV/TV, Tb.Th, and Tb.N, but maximal effects of 100 µg for bone formation parameters such as OV/BV, OS/BS, O.Th, MS/BS, and BFR/BS (at 3 and 9 months). Because the application of 500 µg generally did not further enhance the bone regeneration, 100 µg BMP-2 (i.e., 20- to 400-fold less than previously used in clinical studies [31]) seems to be the maximal local dose needed for the augmentation of bone formation by BMP-2 in the present system.

There are several arguments in favor of a potential clinical relevance or significance of this particular BMP-2 dose, with the aim of improving the stability of the bone to avoid refracturing of the stabilized fracture and to counteract the local catabolic process. These are the remarkable fold-change effects especially in the bone formation parameters, significant effects on the compressive strength at 100 µg (although limited and possibly short-term), and the high effect sizes for dose-dependent differences among the various doses of BMP-2 (between 2.10 and 3.75; i.e., well above the effect

sizes between 0.5 and 1.0 usually assumed in clinical studies). Such improvements may be critical for the long-term improvement of the quality of life for the individual and may justify the additional cost.

Interestingly, other studies in sheep have identified optimal concentrations of BMP-2 comparable with the one in the present study, for example, approximately 10 µg for the osseointegration of titanium implants coated with CPC+BMP-2 [57], or the bone augmentation in an alveolar segmental osteotomy model [30]. Other studies using much higher doses of BMP-2 in other systems (1.05–10.5 mg), although in line with the clinically applied doses, are only partially comparable with the present results, because there was no further enhancement of the effects by 500 µg BMP-2 in the present study [29,58].

It remains to be determined whether the present formulation of the BMP-2-loaded CPC, in which a homogeneous distribution of the BMP-2 with sustained release can be assumed, is suitable for therapy or whether modifications of the delivery system are required to optimize the release kinetics of the biologically active growth factor [59–61].

Cellular effects of BMP-2

The present results also showed that BMP-2 influenced both bone formation (OV/BV, OS/BS, O.Th) and bone resorption parameters such as ES/BS. This is in agreement with the accepted role of BMP-2 in inducing the differentiation and/or activation of both osteoblasts and osteoclasts [62]. This suggests a combined direct or indirect influence of BMP-2 on anabolic and catabolic aspects of bone regeneration, as previously shown for BMP-7 [63]. This combined effect may further enhance the positive action of BMP-2 on bone regeneration. On the other hand, the fact that the structural parameters BV/TV and Tb.Th are still strongly elevated above the level of the untouched bone at 9 months indicates that bone remodeling and the return to physiological levels is not yet completed.

In selected cases (BV/TV assessed by micro-CT, O.Th, and compressive strength; all at 9 months for 100 µg), the addition of BMP-2 to the CPC led to significantly lower values, suggesting a negative effect of BMP-2 on bone formation and/or bone structure. This indicates that the local dose of BMP-2 will have to be carefully titered to exclude inhibiting effects of this BMP on the structure or quality of bone ([47]; own unpublished work).

Adverse effects of BMP-2

Because this was not designed as a safety study, a systematic assessment of the safety profile of the PLGA fiber-reinforced, BMP-2-loaded CPC was not possible. However, there were no signs of adverse effects (e.g., ectopic bone formation or osteolysis, disability or poor outcome, leg or back pain, swelling or wound complications, subsidence or displacement of the implant, urogenital events, and radiculitis) previously reported after the spinal application of high-dose BMP-2 (as high as 1.95–40 mg [31]). In addition, there were no signs of local inflammatory infiltration after the use of the PLGA fiber-reinforced, BMP-2-loaded CPC at any time point, indicating that the cement components have no or negligible pro-inflammatory effects. Furthermore, as previously published, there were no signs of systemic intravascular leakage after CPC injection [64]. Finally, the suggested local dose of 100 µg BMP-2 is between 20 and 400 times lower than the previously applied clinical doses of BMP-2. Although systematic safety studies are clearly needed, the safety profile of low-dose BMP-2 in the present sheep model appears favorable.

Conclusion

BMP-2 significantly augmented the bone formation induced by a PLGA fiber-reinforced CPC in sheep lumbar osteopenia for at least 3 months, thus showing prolonged effects after a single therapeutic application. This included a strengthening of the stability of trabecular bone, as shown by a maximum 1.15-fold increase of the compressive strength, presumably on the basis of both inherent stability of the CPC and strengthening of the bone structure [16,64]. The results indicated that local doses of ≤100 µg BMP-2 may be sufficient for bone induction. Because there were no signs of local or systemic inflammation, all components of BMP-2-free and BMP-2-loaded CPC appeared to be highly biocompatible.

The novel BMP-2-loaded CPC may thus be a suitable candidate to replace the bioinert, non-resorbable, supraphysiologically stiff PMMA cements currently applied in the vertebroplasty/kyphoplasty of osteoporotic vertebral fractures. This approach may also be extended to broader clinical applications such as the therapy of periodontal bone defects or the augmentation of surgical screws.

Acknowledgment

We gratefully acknowledge the financial support by the Carl Zeiss Foundation (doctoral candidate scholarship to S.M.) and the German Federal Ministry of Education and Research (BMBF FKZ 0316205C to J.B and K.D.J.; BMBF FKZ 035577D, 0316205B, and 13N12601 to R.W.K). We gratefully acknowledge the partial financial support of the Deutsche Forschungsgemeinschaft (DFG), grant reference INST 275/241-1 FUGG to K.D.J., and the Thüringer Ministerium für Bildung, Wissenschaft und Kultur (TMBWK), grant reference 62-4264 925/1/10/1/01 to K.D.J.

Nicolas Guena and Alain Lerch, Kasios, are gratefully acknowledged for providing Jectos cement. We gratefully acknowledge E. Mark for performing the osteodensitometry analyses, S. Födisch, G. Grunert, U. Körner, C. Müller, and B. Ukena for excellent technical assistance, and

Dipl.-Sportwiss. E. Kurz and Prof. P. Schlattman for expert statistical advice.

References

[1] Hernlund E, Svedbom A, Ivergard M, Compston J, Cooper C, Stenmark J, et al. Osteoporosis in the European Union: medical management, epidemiology and economic burden. A report prepared in collaboration with the International Osteoporosis Foundation (IOF) and the European Federation of Pharmaceutical Industry Associations (EFPIA). Arch Osteoporos 2013;8:136.

[2] Reginster JY, Burlet N. Osteoporosis: a still increasing prevalence. Bone 2006;38:S4–9.

[3] Teyssedou S, Saget M, Pries P. Kyphopasty and vertebroplasty. Orthop Traumatol Surg Res 2014;100:S169–79.

[4] Ates A, Gemalmaz HC, Deveci MA, Simsek SA, Cetin E, Senkoylu A. Comparison of effectiveness of kyphoplasty and vertebroplasty in patients with osteoporotic vertebra fractures. Acta Orthop Traumatol Turc 2016;50:619–22.

[5] Hulme PA, Krebs J, Ferguson SJ, Berlemann U. Vertebroplasty and kyphoplasty: a systematic review of 69 clinical studies. Spine 2006; 31:1983–2001.

[6] Nouda S, Tomita S, Kin A, Kawahara K, Kinoshita M. Adjacent vertebral body fracture following vertebroplasty with polymethylmethacrylate or calcium phosphate cement: biomechanical evaluation of the cadaveric spine. Spine 2009;34:2613–18.

[7] Trout AT, Kallmes DF, Kaufmann TJ. New fractures after vertebroplasty: adjacent fractures occur significantly sooner. AJNR Am J Neuroradiol 2006;27:217–23.

[8] Uppin AA, Hirsch JA, Centenera LV, Pfiefer BA, Pazianos AG, Choi IS. Occurrence of new vertebral body fracture after percutaneous vertebroplasty in patients with osteoporosis. Radiology 2003;226:119–24.

[9] Blattert TR, Jestaedt L, Weckbach A. Suitability of a calcium phosphate cement in osteoporotic vertebral body fracture augmentation: a controlled, randomized, clinical trial of balloon kyphoplasty comparing calcium phosphate versus polymethylmethacrylate. Spine 2009;34:108–14.

[10] Burguera EF, Xu HH, Weir MD. Injectable and rapid-setting calcium phosphate bone cement with dicalcium phosphate dihydrate. J Biomed Mater Res B Appl Biomater 2006;77:126–34.

[11] Maestretti G, Sutter P, Monnard E, Ciarpaglini R, Wahl P, Hoogewoud H, et al. A prospective study of percutaneous balloon kyphoplasty with calcium phosphate cement in traumatic vertebral fractures: 10-year results. Eur Spine J 2014;23:1354–60.

[12] Khandaker M, Meng Z. The effect of nanoparticles and alternative monomer on the exothermic temperature of PMMA bone cement. Procedia Eng 2015;105:946–52.

[13] Wilke HJ, Mehnert U, Claes LE, Bierschneider MM, Jaksche H, Boszczyk BM. Biomechanical evaluation of vertebroplasty and kyphoplasty with polymethyl methacrylate or calcium phosphate cement under cyclic loading. Spine 2006;31:2934–41.

[14] Gorst NJ, Perrie Y, Gbureck U, Hutton AL, Hofmann MP, Grover LM, et al. Effects of fibre reinforcement on the mechanical properties of brushite cement. Acta Biomater 2006;2:95–102.

[15] Xu HH, Weir MD, Burguera EF, Fraser AM. Injectable and macroporous calcium phosphate cement scaffold. Biomaterials 2006;27:4279–87.

[16] Maenz S, Kunisch E, Muhlstadt M, Bohm A, Kopsch V, Bossert J, et al. Enhanced mechanical properties of a novel, injectable, fiber-reinforced brushite cement. J Mech Behav Biomed Mater 2014;39:328–38.

[17] Maenz S, Hennig M, Muhlstadt M, Kunisch E, Bungartz M, Brinkmann O, et al. Effects of oxygen plasma treatment on interfacial shear strength and post-peak residual strength of a PLGA fiber-reinforced brushite cement. J Mech Behav Biomed Mater 2016;57:347–58.

[18] Verron E, Khairoun I, Guicheux J, Bouler JM. Calcium phosphate biomaterials as bone drug delivery systems: a review. Drug Discov Today 2010;15:547–52.

[19] Urist MR. Bone: formation by autoinduction. Science 1965;150:893–9.

[20] Reddi AH, Huggins C. Biochemical sequences in the transformation of normal fibroblasts in adolescent rats. Proc Natl Acad Sci USA 1972;69:1601–5.

[21] Mi M, Jin H, Wang B, Yukata K, Sheu TJ, Ke QH, et al. Chondrocyte BMP2 signaling plays an essential role in bone fracture healing. Gene 2013;512:211–18.

[22] Scarfi S. Use of bone morphogenetic proteins in mesenchymal stem cell stimulation of cartilage and bone repair. World J Stem Cells 2016; 8:1–12.

[23] Kwiatkowski W, Gray PC, Choe S. Engineering TGF-beta superfamily ligands for clinical applications. Trends Pharmacol Sci 2014;35:648–57.

[24] Turgeman G, Zilberman Y, Zhou S, Kelly P, Moutsatsos IK, Kharode YP, et al. Systemically administered rhBMP-2 promotes MSC activity and reverses bone and cartilage loss in osteopenic mice. J Cell Biochem 2002;86:461–74.

[25] Sarban S, Senkoylu A, Isikan UE, Korkusuz P, Korkusuz F. Can rhBMP-2 containing collagen sponges enhance bone repair in ovariectomized rats?: a preliminary study. Clin Orthop Relat Res 2009;467:3113–20.

[26] Zegzula HD, Buck DC, Brekke J, Wozney JM, Hollinger JO. Bone formation with use of rhBMP-2 (recombinant human bone morphogenetic protein-2). J Bone Joint Surg Am 1997;79:1778–90.

[27] Li M, Liu X, Ge B. Calcium phosphate cement with BMP-2-loaded gelatin microspheres enhances bone healing in osteoporosis: a pilot study. Clin Orthop Relat Res 2010;468:1978–85.

[28] Egermann M, Baltzer AW, Adamaszek S, Evans C, Robbins P, Schneider E, et al. Direct adenoviral transfer of bone morphogenetic protein-2 cDNA enhances fracture healing in osteoporotic sheep. Hum Gene Ther 2006;17:507–17.

[29] Pobloth AM, Duda GN, Giesecke MT, Dienelt A, Schwabe P. High-dose recombinant human bone morphogenetic protein-2 impacts histological and biomechanical properties of a cervical spine fusion segment: results from a sheep model. J Tissue Eng Regen Med 2015;doi:10.1002/term.2049.

[30] Rachmiel A, Aizenbud D, Peled M. Enhancement of bone formation by bone morphogenetic protein-2 during alveolar distraction: an experimental study in sheep. J Periodontol 2004;75:1524–31.

[31] Carragee EJ, Hurwitz EL, Weiner BK. A critical review of recombinant human bone morphogenetic protein-2 trials in spinal surgery: emerging safety concerns and lessons learned. Spine J 2011;11:471–91.

[32] Poynton AR, Lane JM. Safety profile for the clinical use of bone morphogenetic proteins in the spine. Spine 2002;27:S40–8.

[33] Bungartz M, Maenz S, Kunisch E, Horbert V, Xin L, Gunnella F, et al. First-time systematic postoperative clinical assessment of a minimally invasive approach for lumbar ventrolateral vertebroplasty in the large animal model sheep. Spine J 2016;16:1263–75.

[34] Maenz S, Brinkmann O, Kunisch E, Horbert V, Gunnella F, Bischoff S, et al. Enhanced bone formation in sheep vertebral bodies after minimally invasive treatment with a novel, PLGA fiber-reinforced brushite cement. Spine J 2017;17:709–19.

[35] Sachse A, Wagner A, Keller M, Wagner O, Wetzel WD, Layher F, et al. Osteointegration of hydroxyapatite-titanium implants coated with nonglycosylated recombinant human bone morphogenetic protein-2 (BMP-2) in aged sheep. Bone 2005;37:699–710.

[36] Borsari V, Fini M, Giavaresi G, Rimondini L, Consolo U, Chiusoli L, et al. Osteointegration of titanium and hydroxyapatite rough surfaces in healthy and compromised cortical and trabecular bone: in vivo comparative study on young, aged, and estrogen-deficient sheep. J Orthop Res 2007;25:1250–60.

[37] Alaee F, Hong SH, Dukas AG, Pensak MJ, Rowe DW, Lieberman JR. Evaluation of osteogenic cell differentiation in response to bone

morphogenetic protein or demineralized bone matrix in a critical sized defect model using GFP reporter mice. J Orthop Res 2014;32:1120–8.
[38] Faul F, Erdfelder E, Buchner A, Lang AG. Statistical power analyses using G*Power 3.1: tests for correlation and regression analyses. Behav Res Methods 2009;41:1149–60.
[39] Turner AS. The sheep as a model for osteoporosis in humans. Vet J 2002;163:232–9.
[40] Syed Z, Khan A. Bone densitometry: applications and limitations. J Obstet Gynaecol Can 2002;24:476–84.
[41] Plenck HJ. Untersuchung des binde- und stützgewebes (Trichromfärbung nach goldner). In: Böck P, editor. Romeis—mikroskopische technik. Munich, Germany: Urban und Schwarzenberg Verlag; 1989. p. 499.
[42] Knutsen G, Engebretsen L, Ludvigsen TC, Drogset JO, Grontvedt T, Solheim E, et al. Autologous chondrocyte implantation compared with microfracture in the knee. A randomized trial. J Bone Joint Surg Am 2004;86-A:455–64.
[43] Donath K, Breuner G. A method for the study of undecalcified bones and teeth with attached soft tissues. The Sage-Schliff (sawing and grinding) technique. J Oral Pathol 1982;11:318–26.
[44] Parfitt AM, Drezner MK, Glorieux FH, Kanis JA, Malluche H, Meunier PJ, et al. Bone histomorphometry: standardization of nomenclature, symbols, and units. Report of the ASBMR Histomorphometry Nomenclature Committee. J Bone Miner Res 1987;2:595–610.
[45] Delling G. Endokrine osteopathien. Stuttgart, Germany: Gustav Fischer Verlag; 1975.
[46] Dempster DW, Compston JE, Drezner MK, Glorieux FH, Kanis JA, Malluche H, et al. Standardized nomenclature, symbols, and units for bone histomorphometry: a 2012 update of the report of the ASBMR Histomorphometry Nomenclature Committee. J Bone Miner Res 2013;28:2–17.
[47] Zara JN, Siu RK, Zhang X, Shen J, Ngo R, Lee M, et al. High doses of bone morphogenetic protein 2 induce structurally abnormal bone and inflammation in vivo. Tissue Eng Part A 2011;17:1389–99.
[48] Eschler A, Ropenack P, Herlyn PK, Roesner J, Pille K, Busing K, et al. The standardized creation of a lumbar spine vertebral compression fracture in a sheep osteoporosis model induced by ovariectomy, corticosteroid therapy and calcium/phosphorus/vitamin D-deficient diet. Injury 2015;46(Suppl. 4):S17–23.
[49] Eschler A, Roepenack P, Roesner J, Herlyn PK, Martin H, Reichel M, et al. Cementless titanium mesh fixation of osteoporotic burst fractures of the lumbar spine leads to bony healing: results of an experimental sheep model. Biomed Res Int 2016;2016:4094161.
[50] Theiss F, Apelt D, Brand B, Kutter A, Zlinszky K, Bohner M, et al. Biocompatibility and resorption of a brushite calcium phosphate cement. Biomaterials 2005;26:4383–94.
[51] Hannink G, Wolke JG, Schreurs BW, Buma P. In vivo behavior of a novel injectable calcium phosphate cement compared with two other commercially available calcium phosphate cements. J Biomed Mater Res B Appl Biomater 2008;85:478–88.
[52] Dagang G, Haoliang S, Kewei X, Yong H. Long-term variations in mechanical properties and in vivo degradability of CPC/PLGA composite. J Biomed Mater Res B Appl Biomater 2007;82:533–44.
[53] Einhorn TA, Gerstenfeld LC. Fracture healing: mechanisms and interventions. Nat Rev Rheumatol 2015;11:45–54.
[54] Rüedi TP, Buckley RE, Moran CG. Priciples of fracture management. 2nd ed. Stuttgart: Thieme; 2007.
[55] Gruber RM, Ludwig A, Merten HA, Pippig S, Kramer FJ, Schliephake H. Sinus floor augmentation with recombinant human growth and differentiation factor-5 (rhGDF-5): a pilot study in the Goettingen miniature pig comparing autogenous bone and rhGDF-5. Clin Oral Implants Res 2009;20:175–82.
[56] Bungartz M, Kunisch E, Maenz S, Horbert V, Xin L, Gunnella F, et al. GDF5 significantly augments the bone formation induced by an injectable, PLGA-fiber reinforced, brushite-forming cement in a sheep defect model of lumbar osteopenia. Spine J 2017;doi:10.1016/j.spinee.2017.06.007. pii: S1529-9430(17)30269-3. [Epub ahead of print].
[57] Hunziker EB, Jovanovic J, Horner A, Keel MJ, Lippuner K, Shintani N. Optimisation of BMP-2 dosage for the osseointegration of porous titanium implants in an ovine model. Eur Cell Mater 2016;32:241–56.
[58] Pelletier MH, Oliver RA, Christou C, Yu Y, Bertollo N, Irie H, et al. Lumbar spinal fusion with beta-TCP granules and variable Escherichia coli-derived rhBMP-2 dose. Spine J 2014;14:1758–68.
[59] King WJ, Krebsbach PH. Growth factor delivery: how surface interactions modulate release in vitro and in vivo. Adv Drug Deliv Rev 2012;64:1239–56.
[60] Kempen DH, Lu L, Hefferan TE, Creemers LB, Maran A, Classic KL, et al. Retention of in vitro and in vivo BMP-2 bioactivities in sustained delivery vehicles for bone tissue engineering. Biomaterials 2008;29:3245–52.
[61] Luginbuehl V, Meinel L, Merkle HP, Gander B. Localized delivery of growth factors for bone repair. Eur J Pharm Biopharm 2004;58:197–208.
[62] Giannoudis PV, Kanakaris NK, Einhorn TA. Interaction of bone morphogenetic proteins with cells of the osteoclast lineage: review of the existing evidence. Osteoporos Int 2007;18:1565–81.
[63] Maurer T, Zimmermann G, Maurer S, Stegmaier S, Wagner C, Hansch GM. Inhibition of osteoclast generation: a novel function of the bone morphogenetic protein 7/osteogenic protein 1. Mediators Inflamm 2012;2012:171209.
[64] Xin L, Bungartz M, Maenz S, Horbert V, Hennig M, Illerhaus B, et al. Decreased extrusion of calcium phosphate cement versus high viscosity PMMA cement into spongious bone marrow-an ex vivo and in vivo study in sheep vertebrae. Spine J 2016;16:1468–77.

6. DISCUSSION

The work described in the present thesis aimed at developing an injectable, poly (l-lactide-co-glycolide) acid (PLGA)-fiber reinforced, brushite-forming cement (CPC) containing low-dose bone morphogenetic protein BMP-2, which can be used to replace the bioinert, non-resorbable, supraphysiologically stiff PMMA cements currently applied for the vertebroplasty/kyphoplasty of osteoporotic vertebral fractures. In order to confirm the novel PLGA-reinforced CPC as a suitable carrier for BMPs, the first study analyzed the quantity and bioactivity of BMPs released from CPC. Depending on the applied dosage and sample geometry, 25.7% of BMP-2 (within 14 days), between 10 and 34% of GDF5, and between 6 and 17% of BB-1 (within 30/31 days) were released in a bioactive configuration from the CPC, and this release was augmented by the presence of PLGA fibers, suggesting an active contribution of the bioactive BMPs to the healing of bone defects in vivo and validating the CPC as a long-lasting depot-system for a sustained release of the protein.

The development of new drugs or implant devices in the context of osteoporosis requires suitable animal models. The United States Food and Drug Administration (FDA) recommends that new therapeutic agents should undergo testing in the ovariectomized (OVX) rat and in a second, non-rodent, large animal model with intracortical bone remodeling. Beside other animals, e.g. dogs, goats or primates, sheep have been most often used in previous orthopedic field of research, for their similarities to humans regarding bone structure, and anatomy of the thoracic and lumbar spine. For this reason, the second part of the study aimed at establishing a strictly minimally invasive large animal sheep model for lumbar ventrolateral vertebroplasty, which may represent an optimal basis for further studies with CPC. The new sheep model resulted in short operation times (28 ± 2 minutes; mean±standard error of the mean) and X-ray exposure (1.59 ± 0.12 minutes), very limited local trauma (score 0.00 ± 0.00 at 24 hours), short postoperative recovery (2.95 ± 0.29 hours), and rapid decrease of the postoperative impairment score to 0 (3.28 ± 0.36 hours). In addition, the osteoconductivity of the CPC was demonstrated by osteodensitometry (CPC > control), μCT (CPC > control and empty defect), histology/static histomorphometry (CPC > control and empty defect), fluorescence histomorphometry (CPC > control; all $p < 0.05$ for 3 and 9 months), and compressive strength measurements (CPC numerically higher than control; 102% for 3 months and 110% for 9 months). This sheep model was then used in a third study in which the bioresorbable, PLGA-fiber reinforced CPC was loaded with BMP-2, to further enhance and support the complete bone regeneration induced by CPC. Because of the numerous serious adverse effects which have been clinically reported using high doses between 1.95 and 40 mg of BMP-2 for spinal surgery, we aimed at considerably lower doses (1, 5, 100, 500 μg), demonstrating that a single local dose as low as ≤ 100 μg BMP-2 was sufficient to augment middle to long-term bone formation. In particular, compared to untouched controls (L1), CPC+fibers (L4) and/or CPC+fibers+BMP-2 (L5) significantly improved all parameters of bone formation, bone

resorption, and bone structure at 3 and 9 months. Compared to CPC without BMP-2, additional significant effects of BMP-2 were demonstrated for bone structure (bone volume/total volume, trabecular thickness, trabecular number) and formation (osteoid surface/bone surface and mineralizing surface/bone surface), as well as for the compressive strength. Several parameters still showed a significant effect of BMP-2 at the late time point 9 months, supporting the concept that a one-time therapeutic application is sufficient to induce middle to long-term effect. Such study also confirms, with the limitation of different load sharing forces in sheep and humans, the suitability of the present physiological and convenient osteopenia model for the analysis of vertebral augmentation with resorbable and osteoconductive CPC, as well as for dose-response studies with different molecules. The study was not designed as a safety study and was thus not suitable for a systematic assessment of the safety profile of the PLGA-fiber-reinforced, BMP-2-loaded CPC. However, within the limits of the study design, there were no signs of adverse effects previously reported after the clinical use of high-dose BMP-2 for spinal surgery and there were no signs of local inflammation, indicating that all the components of the new cement have no or negligible proinflammatory effects. The study also confirms that PLGA fibers at the present concentration have no negative effect on bone formation (Maenz, Brinkmann et al. 2017), but may rather enhance the osteoconductivity of the CPC. Furthermore, as previously published by our group, in vivo signs of systemic intravascular leakage after the injection of CPC were absent (Xin, Bungartz et al. 2016). Interestingly, local intravascular leakage after in vivo application of CPC was only observed in a very limited percentage of vertebral bodies (approximately 10%) versus 53% in the case of high-viscosity PMMA cement (Kyphon, HV-R12, Medtronic Inc, Milan, Italy). The usage of CPC may thus reduce the risk of cement leakage in comparison with the commonly applied PMMA cement and may bear the potential to lower the frequency or severity of adverse effects.

7. CONCLUSION

Our study demonstrated that the novel BMP-loaded CPC represents a suitable drug delivery system for the release of bioactive BMPs which can contribute to the healing of bone defects. Such effect was observed in vivo after minimally invasive injection of the BMP-2-loaded CPC. After 3 and 9 months, the CPC significantly enhanced the bone formation in sheep lumbar osteopenia, and may thus be a suitable candidate to replace the bioinert, non-resorbable, supraphysiologically stiff PMMA cements currently applied in the vertebroplasty/kyphoplasty of osteoporotic vertebral fractures. Also the two BMPs GDF5 and BB-1 have been tested in vivo by our group, and the results were comparable with the ones of BMP-2-loaded CPC (Bungartz, Kunisch et al. 2017, Gunnella, Kunisch et al. 2017). Future systematic safety studies will have to follow to validate the safety profile of low-dose BMP-2, and eventually, establish the use of BMP-loaded CPC for minimal surgery as well as for broader clinical applications.

LIST OF REFERENCES

Aerssens, J., S. Boonen, G. Lowet and J. Dequeker (1998). "Interspecies differences in bone composition, density, and quality: potential implications for in vivo bone research." Endocrinology **139**(2): 663-670.

Agrawal, V. and M. Sinha (2017). "A review on carrier systems for bone morphogenetic protein-2." J Biomed Mater Res B Appl Biomater **105**(4): 904-925.

Alkhraisat, M. H., C. Rueda, J. Cabrejos-Azama, J. Lucas-Aparicio, F. T. Marino, J. Torres Garcia-Denche, L. B. Jerez, U. Gbureck and E. L. Cabarcos (2010). "Loading and release of doxycycline hyclate from strontium-substituted calcium phosphate cement." Acta Biomater **6**(4): 1522-1528.

Augat, P., U. Simon, A. Liedert and L. Claes (2005). "Mechanics and mechano-biology of fracture healing in normal and osteoporotic bone." Osteoporos Int **16 Suppl 2**: S36-43.

Baroud, G., M. Crookshank and M. Bohner (2006). "High-viscosity cement significantly enhances uniformity of cement filling in vertebroplasty: an experimental model and study on cement leakage." Spine (Phila Pa 1976) **31**(22): 2562-2568.

Barrios, C., L. A. Brostrom, A. Stark and G. Walheim (1993). "Healing complications after internal fixation of trochanteric hip fractures: the prognostic value of osteoporosis." J Orthop Trauma **7**(5): 438-442.

Belkoff, S. M., J. M. Mathis, D. C. Fenton, R. M. Scribner, M. E. Reiley and K. Talmadge (2001). "An ex vivo biomechanical evaluation of an inflatable bone tamp used in the treatment of compression fracture." Spine (Phila Pa 1976) **26**(2): 151-156.

Benneker, L. M. and S. Hoppe (2013). "Percutaneous cement augmentation techniques for osteoporotic spinal fractures." Eur J Trauma Emerg Surg **39**(5): 445-453.

Blattert, T. R., L. Jestaedt and A. Weckbach (2009). "Suitability of a calcium phosphate cement in osteoporotic vertebral body fracture augmentation: a controlled, randomized, clinical trial of balloon kyphoplasty comparing calcium phosphate versus polymethylmethacrylate." Spine (Phila Pa 1976) **34**(2): 108-114.

Blom, E. J., J. Klein-Nulend, J. G. Wolke, K. Kurashina, M. A. van Waas and E. H. Burger (2002). "Transforming growth factor-beta1 incorporation in an alpha-tricalcium phosphate/dicalcium phosphate dihydrate/tetracalcium phosphate monoxide cement: release characteristics and physicochemical properties." Biomaterials **23**(4): 1261-1268.

Blom, E. J., J. Klein-Nulend, L. Yin, M. A. van Waas and E. H. Burger (2001). "Transforming growth factor-beta1 incorporated in calcium phosphate cement stimulates osteotransductivity in rat calvarial bone defects." Clin Oral Implants Res **12**(6): 609-616.

Bohner, M. (2001). "Physical and chemical aspects of calcium phosphates used in spinal surgery." Eur Spine J **10 Suppl 2**: S114-121.

Bohner, M., J. Lemaitre, H. P. Merkle and B. Gander (2000). "Control of gentamicin release from a calcium phosphate cement by admixed poly(acrylic acid)." Journal of Pharmaceutical Sciences **89**(10): 1262-1270.

Bono, C. M., M. B. Harris, N. Warholic, J. N. Katz, E. Carreras, A. White, M. Schmitz, K. B. Wood and E. Losina (2013). "Pain intensity and patients' acceptance of surgical complication risks with lumbar fusion." Spine (Phila Pa 1976) **38**(2): 140-147.

Boonen, S., D. A. Wahl, L. Nauroy, M. L. Brandi, M. L. Bouxsein, J. Goldhahn, E. M. Lewiecki, G. P. Lyritis, D. Marsh, K. Obrant, S. Silverman, E. Siris, K. Akesson and C. S. A. F. W. G. o. I. O. Foundation (2011). "Balloon kyphoplasty and vertebroplasty in the management of vertebral compression fractures." Osteoporos Int **22**(12): 2915-2934.

Bragdon, B., O. Moseychuk, S. Saldanha, D. King, J. Julian and A. Nohe (2011). "Bone morphogenetic proteins: a critical review." Cell Signal **23**(4): 609-620.

Bucay, N., I. Sarosi, C. R. Dunstan, S. Morony, J. Tarpley, C. Capparelli, S. Scully, H. L. Tan, W. Xu, D. L. Lacey, W. J. Boyle and W. S. Simonet (1998). "osteoprotegerin-deficient mice develop early onset osteoporosis and arterial calcification." Genes Dev **12**(9): 1260-1268.

Bungartz, M., E. Kunisch, S. Maenz, V. Horbert, L. Xin, F. Gunnella, J. Mika, J. Borowski, S. Bischoff, H. Schubert, A. Sachse, B. Illerhaus, J. Gunster, J. Bossert, K. D. Jandt, F. Ploger, R. W. Kinne and O. Brinkmann (2017). "GDF5 significantly augments the bone formation induced by an injectable, PLGA fiber-reinforced, brushite-forming cement in a sheep defect model of lumbar osteopenia." Spine J **17**(11): 1685-1698.

Bungartz, M., S. Maenz, E. Kunisch, V. Horbert, L. Xin, F. Gunnella, J. Mika, J. Borowski, S. Bischoff, H. Schubert, A. Sachse, B. Illerhaus, J. Gunster, J. Bossert, K. D. Jandt, R. W. Kinne and O. Brinkmann (2016). "First-time systematic postoperative clinical assessment of a minimally invasive approach for lumbar ventrolateral vertebroplasty in the large animal model sheep." Spine J **16**(10): 1263-1275.

Burton, A. W. and E. Mendel (2003). "Vertebroplasty and kyphoplasty." Pain Physician **6**(3): 335-341.

Bush, T. L. (1991). "Extraskeletal effects of estrogen and the prevention of atherosclerosis." Osteoporos Int **2**(1): 5-11.

Canal, C. and M. P. Ginebra (2011). "Fibre-reinforced calcium phosphate cements: a review." J Mech Behav Biomed Mater **4**(8): 1658-1671.

Cao, W. and L. L. Hench (1996). "Bioactive materials." Ceramics International **22**(6): 493-507.

Carragee, E. J., E. L. Hurwitz and B. K. Weiner (2011). "A critical review of recombinant human bone morphogenetic protein-2 trials in spinal surgery: emerging safety concerns and lessons learned." Spine J **11**(6): 471-491.

Carreira, A. C., W. F. Zambuzzi, M. C. Rossi, R. Astorino Filho, M. C. Sogayar and J. M. Granjeiro (2015). "Bone Morphogenetic Proteins: Promising Molecules for Bone Healing, Bioengineering, and Regenerative Medicine." Vitam Horm **99**: 293-322.

Cashman, K. D. (2007). "Diet, nutrition, and bone health." J Nutr **137**(11 Suppl): 2507S-2512S.

Cenci, S., G. Toraldo, M. N. Weitzmann, C. Roggia, Y. Gao, W. P. Qian, O. Sierra and R. Pacifici (2003). "Estrogen deficiency induces bone loss by increasing T cell proliferation and lifespan through IFN-gamma-induced class II transactivator." Proc Natl Acad Sci U S A **100**(18): 10405-10410.

Cho, T. J., L. C. Gerstenfeld and T. A. Einhorn (2002). "Differential temporal expression of members of the transforming growth factor beta superfamily during murine fracture healing." J Bone Miner Res **17**(3): 513-520.

Cho, T. J., J. A. Kim, C. Y. Chung, W. J. Yoo, L. C. Gerstenfeld, T. A. Einhorn and I. H. Choi (2007). "Expression and role of interleukin-6 in distraction osteogenesis." Calcif Tissue Int **80**(3): 192-200.

Chow, L. C. (2001). "Solubility of calcium phosphates." Monogr Oral Sci **18**: 94-111.

Cooper, C. and L. J. Melton, 3rd (1992). "Vertebral fractures." BMJ **304**(6842): 1634-1635.

Cotten, A., N. Boutry, B. Cortet, R. Assaker, X. Demondion, D. Leblond, P. Chastanet, B. Duquesnoy and H. Deramond (1998). "Percutaneous vertebroplasty: state of the art." Radiographics **18**(2): 311-320; discussion 320-313.

Cummings, S. R., D. M. Black and S. M. Rubin (1989). "Lifetime risks of hip, Colles', or vertebral fracture and coronary heart disease among white postmenopausal women." Arch Intern Med **149**(11): 2445-2448.

Deb, S. (1999). "A review of improvements in acrylic bone cements." J Biomater Appl **14**(1): 16-47.

del Real, R. P., J. G. Wolke, M. Vallet-Regi and J. A. Jansen (2002). "A new method to produce macropores in calcium phosphate cements." Biomaterials **23**(17): 3673-3680.

Deyo, R. A. (2010). "Treatment of lumbar spinal stenosis: a balancing act." Spine J **10**(7): 625-627.

Dimitriou, R., E. Tsiridis and P. V. Giannoudis (2005). "Current concepts of molecular aspects of bone healing." Injury **36**(12): 1392-1404.

Egermann, M., E. Schneider, C. H. Evans and A. W. Baltzer (2005). "The potential of gene therapy for fracture healing in osteoporosis." Osteoporos Int **16 Suppl 2**: S120-128.

Einhorn, T. A. and L. C. Gerstenfeld (2015). "Fracture healing: mechanisms and interventions." Nat Rev Rheumatol **11**(1): 45-54.

Elliott, J. C. (1997). "Structure, crystal chemistry and density of enamel apatites." Ciba Found Symp **205**: 54-67; discussion 67-72.

Englund, U., H. Littbrand, A. Sondell, G. Bucht and U. Pettersson (2009). "The beneficial effects of exercise on BMD are lost after cessation: a 5-year follow-up in older post-menopausal women." Scand J Med Sci Sports **19**(3): 381-388.

Erben, R. G. (1996). "Trabecular and endocortical bone surfaces in the rat: modeling or remodeling?" Anat Rec **246**(1): 39-46.

Galibert P, D. H., Rosat P, et al. (1987). "[Preliminary note on the treatment

of vertebral angioma by percutaneous acrylic vertebroplasty] " Neurochirurgie **33**(2): 166–168.

Gerstenfeld, L. C., Y. M. Alkhiary, E. A. Krall, F. H. Nicholls, S. N. Stapleton, J. L. Fitch, M. Bauer, R. Kayal, D. T. Graves, K. J. Jepsen and T. A. Einhorn (2006). "Three-dimensional reconstruction of fracture callus morphogenesis." J Histochem Cytochem **54**(11): 1215-1228.

Gerstenfeld, L. C., D. M. Cullinane, G. L. Barnes, D. T. Graves and T. A. Einhorn (2003). "Fracture healing as a post-natal developmental process: molecular, spatial, and temporal aspects of its regulation." J Cell Biochem **88**(5): 873-884.

Ginebra, M. P., C. Canal, M. Espanol, D. Pastorino and E. B. Montufar (2012). "Calcium phosphate cements as drug delivery materials." Adv Drug Deliv Rev **64**(12): 1090-1110.

Ginebra, M. P., A. Rilliard, E. Fernandez, C. Elvira, J. San Roman and J. A. Planell (2001). "Mechanical and rheological improvement of a calcium phosphate cement by the addition of a polymeric drug." J Biomed Mater Res **57**(1): 113-118.

Ginebra, M. P., T. Traykova and J. A. Planell (2006). "Calcium phosphate cements as bone drug delivery systems: A review." Journal of Controlled Release **113**(2): 102-110.

Girod Fullana, S., H. Ternet, M. Freche, J. L. Lacout and F. Rodriguez (2010). "Controlled release properties and final macroporosity of a pectin microspheres-calcium phosphate composite bone cement." Acta Biomater **6**(6): 2294-2300.

Gold, D. T. (1996). "The clinical impact of vertebral fractures: quality of life in women with osteoporosis." Bone **18**(3 Suppl): 185S-189S.

Gunnella, F., E. Kunisch, S. Maenz, V. Horbert, L. Xin, J. Mika, J. Borowski, S. Bischoff, H. Schubert, A. Sachse, B. Illerhaus, J. Gunster, J. Bossert, K. D. Jandt, F. Ploger, R. W. Kinne, O. Brinkmann and M. Bungartz (2018). "The GDF5 mutant BB-1 enhances the bone formation induced by an injectable, poly(l-lactide-co-glycolide) acid (PLGA) fiber-reinforced, brushite-forming cement in a sheep defect model of lumbar osteopenia." Spine J **18**(2): 357-369.

Hallberg, I., A. M. Rosenqvist, L. Kartous, O. Lofman, O. Wahlstrom and G. Toss (2004). "Health-related quality of life after osteoporotic fractures." Osteoporos Int **15**(10): 834-841.

He, Z., Q. Zhai, M. Hu, C. Cao, J. Wang, H. Yang and B. Li (2015). "Bone cements for percutaneous vertebroplasty and balloon kyphoplasty: Current status and future developments." Journal of Orthopaedic Translation **3**(1): 1-11.

Hernlund, E., A. Svedbom, M. Ivergard, J. Compston, C. Cooper, J. Stenmark, E. V. McCloskey, B. Jonsson and J. A. Kanis (2013). "Osteoporosis in the European Union: medical management, epidemiology and economic burden. A report prepared in collaboration with the International Osteoporosis Foundation (IOF) and the European Federation of Pharmaceutical Industry Associations (EFPIA)." Arch Osteoporos **8**: 136.

Hofbauer, L. C., F. Gori, B. L. Riggs, D. L. Lacey, C. R. Dunstan, T. C. Spelsberg and S. Khosla (1999). "Stimulation of osteoprotegerin ligand and inhibition of osteoprotegerin production by glucocorticoids in human osteoblastic lineage cells: potential paracrine mechanisms of glucocorticoid-induced osteoporosis." Endocrinology **140**(10): 4382-4389.

Hofbauer, L. C., S. Khosla, C. R. Dunstan, D. L. Lacey, T. C. Spelsberg and B. L. Riggs (1999). "Estrogen stimulates gene expression and protein production of osteoprotegerin in human osteoblastic cells." Endocrinology **140**(9): 4367-4370.

Hofmann, M. P., A. R. Mohammed, Y. Perrie, U. Gbureck and J. E. Barralet (2009). "High-strength resorbable brushite bone cement with controlled drug-releasing capabilities." Acta Biomater **5**(1): 43-49.

Hughes, D. E., A. Dai, J. C. Tiffee, H. H. Li, G. R. Mundy and B. F. Boyce (1996). "Estrogen promotes apoptosis of murine osteoclasts mediated by TGF-beta." Nat Med **2**(10): 1132-1136.

Hulme, P. A., J. Krebs, S. J. Ferguson and U. Berlemann (2006). "Vertebroplasty and kyphoplasty: a systematic review of 69 clinical studies." Spine (Phila Pa 1976) **31**(17): 1983-2001.

Kasten, P., I. Beyen, D. Bormann, R. Luginbuhl, F. Ploger and W. Richter (2010). "The effect of two point mutations in GDF-5 on ectopic bone formation in a beta-tricalciumphosphate scaffold." Biomaterials **31**(14): 3878-3884.

Khairoun, I., M. G. Boltong, F. C. Driessens and J. A. Planell (1998). "Some factors controlling the injectability of calcium phosphate bone cements." J Mater Sci Mater Med **9**(8): 425-428.

Knepper-Nicolai, B., A. Reinstorf, I. Hofinger, K. Flade, R. Wenz and W. Pompe (2002). "Influence of osteocalcin and collagen I on the mechanical and biological properties of Biocement D." Biomol Eng **19**(2-6): 227-231.

Komm, B. S., C. M. Terpening, D. J. Benz, K. A. Graeme, A. Gallegos, M. Korc, G. L. Greene, B. W. O'Malley and M. R. Haussler (1988). "Estrogen binding, receptor mRNA, and biologic response in osteoblast-like osteosarcoma cells." Science **241**(4861): 81-84.

Kong, Y.-Y., U. Feige, I. Sarosi, B. Bolon, A. Tafuri, S. Morony, C. Capparelli, J. Li, R. Elliott, S. McCabe, T. Wong, G. Campagnuolo, E. Moran, E. R. Bogoch, G. Van, L. T. Nguyen, P. S. Ohashi, D. L. Lacey, E. Fish, W. J. Boyle and J. M. Penninger (1999). "Activated T cells regulate bone loss and joint destruction in adjuvant arthritis through osteoprotegerin ligand." Nature **402**: 304.

Kousteni, S., T. Bellido, L. I. Plotkin, C. A. O'Brien, D. L. Bodenner, L. Han, K. Han, G. B. DiGregorio, J. A. Katzenellenbogen, B. S. Katzenellenbogen, P. K. Roberson, R. S. Weinstein, R. L. Jilka and S. C. Manolagas (2001). "Nongenotropic, sex-nonspecific signaling through the estrogen or androgen receptors: dissociation from transcriptional activity." Cell **104**(5): 719-730.

Kousteni, S., L. Han, J. R. Chen, M. Almeida, L. I. Plotkin, T. Bellido and S. C. Manolagas (2003). "Kinase-mediated regulation of common transcription factors accounts for the bone-protective effects of sex steroids." J Clin Invest **111**(11): 1651-1664.

Krolner, B. and B. Toft (1983). "Vertebral bone loss: an unheeded side effect of therapeutic bed rest." Clin Sci (Lond) **64**(5): 537-540.

Lau, E., K. Ong, S. Kurtz, J. Schmier and A. Edidin (2008). "Mortality following the diagnosis of a vertebral compression fracture in the Medicare population." J Bone Joint Surg Am **90**(7): 1479-1486.

Lavelle, W. F., M. A. Khaleel, R. Cheney, E. Demers and A. L. Carl (2008). "Effect of kyphoplasty on survival after vertebral compression fractures." Spine J **8**(5): 763-769.

LeGeros, R. Z. (1982). "Apatitic calcium phosphates: possible dental restorative materials." Journal of Dental Research **61**: 343-343.

Leidig, G., H. W. Minne, P. Sauer, C. Wuster, J. Wuster, M. Lojen, F. Raue and R. Ziegler (1990). "A study of complaints and their relation to vertebral destruction in patients with osteoporosis." Bone Miner **8**(3): 217-229.

Li, M., Y. Shen and T. J. Wronski (1997). "Time course of femoral neck osteopenia in ovariectomized rats." Bone **20**(1): 55-61.

Lopez-Heredia, M. A., G. J. Kamphuis, P. C. Thune, F. C. Oner, J. A. Jansen and X. F. Walboomers (2011). "An injectable calcium phosphate cement for the local delivery of paclitaxel to bone." Biomaterials **32**(23): 5411-5416.

Lyritis, G. P., B. Mayasis, N. Tsakalakos, A. Lambropoulos, S. Gazi, T. Karachalios, M. Tsekoura and A. Yiatzides (1989). "The natural history of the osteoporotic vertebral fracture." Clin Rheumatol **8 Suppl 2**: 66-69.

Maenz, S., O. Brinkmann, E. Kunisch, V. Horbert, F. Gunnella, S. Bischoff, H. Schubert, A. Sachse, L. Xin, J. Gunster, B. Illerhaus, K. D. Jandt, J. Bossert, R. W. Kinne and M. Bungartz (2017). "Enhanced bone formation in sheep vertebral bodies after minimally invasive treatment with a novel, PLGA fiber-reinforced brushite cement." Spine J **17**(5): 709-719.

Maenz, S., E. Kunisch, M. Muhlstadt, A. Bohm, V. Kopsch, J. Bossert, R. W. Kinne and K. D. Jandt (2014). "Enhanced mechanical properties of a novel, injectable, fiber-reinforced brushite cement." J Mech Behav Biomed Mater **39**: 328-338.

Marsell, R. and T. A. Einhorn (2009). "The role of endogenous bone morphogenetic proteins in normal skeletal repair." Injury **40 Suppl 3**: S4-7.

McClung, M. (2007). "Role of RANKL inhibition in osteoporosis." Arthritis Res Ther **9 Suppl 1**: S3.

Melton, L. J., 3rd (1997). "Epidemiology of spinal osteoporosis." Spine (Phila Pa 1976) **22**(24 Suppl): 2S-11S.

Miyazono, K., Y. Kamiya and M. Morikawa (2010). "Bone morphogenetic protein receptors and signal transduction." J Biochem **147**(1): 35-51.

Moerman, E. J., K. Teng, D. A. Lipschitz and B. Lecka-Czernik (2004). "Aging activates adipogenic and suppresses osteogenic programs in mesenchymal marrow stroma/stem cells: the role of PPAR-gamma2 transcription factor and TGF-beta/BMP signaling pathways." Aging Cell **3**(6): 379-389.

Namkung-Matthai, H., R. Appleyard, J. Jansen, J. Hao Lin, S. Maastricht, M. Swain, R. S. Mason, G. A. Murrell, A. D. Diwan and T. Diamond (2001). "Osteoporosis influences the early period of fracture healing in a rat osteoporotic model." Bone **28**(1): 80-86.

Newman, E., A. S. Turner and J. D. Wark (1995). "The potential of sheep for the study of osteopenia: current status and comparison with other animal models." Bone **16**(4 Suppl): 277s-284s.

Nordin, B. E. (1997). "Calcium and osteoporosis." Nutrition **13**(7-8): 664-686.

Nouda, S., S. Tomita, A. Kin, K. Kawahara and M. Kinoshita (2009). "Adjacent vertebral body fracture following vertebroplasty with polymethylmethacrylate or calcium phosphate cement: biomechanical evaluation of the cadaveric spine." Spine (Phila Pa 1976) **34**(24): 2613-2618.

O´Connell, S. L. (1999). The sheep as an experimental model for osteoporosis The University of Melbourne, Melbourne.

Oliveira, M. T., J. Potes, M. C. Queiroga, J. L. Castro, A. F. Pereira, S. Rehman, K. Dalgarno, A. Ramos, C. Vitale-Brovarone and J. C. Reis (2016). "Percutaneous vertebroplasty: a new animal model." Spine J **16**(10): 1253-1262.

Phillips, F. M., B. A. Pfeifer, I. H. Lieberman, E. J. Kerr, 3rd, I. S. Choi and A. G. Pazianos (2003). "Minimally invasive treatments of osteoporotic vertebral compression fractures: vertebroplasty and kyphoplasty." Instr Course Lect **52**: 559-567.

Potes, J. C., Reis J., Capela e Silva, F., Relvas, C., Cabrita, A.S., Simões, J.A. (2008). "The Sheep as an Animal Model in Orthopaedic Research." Experimental Pathology and Health Sciences **2**(1): 29-32.

Reddi, A. H. and C. Huggins (1972). "Biochemical sequences in the transformation of normal fibroblasts in adolescent rats." Proc Natl Acad Sci U S A **69**(6): 1601-1605.

Reed, M. J. and J. M. Edelberg (2004). "Impaired angiogenesis in the aged." Sci Aging Knowledge Environ **2004**(7): pe7.

Reginster, J. Y. and N. Burlet (2006). "Osteoporosis: a still increasing prevalence." Bone **38**(2 Suppl 1): S4-9.

Riggs, B. L., J. Jowsey, P. J. Kelly, J. D. Jones and F. T. Maher (1969). "Effect of sex hormones on bone in primary osteoporosis." J Clin Invest **48**(6): 1065-1072.

Rizzoli, R., J. Branco, M. L. Brandi, S. Boonen, O. Bruyere, P. Cacoub, C. Cooper, A. Diez-Perez, J. Duder, R. A. Fielding, N. C. Harvey, M. Hiligsmann, J. A. Kanis, J. Petermans, J. D. Ringe, Y. Tsouderos, J. Weinman and J. Y. Reginster (2014). "Management of osteoporosis of the oldest old." Osteoporos Int **25**(11): 2507-2529.

Rodriguez, J. P., S. Garat, H. Gajardo, A. M. Pino and G. Seitz (1999). "Abnormal osteogenesis in osteoporotic patients is reflected by altered mesenchymal stem cells dynamics." J Cell Biochem **75**(3): 414-423.

Rosenzweig, B. L., T. Imamura, T. Okadome, G. N. Cox, H. Yamashita, P. ten Dijke, C. H. Heldin and K. Miyazono (1995). "Cloning and characterization of a human type II receptor for bone morphogenetic proteins." Proc Natl Acad Sci U S A **92**(17): 7632-7636.

Scarfi, S. (2016). "Use of bone morphogenetic proteins in mesenchymal stem cell stimulation of cartilage and bone repair." World J Stem Cells **8**(1): 1-12.

Schorlemmer, S., C. Gohl, S. Iwabu, A. Ignatius, L. Claes and P. Augat (2003). "Glucocorticoid treatment of ovariectomized sheep affects mineral density, structure, and mechanical properties of cancellous bone." J Bone Miner Res **18**(11): 2010-2015.

Sierra-Garcia, G. D., R. Castro-Rios, A. Gonzalez-Horta, J. Lara-Arias and A. Chavez-Montes (2016). "[Bone morphogenetic proteins (BMP): clinical application for reconstruction of bone defects]." Gac Med Mex **152**(3): 381-385.

Simonet, W. S., D. L. Lacey, C. R. Dunstan, M. Kelley, M. S. Chang, R. Luthy, H. Q. Nguyen, S. Wooden, L. Bennett, T. Boone, G. Shimamoto, M. DeRose, R. Elliott, A. Colombero, H. L. Tan, G. Trail, J. Sullivan, E. Davy, N. Bucay, L. Renshaw-Gegg, T. M. Hughes, D. Hill, W. Pattison, P. Campbell, S. Sander, G. Van, J. Tarpley, P. Derby, R. Lee and W. J. Boyle (1997). "Osteoprotegerin: a novel secreted protein involved in the regulation of bone density." Cell **89**(2): 309-319.

Smith, C. L. and B. W. O'Malley (2004). "Coregulator function: a key to understanding tissue specificity of selective receptor modulators." Endocr Rev **25**(1): 45-71.

Stein, B. and M. X. Yang (1995). "Repression of the interleukin-6 promoter by estrogen receptor is mediated by NF-kappa B and C/EBP beta." Mol Cell Biol **15**(9): 4971-4979.

Sykaras, N. and L. A. Opperman (2003). "Bone morphogenetic proteins (BMPs): how do they function and what can they offer the clinician?" J Oral Sci **45**(2): 57-73.

Tahara, Y. and Y. Ishii (2001). "Apatite cement containing cis-diamminedichloroplatinum implanted in rabbit femur for sustained release of the anticancer drug and bone formation." J Orthop Sci **6**(6): 556-565.

Takayanagi, H., H. Iizuka, T. Juji, T. Nakagawa, A. Yamamoto, T. Miyazaki, Y. Koshihara, H. Oda, K. Nakamura and S. Tanaka (2000). "Involvement of receptor activator of nuclear factor kappaB ligand/osteoclast differentiation factor in osteoclastogenesis from synoviocytes in rheumatoid arthritis." Arthritis Rheum **43**(2): 259-269.

Tayalia, P. and D. J. Mooney (2009). "Controlled growth factor delivery for tissue engineering." Adv Mater **21**(32-33): 3269-3285.

Thompson, D. D., H. A. Simmons, C. M. Pirie and H. Z. Ke (1995). "FDA Guidelines and animal models for osteoporosis." Bone **17**(4 Suppl): 125S-133S.

Turner, A. S. (2002). "The sheep as a model for osteoporosis in humans." Vet J **163**(3): 232-239.

Unnanuntana, A., B. J. Rebolledo, M. M. Khair, E. F. DiCarlo and J. M. Lane (2011). "Diseases affecting bone quality: beyond osteoporosis." Clin Orthop Relat Res **469**(8): 2194-2206.

Urist, M. R. (1965). "Bone: formation by autoinduction." Science **150**(3698): 893-899.

Verron, E., I. Khairoun, J. Guicheux and J. M. Bouler (2010). "Calcium phosphate biomaterials as bone drug delivery systems: a review." Drug Discov Today **15**(13-14): 547-552.

Verron, E., M. L. Pissonnier, J. Lesoeur, V. Schnitzler, B. H. Fellah, H. Pascal-Moussellard, P. Pilet, O. Gauthier and J. M. Bouler (2014). "Vertebroplasty using bisphosphonate-loaded calcium phosphate cement in a standardized vertebral body bone defect in an osteoporotic sheep model." Acta Biomater **10**(11): 4887-4895.

Voormolen, M. H., W. P. Mali, P. N. Lohle, H. Fransen, L. E. Lampmann, Y. van der Graaf, J. R. Juttmann, X. Jansssens and H. J. Verhaar (2007). "Percutaneous vertebroplasty compared with optimal pain medication treatment: short-term clinical outcome of patients with subacute or chronic painful osteoporotic vertebral compression fractures. The VERTOS study." AJNR Am J Neuroradiol **28**(3): 555-560.

Walsh, W. R., P. Sherman, C. R. Howlett, D. H. Sonnabend and M. G. Ehrlich (1997). "Fracture healing in a rat osteopenia model." Clin Orthop Relat Res(342): 218-227.

Weitzmann, M. N. a. P. R. (2006). "Estrogen deficiency and bone loss: an inflammatory tale." J Clin Invest. **116**(5): 1186-1194.

Wilke, H. J., A. Kettler and L. E. Claes (1997). "Are sheep spines a valid biomechanical model for human spines?" Spine (Phila Pa 1976) **22**(20): 2365-2374.

Xia, Z., L. M. Grover, Y. Huang, I. E. Adamopoulos, U. Gbureck, J. T. Triffitt, R. M. Shelton and J. E. Barralet (2006). "In vitro biodegradation of three brushite calcium phosphate cements by a macrophage cell-line." Biomaterials **27**(26): 4557-4565.

Xiao, Y. T., L. X. Xiang and J. Z. Shao (2007). "Bone morphogenetic protein." Biochem Biophys Res Commun **362**(3): 550-553.

Xin, L., M. Bungartz, S. Maenz, V. Horbert, M. Hennig, B. Illerhaus, J. Gunster, J. Bossert, S. Bischoff, J. Borowski, H. Schubert, K. D. Jandt, E. Kunisch, R. W. Kinne and O. Brinkmann (2016). "Decreased extrusion of calcium phosphate cement versus high viscosity PMMA cement into spongious bone marrow-an ex vivo and in vivo study in sheep vertebrae." Spine J **16**(12): 1468-1477.

Yaltirik, K., A. M. Ashour, C. R. Reis, S. Ozdogan and B. Atalay (2016). "Vertebral augmentation by kyphoplasty and vertebroplasty: 8 years experience outcomes and complications." J Craniovertebr Junction Spine **7**(3): 153-160.

Yimin, Y., R. Zhiwei, M. Wei and R. Jha (2013). "Current status of percutaneous vertebroplasty and percutaneous kyphoplasty--a review." Med Sci Monit **19**: 826-836.

Yuan, H., Y. Li, J. D. de Bruijn, K. de Groot and X. Zhang (2000). "Tissue responses of calcium phosphate cement: a study in dogs." Biomaterials **21**(12): 1283-1290.

A. APPENDIX

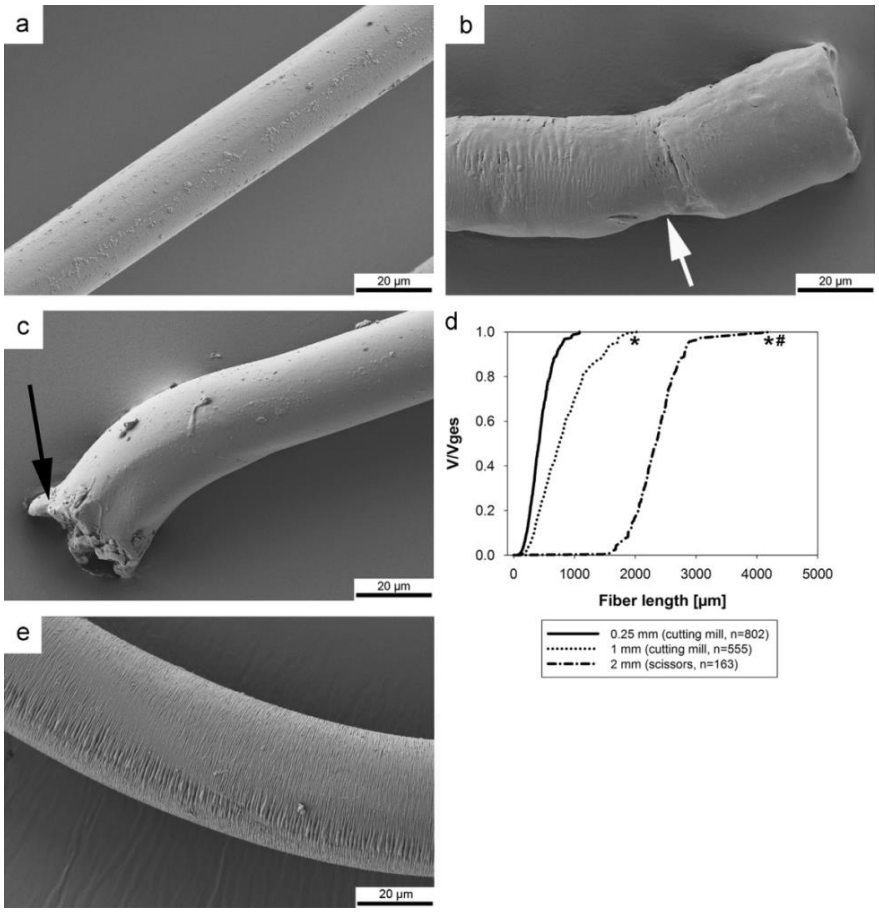

Figure A.1: Morphology of the PLGA fibers. (a) Extruded PLGA fiber with smooth fiber morphology; (b) extruded PLGA fiber chopped in a cutting mill with 0.25 mm sieve insert; a pinch is visible (white arrow); (c) extruded PLGA fiber after cutting with scissors, damage of the fiber ending is detectable (black arrow); (d) cumulative fiber length distribution after cutting with the 3 different approaches (*$p \leq 0.001$ vs. 0.25 mm, #$p \leq 0.001$ vs.1mm); (e) undulated fiber morphology after isopropanol treatment. [*Maenz S et al. Enhanced mechanial properties of a novel, injectable, fiber-reinforced brushite cement. J Mech Behav Biomed Mater 2014 Nov; 39:328-38*]

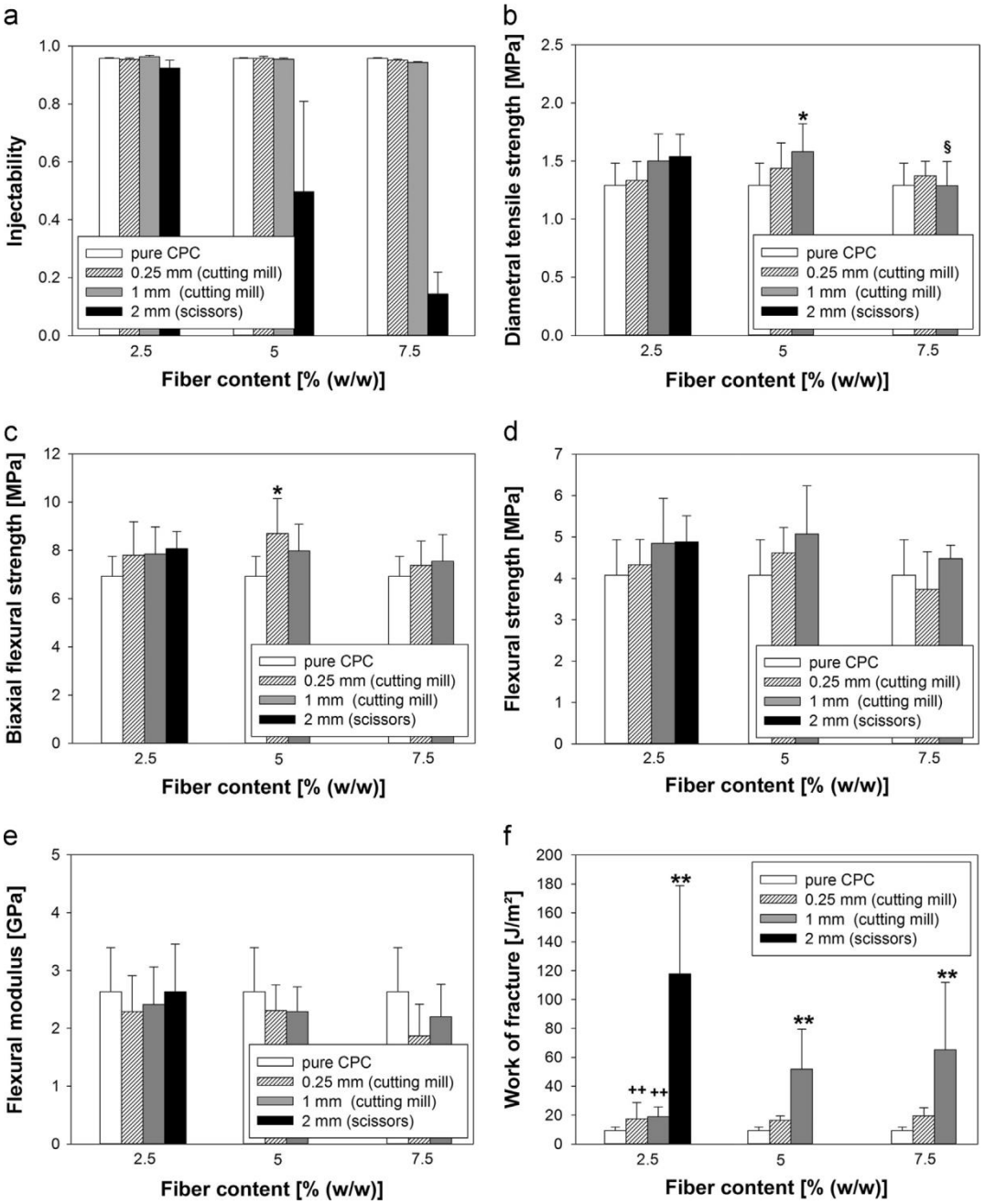

Figure A.2: Injectability and mechanical properties of fiber-reinforced CPCs with different fiber length and content. (a) Injectability (n=3); (b) diametral tensile strength (DTS) (n=10); (c) biaxial flexural (n=10); (d) flexural strength (n=10); (e) flexural modulus (n=10); (f) work of fracture (WOF) (n=10). *p < 0.05 versus pure CPC; **p < 0.01 versus pure CPC; § p < 0.05 versus CPC+5% (w/w) 1 mm; ++ p < 0.01 versus CPC+2.5% (w/w) 2 mm. [*Maenz S et al. Enhanced mechanial properties of a novel, injectable, fiber-reinforced brushite cement. J Mech Behav Biomed Mater 2014 Nov; 39:328-38*]

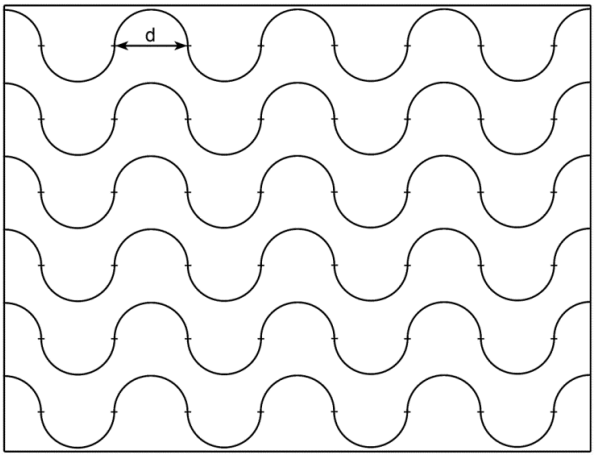

Figure A.3: Schematic representation of the Merz grid. [*Merz WA. Die Streckenmessung an gerichteten Strukturen im Mikroskop und ihre Anwendung zur Bestimmung von Oberflächen-Volumen-Relationen im Knochengewebe. Mikroskopie, 22:132–142, 1967*]

Determination of the histomorphometric parameters

For the histological calculations, the following parameters were determined in 20 fields of each individual vertebral body in the immediate vicinity of the injection channel using a Merz counting reticule (please refer to the Material and Methods section of Chapter 3; pag.):

F = Number of measuring fields

P = Number of hits (points) over mineralized bone and osteoid

P_0 = Number of hits over osteoid

I = Total intersection number of the wave lines with the trabecular bone surface

Io = Intersections of the wave lines with osteoid

I_H = Intersections of the wave lines with Howship`s lacunae containing osteoclasts

k = $\pi \times d / 4$ [µm] (1)

where d is the distance between 2 adjacent points in the counting net.

The 7 parameters calculated below correspond to the recommendations of the International Committee of the American Society for Bone and Mineral Research (ASBMR):

Bone volume/total volume (BV/TV): mineralized and non-mineralized fraction of the bone (includes the entire bone with cavities and appendix tissue)

$$BV/TV = P \times 100 / (F \times 48) \quad [\%] \quad (2)$$

Trabecular thickness (Tb.Th): average absolute thickness of the trabeculae

$$Tb.Th = P \times k / I \quad [\mu m] \quad (3)$$

Trabecular number (Tb.N): number of trabeculae per mm (derived from bone volume/total volume and trabecular thickness)

$$Tb.N = BV/TV / Tb.Th \quad [1/mm] \quad (4)$$

Osteoid volume (OV/BV): non-mineralized fraction of the bone

$$OV/BV = P_0 \times 100 / P \quad [\%] \quad (5)$$

Osteoid surface (OS/BS): non-mineralized surface fraction related to the total bone surface independent of the osteoblast coverage

$$OS/BS = I_O \times 100 / I \quad [\%] \quad (6)$$

Osteoid thickness (O.Th): average absolute thickness of non-mineralized bone tissue

$$O.Th = P_0 \times k \times 100 / I_O \quad [\mu m] \quad (7)$$

Eroded Surface (ES/BS): surface proportion of resorption lacunae related to the total trabecular bone surface independent of the osteoclast coverage

$$ES/BS = I_H \times 100 / I \quad [\%] \quad (8)$$

LIST OF TABLES

LIST OF FIGURES

ACKNOWLEDGMENTS

My life has been shaped by so many amazing people during the past three years. Without their support and assistance throughout the research project, the completion of this Doctoral study would not have been achieved.

In particular, I'm beyond thankful to my principal supervisor Prof. Med. Dr. Raimund W. Kinne for his guidance and professional support; I express here my deepest gratitude and appreciation for his incredible passionate spirit, fierce determination and work ethic.

I would like to thank all the members of the Experimental Rheumatology Lab group (Friedrich Schiller University, Jena). In particular Dr. E. Kunisch, Dr. M. Stoica and my friend Pavan Kalla Kumar for their suggestions and constructive ideas; B. Ukena, C. Müller, U. Körner, S. Födisch and G. Günert for their excellent technical assistance. It has been an absolute privilege to have worked with them.

I gratefully aknowdlege the Otto Schott Institute of Materials Research (Friedrich Schiller University, Jena), the Institute of Laboratory Animal Sciences and Welfare (Jena University Hospital, Jena), Dr. Med. O. Brinkmann and Dr. Med. M. Bungartz from the Department of Orthopedics (Jena University Hospital, Waldkrankenhaus "Rudolf Elle", Eisenberg) for the cooperation and the valuable help in performing the animal experiments.

Finally, the greatest thanks of all to my parents for providing me support and encouragement; to my grandparents whose spirit will always be my guide, because love knows no bounds; to Robert for loving me at my best and my worst and, therefore, for teaching me the meaning of true love.

I am indebted to each and every one of these people for their unconditional friendship, advice, tough love and inspiration.

CURRICULUM VITAE

Personal data

Name: Francesca Gunnella

Address: Werner-Seelenbinder Straße 39, 07747 Jena

Email: fgunnella@alice.it

Date of birth: 03.04.1988

Place of birth: Rieti, Italy

Academic education and degrees

09/02-07/07 High school Liceo Scientifico "C. Jucci", Rieti, Italy (Final exam grade: 100/100)

10/07-10/11 **Bachelor Degree in Biotechnology**
(Universita´degli Studi di L´Aquila, L´Aquila, Italy); Title of the Dissertation: "Quantification of bone resorption serum markers in a novel murine model of Autosomic Dominant Osteopetrosis via ELISA assays" (Grade: 110/110 cum laude)

10/11-07/13 **Master Degree in Molecular and Cellular Biotechnology**
(Universita´degli Studi di L´Aquila, L´Aquila, Italy); Title of the Dissertation: "Phenotype of the first Autosomal Dominant Osteopetrosis (ADO) disease model the p.G213R-*clcn7* knock-in mouse" (Grade: 110/110 cum laude)

02/15-present **Doctoral studies**
(Faculty of Medicine , Friedrich Schiller University Jena, Germany)

Working and research experience

05/14-11/14 **Quality control analyst**
Bioscience Divison; Microbiology Unit of Baxter Intern., Rieti, Italy

02/15-present **PhD researcher**
Experimental Rheumatology Unit, Department of Orthopedics, Jena University Hospital, Waldkrankenhaus "Rudolf Elle", Eisenberg, Germany

POSTER PRESENTATIONS

Gunnella F, Maenz S, Kunisch E, Illerhaus B, Bungartz M, Brinkmann O, Bossert J, Kinne RW; (October 2016). PLGA-fiber reinforcement of injectable calcium phosphate cement enhances bone regeneration in an in vivo vertebral body augmentation model. ("Best Experimental Papers" section). Deutscher Kongress für Ortophädie und Unfallchirurgie (DKOU), Berlin, Germany.

Gunnella F, Bungartz M, Maenz S, , Kunisch E, Brinkmann O, Bossert J, Kinne RW; (May 2017). Systematic post-operative clinical assessment of lumbar ventrolateral vertebroplasty in the large animal model sheep using a minimally-invasive approach. 4th Euro BioMAT 2017, Weimar, Germany.

Gunnella F, Kunisch E, Bungartz M, Brinkmann O, Bossert J, Kinne RW; (October 2017). GDF5 significantly augments the bone formation induced by an injectable, PLGA-fiber reinforced, brushite-forming cement in a sheep defect model of lumbar osteopenia. ("Best Experimental Papers" section) Deutscher Kongress für Ortophädie und Unfallchirurgie (DKOU), Berlin, Germany.

LIST OF PUBLICATIONS BY CANDIDATE

The current work comprises several research papers, some of which have been already published, while others are under review or ready for submission in recognized peer-review academic journals. The following three papers have been included in the thesis:

1. **Gunnella F**, Kunisch E, Maenz S, Bossert J, Jandt KD, Plöger F, Kinne RW. In vitro release of bioactive bone morphogenetic proteins (GDF5, BB-1, and BMP-2) from a PLGA fiber-reinforced, brushite-forming calcium phosphate cement (submitted to *The Spine Journal*; under peer-review process).
2. Bungartz M, Kunisch E, Horbert V, Xin L, **Gunnella F**, Mika J, Borowski J, Bischoff S, Schubert H, Sachse A, Illerhaus B, Günster J, Jandt KD, Kinne RW, Brinkmann O. First-time systematic postoperative clinical assessment of a minimally invasive approach for lumbar ventrolateral vertebroplasty in the large animal model sheep. *The Spine Journal* 2016;16(10):1263-1275.
3. **Gunnella F**, Kunisch E, Bungartz M, Maenz S, Horbert V, Xin L, Mika J, Borowski J, Bischoff S, Schubert H, Hortschansky P, Sachse A, Illerhaus B, Günster J, Bossert J, Jandt KD, Plöger F, Kinne RW, Brinkmann O. Low-dose BMP-2 is sufficient to enhance the bone formation induced by an injectable, PLGA fiber-reinforced, brushite-forming cement in a sheep defect model of lumbar osteopenia. *The Spine Journal* 2017;17(11):1699-1711.

Other published journal papers as first author or co-author:

4. Maenz S, Brinkmann O, Kunisch E, Horbert V, **Gunnella F**, Bischoff S, Schubert H, Sachse A, Xin L, Günster J, Illerhaus B, Jandt KD, Bossert J, Kinne RW, Bungartz M. Enhanced bone formation in sheep vertebral bodies after minimally-invasive treatment with a novel, PLGA-fiber reinforced brushite cement. *The Spine Journal* 2017;17(5):709-719.
5. Bungartz M, Kunisch E, Maenz S, Horbert V, Xin L, **Gunnella F**, Mika J, Borowski J, Bischoff S, Schubert H, Sachse A, Illerhaus B, Günster J, Bossert J, Jandt KD, Plöger F, Kinne RW, Brinkmann O. GDF5 significantly augments the bone formation induced by an injectable, PLGA fiber-reinforced, brushite-forming cement in a sheep defect model of lumbar osteopenia. *The Spine Journal* 2017 Nov;17(11):1685-1698.
6. **Gunnella F**, Kunisch E, Maenz S, Horbert V, Xin L, Mika J, Borowski J, Bischoff S, Schubert H, Sachse A, Illerhaus B, Günster J, Bossert J, Jandt KD, Plöger F, Kinne RW, Brinkmann O, Bungartz M. The GDF5 mutant BB-1 enhances the bone formation induced by an injectable, PLGA-fiber reinforced, brushite-forming cement in a sheep defect model of lumbar osteopenia. *The Spine Journal* 2018 Feb;18(2):357-369.

Submitted journal manuscripts under review:

7. Kunisch E, **Gunnella F**, Wagner S, Dees F, Maenz S, Bossert J, Jandt KD, Kinne RW. The PGLA fiber component of brushite-forming calcium phosphate cement induces the osteogenic differentiation of human adipose tissue-derived stem cells (submitted to *The Spine Journal*; under peer-review process).

Manuscripts in preparation for submission:

8. Maenz S, Brinkmann O, Hasenbein I, Braun C, Kunisch E, Horbert V, **Gunnella F**, Sachse A, Bischoff S, Schubert H, Jandt KD, Bossert J, Kinne RW and Bungartz M. The old sheep: A convenient and suitable model for senile osteopenia.

EHRENWÖRTLICHE ERKLÄRUNG

Hiermit erkläre ich, dass mir die Promotionsordnung der Medizinischen Fakultät der Friedrich-Schiller-Universität bekannt ist,

ich die Dissertation selbst angefertigt habe und alle von mir benutzten Hilfsmittel, persönlichen Mitteilungen und Quellen in meiner Arbeit angegeben sind,
mich folgende Personen bei der Auswahl und Auswertung des Materials sowie bei der Herstellung des Manuskripts unterstützt haben:

1. Prof. Med. Dr. Raimund W. Kinne (Universitätsklinikum Jena, Arbeitsgruppe für Experimentelle Rheumatologie)
2. Dr. E. Kunisch; Frau B. Ukena, G. Grunert, S. Födisch and C. Müller (Arbeitsgruppe für Experimentelle Rheumatologie)
3. Prof. Dr. K. D. Jandt, Dr. J. Bossert Dr. S. Maenz, (Friedrich-Schiller-Universität Jena, Otto-Schott-Institut für Materialforschung)
4. Institut für Versuchstierkunde und Tierschutz (Universitätsklinikum Jena)
5. Dr. M. Bungartz, Dr. O. Brinkmann (Universitätsklinikum Jena, Lehrstuhl für Orthopädie)
6. Dr. B. Illerhaus (Bundesanstalt für Materialforschung und -prüfung)
7. Dr. Frank Plöger (BIOPHARM GmbH, Heidelberg, Germany) and Dr. P. Hortschansky (Leibniz-Institute for Natural Products Research and Infection Biology – Hans-Knoell-Institute, Jena, Germany),

die Hilfe eines Promotionsberaters nicht in Anspruch genommen wurde und dass Dritte weder unmittelbar noch mittelbar geldwerte Leistungen von mir für Arbeiten erhalten haben, die im Zusammenhang mit dem Inhalt der vorgelegten Dissertation stehen,

dass ich die Dissertation noch nicht als Prüfungsarbeit für eine staatliche oder andere wissenschaftliche Prüfung eingereicht habe und

dass ich die gleiche, eine in wesentlichen Teilen ähnliche oder eine andere Abhandlung nicht bei einer anderen Hochschule als Dissertation eingereicht habe.

Ort, Datum Francesca Gunnella